CIVIL ENGINEERING STUDIES

STRUCTURAL RESEARCH SERIES NO. 294

THE EFFECT OF PLASTIC PRESTRAINS ON THE LOW CYCLE FATIGUE BEHAVIOR OF TITANIUM

Metz Reference Room
Civil Engineering Department
B106 C. E. Building
University of Illinois
Urbana, Illinois 61801

by
J. B. RADZIMINSKI
and
W. H. MUNSE

DEPARTMENT OF CIVIL ENGINEERING
UNIVERSITY OF ILLINOIS
URBANA, ILLINOIS
AUGUST, 1965

THE EFFECT OF PLASTIC PRESTRAINS ON THE LOW CYCLE FATIGUE BEHAVIOR OF TITANIUM

by

J. B. Radziminski

and

W. H. Munse

Department of Civil Engineering

University of Illinois

Urbana, Illinois

August, 1965

ABSTRACT

Considerable interest has recently been centered on the low cycle fatigue properties of materials suitable for use in the construction of space and hydro-space vehicles. The current study presents an evaluation of the influence of large plastic prestrains, both tensile and compressive, on the room temperature static tensile ductility and low cycle fatigue resistance of a commercially pure titanium, RS-70. Fatigue failures at lives ranging from 1/4 to 10^3 cycles were examined.

A number of polished "hourglass-shaped" specimens were tested to failure in static tension following the application of axial plastic pre-compressive strains of various magnitudes. The true (natural) fracture strain was found to decrease in direct proportion to the severity of precompression. The true tensile stress at fracture, however, was not materially altered by the application of the prior compressive strain.

Controlled-strain axial fatigue tests were conducted on specimens of the virgin titanium and on specimens initially subjected to two levels of plastic precompressive strain. The tests were performed at nominal strain ratios of 0, 1/2, and 3/4 to introduce the additional parameter of positive mean strain (tensile prestrain) into the cyclic program. The constant total strain ranges varied from approximately 0.01 to 0.20.

The results of the fatigue tests revealed that, in the low cycle region, both tensile and compressive prestrains reduced the basic fatigue resistance of titanium, the reduction in life increasing in direct relation to the magnitude of the prestrain. This detrimental influence, quite pronounced for large total strain ranges, gradually diminished for progressively smaller

constant ranges, however, and became relatively insignificant as the strain cycle approached a fully elastic condition.

A semi-empirical relationship has been developed which quantitatively relates the appropriate test variables to the observed ability of a ductile material to resist failure by fatigue. The proposed relationship expresses the decreasing influence of axial prestrains on subsequent controlled-strain low cycle fatigue behavior. The estimated range of applicability of the expression is confined to fatigue lives varying from the static tension test at one limit to approximately 10^3 cycles to failure at the other.

A good correlation was obtained between the proposed fatigue relationship and the titanium test results for each condition of prestrain and strain ratio examined. Further support was provided by low cycle fatigue results for an aluminum alloy, 2024-T4, the data having been obtained from a previous study.

ACKNOWLEDGEMENT

This project was conducted as a doctoral research study in the Department of Civil Engineering of the University of Illinois. The titanium used in the investigation was made available by the U. S. Navy Marine Engineering Laboratory, Annapolis, Maryland, through Mr. W. L. Williams.

The authors wish to acknowledge the assistance given them by Messrs. E. E. Kirby and D. F. Lange, laboratory technicians. Their careful preparation of the test specimens and helpful suggestions regarding the experimental phases of the investigation were greatly appreciated.

The authors also express their thanks to Mrs. H. E. Dittmer for her excellent typing of the final manuscript.

TABLE OF CONTENTS

		Page
LIST OF TABLES		vi
LIST OF FIGURES		vii
I.	INTRODUCTION	1
II.	FATIGUE BEHAVIOR OF METALS	3
	A. Long Life Fatigue Behavior	3
	B. Low Cycle Fatigue Behavior	4
	1. Introductory Remarks	4
	2. Controlled-Load Tests	4
	3. Controlled-Deformation Tests	6
	(a) General	6
	(b) Effect of Plastic Prestrains on Hysteresis Behavior and Fatigue Life	9
	4. Analysis of Controlled-Deformation Test Results	14
III.	DEVELOPMENT OF HYPOTHESIS	20
	A. General Review	20
	B. Hypothesis	21
	1. Introductory Remarks	21
	2. Cyclic Controlled-Strain Parameters	22
	3. Reversed Strain Cycling About Zero Mean Strain	23
	4. Effect of Tensile and Compressive Prestrains	25
IV.	EXPERIMENTAL PROGRAM	30
	A. Scope	30
	B. Material, Equipment, and Testing Procedures	30
	1. Material Description and Specimen Preparation	30
	2. Equipment	32
	3. Testing Procedures	34
	(a) Static Precompression and Tension Tests	34
	(b) Cyclic Controlled-Strain Tests	36
V.	PRESENTATION AND ANALYSIS OF TEST RESULTS	39
	A. Test Results	39
	1. Static Precompression and Tension Tests	39
	2. Cyclic Controlled-Strain Tests	39
	B. Analysis of Results	43
	1. Direct Application of Cyclic Stress-Strain Data	43
	2. Use of Approximate Relationships	48
	C. Correlation with Existing Data	50

TABLE OF CONTENTS (Continued)

		Page
VI.	SUMMARY AND CONCLUSIONS	54
	A. Summary	54
	B. Conclusions	56
LIST OF REFERENCES		59
TABLES		63
FIGURES		69
APPENDIX A:	GLOSSARY OF TERMS	111
APPENDIX B:	CALCULATION OF DIAMETRAL AND LONGITUDINAL STRAINS	113
APPENDIX C:	COMPARISON OF LOW CYCLE AND LONG LIFE FATIGUE OF TITANIUM	116

LIST OF TABLES

Table		Page
1.	Results of Static Tension Tests for Specimens Subjected to Various Plastic Precompressive Strains	63
2.	Results of Fatigue Tests for Commercially Pure Titanium RS-70 - Initially Uncompressed Specimens.	64
3.	Results of Fatigue Tests for Commercially Pure Titanium RS-70 - Specimens Precompressed to -0.167 Av. Strain.	65
4.	Results of Fatigue Tests for Commercially Pure Titanium RS-70 - Specimens Precompressed to -0.323 Av. Strain.	66
5.	Results of Fatigue Tests for 2024-T4 Aluminum Alloy	67

LIST OF FIGURES

Figure		Page
1.	Comparison of Controlled-Load and Controlled-Deformation Fatigue Behavior	69
2.	Components of Total Strain Range for Controlled-Strain Cycling	70
3.	Illustration of Controlled-Strain Cycling About a Tensile Mean Strain	71
4.	Cyclic Stress-Strain Diagrams for Various Conditions of Mean Strain	72
5.	Effect of Large Tensile Mean Strains on Low Cycle Fatigue Behavior	73
6.	Parameters Encountered in Controlled-Strain Cycling About Zero Mean Strain	74
7.	Parameters Encountered in Controlled-Strain Cycling About a Tensile Mean Strain	75
8.	Parameters Encountered in Controlled-Strain Cycling After Precompression	76
9.	Illustration of Controlled-Strain Cycling About a Positive Mean Strain After Precompression	77
10.	Details of Test Specimen	78
11.	Traveling Microscope Assembly	79
12.	Rectangular Frame Diameter Gage	79
13.	60,000 Lb. Universal Testing Machine	80
14.	Loading-Head and Sleeve Assembly	80
15.	Method of Compressive Load Application	81
16.	Method of Tensile Load Application	81
17.	50,000 Lb. Fatigue Testing Machine	82
18.	Pull-Head Assembly for Fatigue Machine	83
19.	Pull-Head Assembly with Specimen and Gage Placed in Position	83

LIST OF FIGURES (Continued)

Figure		Page
20.	Specimen Precompressed to -0.32 Strain Beside Virgin Specimen.	84
21.	Static Stress-Strain Diagrams for Specimens Subjected to Various Plastic Precompressive Strains.	85
22.	Fracture Appearance of Typical Static and Fatigue Test Specimens	86
23.	Schematic Representation of Cyclic Controlled-Strain Tests Used in Current Study	87
24a.	Cyclic Stress History of Initially Uncompressed Specimens, R = 0	88
24b.	Cyclic Stress History of Initially Uncompressed Specimens, R = 1/2	89
24c.	Cyclic Stress History of Initially Uncompressed Specimens, R = 3/4	90
25a.	Cyclic Stress History of Specimens Precompressed to -0.167 Av. Strain, R = 0	91
25b.	Cyclic Stress History of Specimens Precompressed to -0.167 Av. Strain, R = 1/2	92
26a.	Cyclic Stress History of Specimens Precompressed to -0.323 Av. Strain, R = 0	93
26b.	Cyclic Stress History of Specimens Precompressed to -0.323 Av. Strain, R = 1/2	94
27.	Cyclic Stress-Strain Diagrams for Initially Uncompressed Specimens	95
28.	Cyclic Stress-Strain Diagrams for Specimens Precompressed to -0.167 Av. Strain.	96
29.	Cyclic Stress-Strain Diagrams for Specimens Precompressed to -0.323 Av. Strain.	97
30.	Reduction in Static Fracture Ductility as a Result of Precompression.	98
31.	Elastic-Plastic Strain Ratio for Initially Uncompressed Specimens	99

LIST OF FIGURES (Continued)

Figures		Page
32.	Elastic-Plastic Strain Ratio for Specimens Precompressed to -0.167 Av. Strain.	100
33.	Elastic-Plastic Strain Ratio for Specimens Precompressed to -0.323 Av. Strain.	101
34a.	Fatigue Test Results for Initially Uncompressed Specimens ($\Delta\epsilon_t$ vs. N_f).	102
34b.	Fatigue Test Results for Initially Uncompressed Specimens (ϵ_{max} vs. N_f)	103
35.	Fatigue Test Results for Specimens Precompressed to -0.167 Av. Strain.	104
36.	Fatigue Test Results for Specimens Precompressed to -0.323 Av. Strain.	105
37.	Fatigue Test Results for All Specimens Strain Cycled at R = 0	106
38.	Elastic-Plastic Strain Ratio for 2024-T4 Aluminum Alloy, Zero Mean Strain.	107
39.	Elastic-Plastic Strain Ratio for 2024-T4 Aluminum Alloy, Various Mean Strains.	108
40a.	Fatigue Test Results for 2024-T4 Aluminum Alloy ($\Delta\epsilon_t$ vs. N_f).	109
40b.	Fatigue Test Results for 2024-T4 Aluminum Alloy (ϵ_{max} vs. N_f)	110

I. INTRODUCTION

Fatigue, the progressive deterioration and eventual fracture of a material under the action of repetitive reversal of stress, has been the object of extensive study for many years. As a result of practical design requirements, emphasis has been placed on fatigue behavior of structural metals in the life range beyond 10^4 cycles which is associated with essentially elastic deformations. Under such conditions, the deterioration process initiates with the formation, possibly at a small fraction of the total cyclic life,[1]* of fine micro-cracks which progress at first slowly and erratically through the structure of the test material. These fissures eventually interconnect to form macro-cracks which, depending upon the test conditions, can lead relatively rapidly to complete fracture. The entire region encompassed by this behavior pattern is generally referred to as the "long life" fatigue range.

Recently, considerable attention has been given to the "low cycle" fatigue range which covers cyclic behavior varying from fracture in simple monotonic tension at one extreme to lives between 10^3 and 10^4 cycles at the other. This interest stems to a large degree from a recognition of the lower cyclic life requirements during the period of usefulness encountered in missiles, certain space and aero-space vehicle components, high-pressure hydro-space vessels, etc., together with the prime concern for weight minimization in these applications. The low cycle fatigue region, especially at the shorter life end of the spectrum, is normally associated with gross plastic deformations leading to ductile fractures more closely resembling static tensile failures than the typical striated fatigue fracture surfaces identified with slow crack propagation under nominally elastic stresses. Concern has been expressed that the term "fatigue"

---

* Numbers in parentheses refer to corresponding entries in List of References.

is somewhat a misnomer in the former region, and that "cyclic, ductile-type" failure may be more descriptive terminology. However, for the course of this study, "low cycle" fatigue is used in referring to behavior in the entire range of lives examined (maximum of approximately 10^3 cycles) even though transitions in fracture appearance are evidenced.

For a ductile material cycled between constant limits of strain, significant alterations in the magnitude of the resultant mechanical hysteresis loop can occur during the early stages of testing. It has been found that both the hysteresis behavior and low cycle fatigue resistance may be materially affected by severe plastic prestraining (or cold-working) prior to cycling. To examine these effects in detail, small polished specimens of a commercially pure titanium (manufacturer's designation RS-70) were subjected to single applications of axial plastic prestrain, both tensile and compressive. The specimens were then cycled between various controlled strain limits to produce failures in the low cycle fatigue range, i.e., maximum lives slightly beyond 10^3 cycles. The objectives of this study were threefold: 1) to examine the basic low cycle fatigue behavior of axially loaded titanium specimens; 2) to determine the range of influence of plastic prestrains on this fatigue behavior; and 3) to combine the relevant parameters involved into a fatigue relationship based upon a physical and intuitive analysis of the observable material behavior mechanisms. The final goal, of course, has been to develop reasonably conservative failure criteria, relating quantities easily obtained from a minimum amount of testing, for utilization by the engineer faced with low cycle fatigue design problems.

II. FATIGUE BEHAVIOR OF METALS

A. Long Life Fatigue Behavior

Exhaustive studies of many materials which behave elastically under small stresses have shown that a linear relationship exists, for a wide range of lives, between the applied stress and fatigue life when related on a log-log basis.[2] As the stress range is decreased, a knee is observed in the S-N curve at about 10^6 cycles, below which some materials appear to suffer no permanent deterioration regardless of the number of additional applied cycles of stress. This lower point is commonly referred to as the "fatigue limit" or "endurance limit."

Throughout the entire long life fatigue range, many parameters have been recognized as affecting the nature of the basic S-N relationship. Besides those factors relating to the mechanical properties of the material itself, other geometric and environmental influences can affect fatigue behavior. For a constant range of cyclic stress, a superimposed tensile mean stress reduces the resultant fatigue life.[3] Similarly, reductions in resistance result from the introduction of notches and increased roughness in the surface finish of a test specimen. Environments of high or low temperature, and high corrosiveness likewise alter the basic S-N relationship. To properly assess the fatigue resistance of a particular material or structural component, therefore, it is important to recognize and, where possible, to evaluate separately each of the factors contributing to the observed behavior.

The short discussion above is presented in way of introduction to observations of analogous response to the testing conditions in the low cycle fatigue region.

B. Low Cycle Fatigue Behavior

1. Introductory Remarks

The range of low cycle fatigue lives is usually associated with loads which create deformations well beyond the limit of linearity between stress and strain. Considerable variation occurs in the hysteresis behavior resulting from reversal of loading during the cycling process; these changes depend upon whether stress or strain range is the controlled test parameter. Consequently, low cycle fatigue tests must be further defined as either constant-load (nominal stress) or constant-deformation (strain) tests. Comprehensive reviews of the literature concerning both types of tests have been prepared by Benham[4] and Yao.[5]

Significant changes in the hysteresis condition and subsequent fatigue behavior are also incurred as a result of severe prestraining prior to cycling. As this is an area of primary concern in the present study, a separate section is devoted to a review of the work of previous investigators who have examined the effects of prestraining on low cycle fatigue life. Observations from these earlier studies have provided the foundation upon which the relationships presented herein have been developed, and then verified by the current testing program.

2. Controlled-Load Tests

Since the present investigation concerns fatigue behavior under conditions of controlled strains, only a brief description of constant-load range tests need be included for purposes of general comparison. In an early investigation using direct axial loads, Hartmann and Stickley[6] obtained results for 17S-T aluminum alloy for fatigue lives between 1/2 and 5×10^8 cycles. It should be noted that the upper limit of the S-N curve in the low cycle region is

3. Controlled-Deformation Tests

(a) General

Certain disadvantages arise in controlled-load fatigue testing of ductile materials when the applied loads are such that minor changes in stress are accompanied by large strain variations. Besides the difficulty of maintaining the load at a given level near the ultimate, changes in the hysteresis loop contour during cycling often produce pronounced "cyclic creep" conditions resulting in progressive specimen necking with increasingly higher true stresses.[14,15] Recognizing these difficulties, many investigators have adopted strain as the controlled parameter in low cycle fatigue studies. Early studies usually involved the measurement of engineering strains, i.e., changes in gage length of cylindrical or sheet specimens. However, the highly localized nature of low cycle fatigue damage in areas of largest plastic strain has led to wide acceptance of "true" strains in the control of tests and analysis of data.* To effectively measure such localized deformations, "hourglass-shaped" axial test specimens, which confine the maximum strains to a small region, are often used.[16-18] A specimen configuration of this type has been used in the conduct of the present experimental investigation. It must be recognized, however, that these "true" strains are still based upon gross changes in cross-sectional area, which do not describe the complex conditions at the center of the highly strained volume nor the effect of the taper radius (radius of curvature at test section) of the specimen. Nevertheless, these strain measurements have been most effective in analyzing the relative low cycle fatigue behavior of different materials, and the influence of various test parameters on a given material. In the following discussion of experimental work to date, it must be remembered that many specimen

* "True" refers to the concept of natural (logarithmic) strains computed from measurements taken at the position of greatest local deformation.

types and strain measurement techniques have been employed, so that care must be exercised when comparing results.

As early as 1912, Kommers[19] recognized the importance of repeated deflections in low cycle fatigue from a study of cyclic bending tests. However, as a result of the emphasis on elastic behavior in design, the literature pertaining to cyclic controlled-strain fatigue tests was sparse in the United States during the first half of this century. In 1948, Liu et al.[16] conducted reversed strain, axial fatigue tests of 24S-T aluminum alloy. The magnitudes of the plastic strains resulted in failures between 1 and 7 cycles. During the subsequent years, Coffin and his colleagues[18,20-24] have contributed significantly to the present state of knowledge of low cycle fatigue. In the course of their studies of low carbon and stainless steels, copper, nickel, and aluminum alloys, they have examined the effect of temperature, prior annealing, and plastic prestraining on the contour of the hysteresis loop and fatigue life resulting from axial constant strain range cycling. Their results have indicated that, for a wide variety of materials, a linear relationship exists on a log-log basis between the plastic component of the cyclic total controlled-strain range, $\Delta\epsilon_p$,* and the corresponding fatigue life, N_f. (Refer to Fig. 2 for definition of cyclic strain components.) Similar to constant-load data presentation, the failure line is extrapolated to the fracture condition in a static tension test, the intercept on the strain axis being related in this case to the fracture strain of the material. Low,[25,26] based on plane bending fatigue tests at constant angular deformations, established a straight line correlation between the maximum fibre strain and life on a log-log basis for strains to a minimum of 0.004**.

---

* A glossary of terms is presented in Appendix A.

** The decimal equivalent of strain in percent is used throughout. Thus, 0.004 = 0.4 percent strain, etc.

The corresponding life at this strain was approximately 10^4 cycles. The materials examined included 3 steels and 2 aluminum alloys.

In a more recent investigation, Gross[27] found that the total strain range, $\Delta\varepsilon_t$, provided a more consistent linear log-log relationship with low cycle fatigue life. His flexural tests were conducted on a variety of materials (5 steels, 5 nickel-base, 6 aluminum-base, and 3 copper-base alloys) subjected to a number of different test conditions (plain and notched specimens, weldments, variable cycle pattern, and air and salt water atmospheres). Fatigue lives included the range from 10^2 to 10^5 cycles. A similar correlation using $\Delta\varepsilon_t$ was obtained by Wells and Sullivan[28] for tests on a nickel-base superalloy, Udimet 700, at cyclic total strain ranges from 0.028 to 0.008 with fatigue lives to a maximum of 10^4 cycles. When the entire spectrum of fatigue life is considered, however, there is actually a decrease in the slope of the log $\Delta\varepsilon_t$-log N_f curve as the long life region is approached, the transition area usually occurring near 10^3 cycles for ductile metals. The curve then follows the normal long life fatigue relationship in the range where strain becomes proportional to stress, and finally flattens out for those materials which exhibit a fatigue limit. In a series of axial fatigue tests which included lives extended from the low to intermediate life range, R. W. Smith *et al.*[29] observed this decrease in the slope of the log $\Delta\varepsilon_t$-log N_f curve. A wide variety of metals were examined in the study, including 6 steels, beryllium, Inconel X, a titanium, and 3 aluminum alloys. Similar transition behavior has been reported and analyzed by Morrow and Tuler[30] in tests with two nickel-base alloys, Inconel 713C and Waspaloy. A typical qualitative curve encompassing the entire fatigue life range based upon cyclic total strain range is presented in Fig. 1b for comparison with the load-life curve shown in Fig. 1a.

(b) Effect of Plastic Prestrains on Hysteresis Behavior and Fatigue Life

The observations of linearity between either $\Delta\epsilon_t$ or $\Delta\epsilon_p$ and N_f on a log-log basis discussed in the preceding section are based largely on fatigue studies in which the strains are subject to complete reversal, i.e., mean strain is zero; or zero strain-maximum strain conditions, i.e., mean strain is half the maximum strain. Important variations in the basic behavior are evidenced, however, when the material is subjected to severe plastic prestrain, either tensile or compressive, before cycling is undertaken.* Before examining these effects in detail, a brief review of the changes in static tensile ductility observed for metals under similar conditions of prestrain is in order.

When a ductile material is plastically deformed in tension and the load then removed, the unloading curve remains elastic. Unless the material ages rapidly at the test temperature, the reloading curve will also remain essentially elastic to a point close to the initial maximum strain after which plastic deformations again predominate.(31) The stress-strain curve then continues along a path coincident with the curve for a specimen loaded monotonically to fracture. Thus, the retained ductility upon reloading is simply the static fracture strain less the initial tensile plastic prestrain. This behavior has been verified by Bridgman(32) (for steel), and Liu and Sachs(33) (for aluminum).

Similar behavior is exhibited when the material is subjected to a large initial plastic compressive strain. Bridgman,(32) after heat-treating low carbon steel specimens to a series of nine different conditions, precompressed these specimens to total axial compressive strains of -1.25. The specimens were then tested to failure in simple tension. For each of the conditions of

---

* Reversed strain cycling after a single plastic strain application (prestrain) may be alternatively interpreted as cycling about a particular mean strain value, ϵ_m, the terms thus becoming completely interchangeable, Fig. 3.

heat-treatment, the precompressed specimens exhibited reduced fracture ductility relative to similarly treated specimens which were not precompressed. Polakowski[34] studied the effect of cold-working on the stress-strain relationship of aluminum, copper, and low carbon steel. Static tension tests, conducted after the initial cold-working, indicated that the tensile strength for these materials increased significantly whereas the fracture ductility was severely reduced. In each instance the reduction in ductility became more pronounced with greater prior cold-working. Drucker et al.[35] subjected E-steel to various plastic precompressive strains from -0.10 to -0.47. Subsequent tensile tests on the precompressed specimens again showed a significant and continuous reduction in ductility with increasing amounts of precompression. Similar results are reported by Yao[36] for his "one-cycle" tests with ABS-C and E-steels.

In low cycle fatigue, changes in the height of the hysteresis loop during the progress of constant-strain-range cycling have been reported in a number of studies. Such variations in stress magnitude are referred to here as "cyclic hardening" or "cyclic softening" rather than "strain hardening," which is normally associated with the post-yield slope of the static stress-strain curve. A thorough review of the literature on this particular phase of cyclic behavior has recently been reported by Tuler and Morrow.[37]

In an early study in the United States with annealed 24S-T aluminum, Liu[16] et al. observed, for constant alternating strain ranges from 0.12 to 0.30, that marked hardening occurred in the first and second strain reversals. The hysteresis loop then remained quite stable until final failure. It should be noted that the simple tensile fracture strain for the material was approximately 0.38 and that the very large cyclic strains involved led to failures in 7 cycles or less.

Later, Liu[38] found for the same aluminum that cyclic hardening occurred in the first few cycles even after the material had been initially strained in compression as high as -0.18; above this value, cyclic softening was observed following the precompression. For each of these tests the total strain range was controlled at 0.12. Thus it is apparent that the cyclic hysteresis behavior depends not only upon the strain range, but on the amount of plastic prestrain (tensile or compressive) as well. Liu also found that, for the constant cyclic strain range studied, the number of cycles to failure decreased with increasing precompressive strain.

In an early paper, Coffin[20] observed that annealed 347 stainless steel will cyclically harden under reversed strains, whereas the same material will undergo cyclic softening after an initial large (0.15 or 0.30) tensile prestrain. Polakowski[34] obtained similar results for flexural controlled-strain tests of copper and aluminum. In the annealed condition these materials hardened during cyclic straining. When subjected to prior cold-working, however, both metals would soften during continued cycling at moderate strains, the degree of softening varying in direct relation to the amount of initial cold-work. Based on these experiments, Polakowski postulated that, under cyclic straining at a constant level, a given material will eventually stabilize at the same hardness (hysteresis condition) regardless of the initial state of the material. This hypothesis has largely been confirmed in later studies, particularly for ductile metals at small or moderate ranges of repeated plastic strain.

Coffin and Tavernelli[18] performed a series of cyclic axial strain tests on 2S aluminum in the annealed condition and after it had been subjected to prestrains, tensile and compressive, of 0.10 to 0.40. Again the authors observed that "either strain hardening or strain softening can occur, depending both upon the degree of prior strain and the amplitude of the diametral strain

range used in cycling." In general, for those specimens subjected to tensile prestrains, the transition from cyclic hardening to softening was found to occur for ranges of strain below 0.10. As with the work of Polakowski, it was noted, for a given constant strain range, that the eventual stable stress condition reached during cycling would be about the same independent of the amount of prestrain, unless, of course, fatigue fracture intervened before the adjustments were completed.

Pian and D'Amato[17] examined the effect of tensile mean strain on the hysteresis changes and fatigue lives encountered during controlled cyclic straining of 2024 aluminum alloy. Their data are presented in terms of the strain range and the "strain ratio," i.e., ratio of minimum to maximum strain, which in turn uniquely define the mean strain. As with earlier tests on aluminum, the authors found that the occurrence of cyclic hardening or softening was dependent upon the magnitude of the mean strain and the cyclic strain range. It was also noted that large mean strains had a detrimental effect on fatigue life relative to those cycled about a zero mean, especially at the shorter lives associated with large total strain ranges.

In a subsequent study with the same material, D'Amato[39] presented a number of significant observations encompassing the realm of low cycle fatigue. A series of tests were performed on hourglass-shaped specimens with taper radius of 1-1/2 in. for which the fracture strain in static tension was approximately 0.38. The cyclic controlled total strain ranges varied from 0.01 to 0.345 with mean strains of -0.075, 0, 0.075, 0.135, 0.185, and 0.275. For each test specimen, the stress history during cycling was also examined. In analyzing the data, the "stable" elastic component of the total strain range was determined by taking an average value of the cyclic stress range over the entire lifetime of the specimen.

To obtain an indication of the effect of strain cycling on the stable stress state for the material, D'Amato constructed stress-strain diagrams using half the cyclic total strain range as abscissa and the average cyclic stress amplitude as ordinate. A given cyclic strain range and its corresponding average stress amplitude would be represented as a single point on this curve. For each of the strain ranges studied, a point was thus plotted on the diagram, these points then being connected to form a "cyclic stress-strain" curve. Separate curves were constructed for each of the mean strains examined. Comparing these curves, it was observed that those representing the greater mean strains were generally above the curves for small mean strains, whereas all the cyclic curves were above the static tensile test stress-strain diagram. An illustration of these observations is shown in Fig. 4. (For some metals, especially those subjected to severe initial cold-working, the cyclic stress-strain curve will lie below that for the static tension test, Ref. 29.) D'Amato concluded from this deviation of the cyclic stress-strain diagram relative to the static tension curve that the "tensile test cannot be used to relate the stress and strain for the fatigue tests."

The fatigue lives of the 1-1/2 in. taper radius specimens were then compared with the cyclic total strain range, $\Delta\varepsilon_t$, and the plastic strain range, $\Delta\varepsilon_p$. Using the total strain range it was found, on a log-log basis, that fatigue life decreases with increasing mean strain for a given constant range of strain. This adverse effect of mean strain on fatigue behavior was diminished at the lower strain ranges, however, and tended to "wash out" as conditions approached fully elastic stress reversals. Between 10^3 and 10^4 cycles to failure the curves for the different mean strains converged and continued into the long life fatigue region at a flatter slope. A sketch of this general behavior is shown in Fig. 5a.

When the fatigue lives were compared to the plastic strain range, on the other hand, a divergence downward from the linear log-log relationship occurred prior to 1000 cycles. The point of divergence was manifested earlier with increasing mean strain, Fig. 5b. This occurred as a consequence of the high stresses involved in the initial strain application, the subsequent cyclic hysteresis adjustments not being able to develop before fatigue failure intervened. It is apparent, therefore, that fatigue relationships developed for tests at zero mean strain cannot always be conservatively used to relate to data obtained for large mean strains (severe initial prestraining or cold-working).

Gerberich[40] also performed a series of cyclic axial tests to examine the effect of mean strain on the low cycle fatigue behavior of 2024 aluminum, and compared his results with those of Liu et al.,[16] and Pian and D'Amato.[17] Based on these studies he concluded that increasing the mean strain will decrease fatigue life in the low cycle region, but that the effect of the mean strain "progressively decreases as the number of cycles to failure increases." Similar results were reported by Sachs[41] et al. for cyclic bending tests of A-302 steel, and 5454-0 and 2024 aluminum alloys. The effect of prestraining was found to become insignificant beyond 10^4 cycles when fatigue life was compared to the total cyclic strain range, $\Delta\varepsilon_t$. These tests were later expanded to include axial fatigue data for A-302 and A-225 steels and 5454-0 aluminum with lives ranging to a maximum of approximately 400 cycles.[42,43] In general, the conclusions reached in the earlier studies were confirmed.

4. Analysis of Controlled-Deformation Test Results

In analyzing the effect of stress concentrations on the fatigue behavior of a material strain cycled in bending, Orowan[44] postulated that fracture occurs "when a critical value of the total absolute plastic strain is reached." The

resulting expression:

$$\Delta\epsilon_p \cdot N_f = C \tag{2.1}$$

where C is a constant, is represented as a straight line on a log-log graph in direct analogy to the typical S-N diagram associated with the long life fatigue range.

Later, Manson[45] and Coffin[20] found that a modification of the basic equation was required to more accurately describe their experimental data:

$$\Delta\epsilon_p \cdot N_f^{\,a} = C \tag{2.2}$$

where a is also a constant which represents the slope of the log $\Delta\epsilon_p$-log N_f curve. In an analysis of the results of several investigators, Tavernelli and Coffin[22] suggested that, for reversed cyclic strains at room and elevated temperatures, the exponent in the above equation may be conservatively taken as 0.5:

$$\Delta\epsilon_p \cdot N_f^{\,0.5} = C \tag{2.3}$$

Recognizing that the constant C may be related to the static fracture strain in simple tension, ϵ_f, and assuming that the static tension test represents a "fatigue" life of 1/4 cycle, the authors calculated C as:

$$C = \epsilon_f \cdot \left(\frac{1}{4}\right)^{0.5} = \frac{\epsilon_f}{2}$$

Thus Eq. (2.3) may be expressed as:

$$\Delta\epsilon_p \cdot N_f^{\,0.5} = \frac{\epsilon_f}{2} \tag{2.4}$$

The fracture strain was taken as the "true" strain found from the reduction in area for a uniaxial static tension test:

$$\epsilon_f = \ell n \frac{A_o}{A_f} \tag{2.5}$$

where A_o and A_f are the initial and final cross-sectional areas, respectively. Equation (2.4) was found reasonably satisfactory by Tavernelli and Coffin,[22] although "best-fit" curves for the data using a slope of -0.5 did not intersect the strain axis at ϵ_f for all materials and test conditions.

Martin,[46] using an analysis based upon an energy criterion, suggested that the constant C be represented by $\epsilon_f\sqrt{2}$:

$$\Delta\epsilon_p \cdot N_f^{0.5} = \frac{\epsilon_f}{\sqrt{2}} \tag{2.6}$$

This equation was found to offer better predictions of fatigue life than Eq. (2.4) for room temperature, axial strain test data of several materials. The reverse was true, however, for conditions of flexural fatigue and elevated temperature cycling.

Recently, it has been common for authors to view the strain axis intercept as an "apparent" fracture ductility factor, ϵ_f', which, although varying somewhat from the true fracture strain, can be closely related to it for purposes of comparison of different materials, i.e., $\epsilon_f' = f(\epsilon_f)$.

A number of investigators have also found that the exponent 0.5 in Eq. (2.3) proposed by Coffin is not satisfactory for all data. Benham[47] (for copper), and Dubuc[13] (for low carbon steel and brass) reported the exponent of N_f to be slightly greater than 0.5. In an analysis of cyclic data for Inconel, 347 stainless steel, and titanium tested at elevated temperatures, Majors[48] reported this exponent to range from 0.35 to 0.82. Gross[27] found the value varied from 0.42 to 2.40 for several different materials and test environments. It appears, then, that the exponent of N_f in Eq. (2.2) best

representative of low cycle fatigue data is dependent upon both the material and testing conditions. These conditions include temperature, frequency of cycling, testing environment and specimen geometry. It would not be wise, with the present state of knowledge, to presuppose a value of a, but rather, to determine a suitable exponent by performing at least a minimum number of cyclic tests.

To obtain a single expression applicable in both the low cycle and long life fatigue regions for reversed cyclic strain tests, Langer[49] proposed a relationship based upon the total strain range, $\Delta\epsilon_t$:

$$\Delta\epsilon_t = \Delta\epsilon_p + \Delta\epsilon_e \tag{2.7}$$

where $\Delta\epsilon_e$ is the stable cyclic elastic strain range, i.e., $\Delta\epsilon_e = \Delta\sigma_s/E$, Fig. 2. Substituting Eq. (2.4) for the plastic component into the above:

$$\Delta\epsilon_t = \frac{\epsilon_f}{2N_f^{0.5}} + \Delta\epsilon_e = \frac{\epsilon_f}{2N_f^{0.5}} + \frac{\Delta\sigma_s}{E}$$

Langer then approximated the total stress range as twice the maximum stress at the material's fatigue limit, $2S_e$:

$$\Delta\epsilon_t = \frac{\epsilon_f}{2N_f^{0.5}} + \frac{2S_e}{E}$$

Multiplying by E/2, and taking the resulting product, $\Delta\epsilon_t \cdot E/2$, as a measure of a "pseudo-stress" amplitude, S_a, the equation becomes:

$$S_a = \frac{E \cdot \epsilon_f}{4N_f^{0.5}} + S_e \tag{2.8}$$

Tavernelli and Coffin[23] compared Eq. (2.8) with data for a variety of metals and found it to be conservative. Gross,[27] however, found the

relationship to range from "ultra-conservative to unconservative" when compared with his flexural fatigue results.

Morrow and Tuler,[30] rather than approximating $\Delta\epsilon_e$ in Eq. (2.7) by a fatigue limit condition, substituted the actual stress vs. life linear log-log relationship normally observed in the long life fatigue range:

$$\Delta\epsilon_e = \frac{\Delta\sigma}{E} = \frac{2\sigma_f'}{E(2N_f)^b} \tag{2.9a}$$

where σ_f' is a fatigue strength coefficient (measure of the static tensile strength), $2\sigma_f'/E$ is the elastic strain axis intercept at $2N_f = 1$, and $-b$ is the slope of the log $\Delta\epsilon_e$-log $2N_f$ curve. $2N_f$ is the number of strain "reversals" or "half-cycles" to failure. To this the authors added the term expressing a relationship between plastic strain range and fatigue life in the low cycle region:

$$\Delta\epsilon_p = \frac{2\epsilon_f'}{(2N_f)^c} \tag{2.9b}$$

where $2\epsilon_f'$ is the plastic strain axis intercept at $2N_f = 1$, and $-c$ is the slope of the log $\Delta\epsilon_p$-log $2N_f$ curve. Thus, by substitution of Eqs. (2.9a and b) in Eq. (2.7), the entire fatigue life spectrum is represented by:

$$\Delta\epsilon_t = \frac{2\epsilon_f'}{(2N_f)^c} + \frac{2\sigma_f'}{E(2N_f)^b} \tag{2.10}$$

Gerberich[40] expressed the effect of mean strain on low cycle fatigue behavior by introducing that parameter into the basic fatigue relationship:

$$\Delta\epsilon_p \cdot N_f^{0.5} = \epsilon_f' - \epsilon_m$$

or

$$N_f = \left[\frac{\epsilon_f' - \epsilon_m}{\Delta\epsilon_p}\right]^2 \tag{2.11}$$

where ϵ_f' is the apparent fracture strain and ϵ_m is the cyclic mean strain (or plastic prestrain). In later investigations[41-43] the plastic strain component in Eq. (2.11) was replaced by the total strain range:

$$N_f = \left[\frac{\epsilon_f' - \epsilon_m}{\Delta\epsilon_t}\right]^2 \tag{2.12}$$

This expression was found to be satisfactory in cyclic axial strain tests for a number of materials and for lives up to about 400 cycles. For large mean strains, however, the equation does not adequately predict the authors' observation that the effects of prestraining "appear to become insignificant somewhere above 1000 cycles."[43]

This concludes a brief summary of present information on the behavioral aspects of low cycle fatigue in materials subjected to large cyclic strains. In the following chapter an expression is presented which combines the influences of prestraining and subsequent hysteresis behavior inasmuch as they affect low cycle fatigue resistance. This relationship, hopefully applicable to a variety of ductile materials, will then be verified by axial controlled-strain tests of a commercially pure titanium.

III. DEVELOPMENT OF HYPOTHESIS

A. General Review

The low cycle fatigue hypothesis presented in this chapter has been developed in part from an analysis of the behavior encountered during prior cyclic controlled-strain studies. It is important, therefore, to summarize the conclusions drawn from earlier observations of the various test parameters and related fatigue resistance before proceeding. The following remarks are, in general, applicable to ductile materials (static tensile fracture strain, $\epsilon_f > 0.1$) subjected to constant total strain range cycling at room temperature:

(1) For completely reversed cyclic strain tests of the virgin material (not subjected to a large plastic prestrain application) the resultant low cycle fatigue behavior may be represented by a linear log-log relationship between either the total strain range, $\Delta\epsilon_t$, or the plastic strain range, $\Delta\epsilon_p$, and fatigue life, N_f. The slopes of the failure curves are dependent upon both material factors and test conditions.

(2) The relative position of these fatigue curves for different materials may be directly related to the static tensile ductility of each material; i.e., the failure line for a metal of high tensile fracture strain will normally lie above that for a material possessing a lower fracture strain.

(3) Significant variations in the shape of the hysteresis loop occur during cyclic straining. These changes usually stabilize to a "steady-state" condition within a proportionately few cycles unless fatigue failure intervenes. The degree of cyclic hardening or softening that takes place is dependent upon both the strain range and the condition of mean strain. The stress-strain diagram obtained from a static tension test cannot, therefore,

be satisfactorily used to describe the stable stress conditions obtained during cyclic straining.

(4) Plastic prestraining,* either tensile or compressive, decreases the low cycle fatigue resistance of a material in proportion to the magnitude of prestrain. This reduction, most pronounced at very low lives, results from the combination of a loss of ductility caused by the prestraining, and the large strain ranges which preclude any beneficial cyclic adjustments in the hysteresis condition prior to failure. At smaller constant strain ranges, however, the influence of prestrain progressively diminishes as the material is able to stabilize with cycling to a condition closer to that of an initially undeformed test specimen. This process becomes complete as the strain reversals approach elastic conditions, with fatigue behavior (based on total strain range) practically independent of prestrain in the long life region. Thus, as Morrow and Tuler[30] observe, "The resistance to repeated total strain is dependent on ductility at short lives, strength at long lives, and a combination of ductility and strength at intermediate lives."

B. Hypothesis

1. Introductory Remarks

The primary objective of this study has been the development of a fatigue relationship, based on controlled total strain range tests, which includes the effects of prestrain, both tensile and compressive, on the mechanisms operative in the low cycle behavior of ductile metals. This relationship is presented in terms of $\Delta\epsilon_t$ as the independent variable, for the total strain range, rather than the plastic component, $\Delta\epsilon_p$, was kept constant during each

---

* The equivalence of cycling about a particular mean strain, and reversed strain cycling subsequent to a plastic prestrain application has been noted earlier, Fig. 3.

cyclic test. Such an expression is thus readily adaptable to design requirements. Furthermore, the variations in hysteresis behavior evident during the cycling process, especially for severe prestrains and large strain ranges, make it difficult to assign appropriate "stable" plastic (or elastic) strain components for particular constant total ranges of strain.

It must be emphasized that the expressions developed herein are applicable to the low cycle fatigue domain only, and should not be extrapolated to the long life region. They are thus bounded by the simple tension test at one extreme and small cyclic plastic strain reversals (i.e., $\Delta\epsilon_p$ of the same order of magnitude as $\Delta\epsilon_e$) at the other. An approximate upper limit on life may be taken at about 10^3 cycles. An alternate approach for determining the range of applicability would be to obtain the normal log S-log N_f curve (converted to strain) for the long life region and extend it to the point of intersection with the low cycle curve.

2. Cyclic Controlled-Strain Parameters

Before continuing with the development of the hypothesis, an explanation of the terms used to define the basic parameters encountered in controlled-strain cycling is necessary. For constant total strain range tests, the components of the total range, Fig. 6 are:

$$\Delta\epsilon_t = \Delta\epsilon_e + \Delta\epsilon_p \tag{3.1}$$

$$\Delta\epsilon_e = \frac{\Delta\sigma_s}{E} \tag{3.2}$$

where $\Delta\epsilon_e$ and $\Delta\epsilon_p$ are the cyclic elastic and plastic strain ranges, respectively. In Eq. (3.2), $\Delta\sigma_s$ is the magnitude of the cyclic range of stress after a "stable" hysteresis loop has been established (defined herein at half the fatigue life, $N_f/2$), and E is the elastic modulus of the material.

For controlled-strain cycling following an initial tensile plastic strain application (i.e., cycling about a tensile mean strain), the test variables, Fig. 7, include:

$$\text{cyclic mean strain} \qquad \epsilon_m = \frac{1}{2}\,(\epsilon_{max} + \epsilon_{min}) \tag{3.3}$$

$$\text{cyclic strain ratio} \qquad R = \frac{\epsilon_{min}}{\epsilon_{max}} \tag{3.4}$$

where ϵ_{max} and ϵ_{min} are the limiting values of the total strain range, $\Delta\epsilon_t = \epsilon_{max} - \epsilon_{min}$. Combining this with Eq. (3.3):

$$\Delta\epsilon_t = 2\,(\epsilon_{max} - \epsilon_m) \tag{3.5}$$

By controlling $\Delta\epsilon_t$ and R, the mean strain is also uniquely determined:

$$\epsilon_m = \frac{1}{2}\,\Delta\epsilon_t\,\left(\frac{1 + R}{1 - R}\right) \tag{3.6}$$

Note also from Eqs. (3.4) through (3.6) that, in analyzing fatigue data, the value of $\Delta\epsilon_t$ corresponding to a static tension test (i.e., for $\epsilon_{max} = \epsilon_f$ and $N_f = 1/4$ cycle) varies with the type of cyclic test under consideration. Thus, by definition, for complete reversal cycling, $R = -1$, $\Delta\epsilon_{t(1/4)} = 2\epsilon_f$; for $R = 0$, $\Delta\epsilon_{t(1/4)} = \epsilon_f$; etc.

For convenience of presentation, the additional variables related to precompressive straining will be introduced as they arise in the development of the hypothesis.

3. Reversed Strain Cycling About Zero Mean Strain

The low cycle fatigue behavior of a ductile material subjected to controlled total cyclic strain ranges about a zero mean, Fig. 6, may be represented by:

$$\Delta\epsilon_t \cdot N_f^m = C$$

or

$$N_f = \left[\frac{C}{\Delta\epsilon_t}\right]^{1/m} \tag{3.7}$$

where N_f is the cyclic life to complete specimen separation (fracture), and C and m are constants. The negative of the exponent, -m, is the slope of the log $\Delta\epsilon_t$-log N_f curve. No fixed value of m is suggested; it should be determined from the actual experimental data obtained for the particular material and test conditions under investigation. It is considered a fatigue test property and not a universal constant.

The constant C is related to the static tensile ductility and may be expressed as:

$$C = \epsilon_f' = f(\epsilon_f) \tag{3.8}$$

where ϵ_f' is considered an "apparent" fracture ductility and ϵ_f is the logarithmic or "true" static tensile fracture strain. (Refer to discussion in Chapter II.)

Since both the specimen type and test condition (uniaxial cycling) for the current fatigue study are the same as those used in the static tension tests, it is anticipated that the constant C can be represented directly by the true fracture strain in Eqs. (3.8) and (3.7):

$$C = \epsilon_f$$

$$\therefore \quad N_f = \left[\frac{\epsilon_f}{\Delta\epsilon_t}\right]^{1/m} \tag{3.9}$$

The intercept on the total strain range axis representative of the static tensile fracture strain is assumed to occur at a "fatigue" life of 1/4 cycle. For cyclic tests, the sequence then continues around the hysteresis

loop as shown in Fig. 6. A full cycle is completed as the original state of zero stress is again reached after the compression portion of the loop has been traversed. It is obvious that extrapolation to a minimum life of 1/4 cycle is somewhat arbitrary, for a smooth fatigue life "curve" does not strictly exist in this region. The "curve" is actually a series of discrete steps in that a specimen not failing at the first tensile load application (N = 1/4) cannot fail until at least the second tensile load application, N > 1, etc.

If a specimen, after being subjected to a number of fatigue cycles, fails before the set maximum tensile strain for the next cycle is attained, its total life is considered to be the number of complete cycles plus a partial cycle:

$$\text{partial cycle} = \frac{1}{4}\left(\frac{\epsilon_{fail} - \epsilon_{min}}{\Delta\epsilon_t}\right) \tag{3.10}$$

where ϵ_{fail} is the strain at the instant of failure. Of course, this additional fraction is of little consequence for lives beyond about 10 cycles.

4. Effect of Tensile and Compressive Prestrains

The effects of prestraining on low cycle fatigue resistance, previously discussed qualitatively, can now be incorporated into the basic fatigue relationship, Eq. (3.9). The influence of tensile prestrain (mean strain) will be introduced first, followed by a similar discussion for precompressive strains. The separate results will then be combined into a single expression.

It has been established that, for a material subjected to a tensile prestrain, ϵ_m, if the load is then reapplied continuously to fracture, the retained ductility available after the prestrain, Fig. 7, is:

$$\text{retained ductility} = \epsilon_f - \epsilon_m$$

It follows that in describing cyclic strain testing about a particular tensile mean strain, ϵ_m, the intercept on the strain axis at N_f = 1/4 cycle, representative of the static tension test following a single identical strain application, should also be proportional to $\epsilon_f - \epsilon_m$.

For the remainder of the low cycle fatigue region, however, there is a gradual transition from a fatigue resistance dependent upon reserve ductility properties at low cyclic lives (large plastic deformations) to a resistance related directly to material strength for longer lives (small plastic deformations). Thus, as the controlled cyclic strain range is decreased, the adverse effects on fatigue behavior of large plastic prestrains are continuously reduced and become insignificant for strain reversals approaching elastic conditions. As a result, the log $\Delta\epsilon_t$-log N_f curves corresponding to various magnitudes of prestrain eventually converge with the failure curve for complete reversal tests, $\epsilon_m = 0$.

Any analytical description of this behavior, when introduced into the fatigue life relationship, should satisfy the following limits:

$$N_f = \left[\frac{\epsilon_f - f(\epsilon_m)}{\Delta\epsilon_t}\right]^{1/m} \tag{3.11}$$

where

$$f(\epsilon_m) \rightarrow \epsilon_m \qquad \text{as} \qquad \Delta\epsilon_t \rightarrow \epsilon_f ; (R = 0)$$

$$f(\epsilon_m) \rightarrow 0 \qquad \text{as} \qquad \Delta\epsilon_p \rightarrow 0;\ \Delta\epsilon_t \rightarrow \Delta\epsilon_e$$

It is postulated that the function $f(\epsilon_m)$ may be expressed by the following continuous relationship, which inter-relates the governing variables and satisfactorily depicts the limiting conditions stipulated above:

$$f(\epsilon_m) = \frac{\Delta\epsilon_p}{\Delta\epsilon_t}(\epsilon_m) = \left(1 - \frac{\Delta\epsilon_e}{\Delta\epsilon_t}\right)(\epsilon_m) \tag{3.12}$$

To obtain the plastic strain range, it is necessary to establish the cyclic stress-strain relationship for each value of mean strain or strain ratio. For the materials examined in this study, however, it will be subsequently shown that the cyclic stress-strain curve for R = 0 (or, preferably, R = -1) can be used to represent other strain ratios as well. Thus only a minimum of actual cyclic testing will be required to determine the necessary parameters.

Substituting the above expression into Eq. (3.11):

$$N_f = \left[\frac{\epsilon_f - \frac{\Delta\epsilon_p}{\Delta\epsilon_t} (\epsilon_m)}{\Delta\epsilon_t} \right]^{1/m} \tag{3.13}$$

Note that this equation reflects the decreasing influence of mean strain as the cyclic strains approach elastic reversals ($\Delta\epsilon_p \rightarrow 0$).

Although there is comparatively little information in the literature regarding the effect of large initial compressive strains on subsequent low cycle fatigue lives, the available data do indicate that the hysteresis changes accompanying progressive cycling follow behavior patterns similar to those for pretensioned specimens. It would be expected, then, that the effect of initial hardening and loss of ductility due to a single large plastic precompressive strain application, though detrimental at very short cyclic lives, should again by essentially "washed out" at the longer lives associated with small plastic strain ranges.

Denoting the fracture strain in a static tension test following pre-compression, Fig. 8, as ϵ_f^{pc}, the reduction in ductility relative to that of an initially undeformed specimen is:

$$\epsilon_r^{pc} = \epsilon_f - \epsilon_f^{pc} \tag{3.14}$$

where the ductility reduction, ϵ_r^{pc}, is in turn related to the amount of initial compressive strain, ϵ_{pc}. (For the titanium investigated in this study ϵ_r^{pc} was found to be directly proportional to ϵ_{pc}.)

The anticipated diminishing influence of ϵ_r^{pc} with fatigue cycling at decreasing constant total strain ranges may be introduced into the basic fatigue life relationship in a manner analogous to that postulated for tensile prestrains. By transferring the origin of the reference axes from 0 to 0' in Fig. 8 and imposing the same limiting conditions on the expression for fatigue life, Eq. (3.9) becomes:

$$N_f = \left[\frac{\epsilon_f - \frac{\Delta\epsilon_p}{\Delta\epsilon_t}(\epsilon_r^{pc})}{\Delta\epsilon_t}\right]^{1/m} \tag{3.15}$$

where

$$\frac{\Delta\epsilon_p}{\Delta\epsilon_t}(\epsilon_r^{pc}) \rightarrow \epsilon_r^{pc} \qquad \text{as} \qquad \Delta\epsilon_t \rightarrow 2\epsilon_f^{pc};(R = -1)$$

$$\frac{\Delta\epsilon_p}{\Delta\epsilon_t}(\epsilon_r^{pc}) \rightarrow 0 \qquad \text{as} \qquad \Delta\epsilon_p \rightarrow 0;\ \Delta\epsilon_t \rightarrow \Delta\epsilon_e$$

A third situation now presents itself, whereby a material subjected to a large initial compressive strain is then strain-cycled about other arbitrary values of "positive" mean strain, Fig. 9. Note that mean strain, a positive quantity, must be measured relative to the reference axes with origin at 0'. It is assumed that low cycle fatigue resistance resulting from such conditions may be predicted by combining the separate effects of compressive prestrain and variable mean strain into the single relationship:

$$N_f = \left[\frac{\epsilon_f - \frac{\Delta\epsilon_p}{\Delta\epsilon_t}(\epsilon_r^{pc} + \epsilon_m)}{\Delta\epsilon_t}\right]^{1/m} \tag{3.16}$$

For fatigue studies in which the specimen type and cyclic test conditions differ from those used to determine the simple tensile test properties, better extrapolation to N_f = 1/4 cycle may be obtained by substituting an apparent ductility, ϵ_f', for the actual fracture strain, ϵ_f, in Eq. (3.16):

$$N_f = \left[\frac{\epsilon_f' - \frac{\Delta\epsilon_p}{\Delta\epsilon_t} (\epsilon_r^{pc} + \epsilon_m)}{\Delta\epsilon_t} \right]^{1/m} \tag{3.17}$$

Equations (3.16) and (3.17) are thus in a sufficiently general form to be directly applicable to the various cyclic conditions examined in this section. These relationships are compared with data obtained from the experimental program described in the next chapter and with other existing data.

IV. EXPERIMENTAL PROGRAM

A. Scope

The purpose of the experimental phase of this study was to establish the validity of the proposed hypothesis, Eq. (3.16), through a program of tests with titanium in which the applicable physical quantities could be examined. To determine the effect of precompression on tensile ductility, 8 specimens were first subjected to varying amounts of axial plastic precompressive strain, and then tested to failure in static tension. Fatigue studies were conducted on specimens initially in an undeformed condition and on others first subjected to precompression (two levels of compressive prestrain were studied). For each of these three conditions, the specimens were axially cycled at controlled strain ranges for strain ratios of 0 and 1/2. A number of initially uncompressed specmens were also tested at R = 3/4. In all, a total of 30 cyclic fatigue specimens were tested in the investigation.

B. Material, Equipment, and Testing Procedures

1. Material Description and Specimen Preparation

The material used in the experimental program, a commercially pure titanium (manufacturer's designation RS-70), was supplied by the U. S. Navy Marine Engineering Laboratory, Annapolis, Maryland. The material was furnished in plate form, 8 in. x 30 in. x 2 in. thick. The chemical composition of the titanium is as follows:

Titanium RS-70
Chemical Composition, percent

Fe	C	N	H_2	O_2
0.09	0.03	0.007	0.0073	0.317

Details of the test specimens are shown in Fig. 10. The specimens have a 1 in. taper radius and a diameter of 1/2 in. at the minimum cross-section. The specimen blanks were cut from the parent plate with the 1-1/2 in. dimension of the specimen being obtained by milling down the 2 in. plate thickness. The longitudinal axis of each specimen was parallel to the rolling direction of the plate. Since it has been demonstrated that the static fracture strain will vary with specimen geometry,[39] the tensile properties applicable to the hypothesis were obtained from the same specimen configuration used in the fatigue tests.

Use of the hourglass-shaped specimens requires further explanation. "Ductile-type" failures obtained in very low cycle fatigue tests result from large localized plastic deformations in the test material. In a cylindrical test specimen the initiation of such a fracture will occur as a consequence of necking at a critical section along the specimen axis. It is difficult to predict the exact point of origin of necking or to obtain a satisfactory direct measurement of the localized longitudinal strains in that region. By using tapered specimens, however, the region of greatest deformation is concentrated at the minimum cross-section where measurements of diameter change are easily performed. The diametral and longitudinal strains can then be calculated directly from these measured values, as explained subsequently. It should be remembered that even such "true" strain (and "true" stress) calculations are only average values in that variations through the cross-section are not considered.

After the specimen blank had been cut, the test section was machined to the proper configuration. The ends of the specimen were "squared-off" perpendicular to the longitudinal axis and the holes drilled through the pull-heads.

The test section of each specimen was polished using Nos. 120, 220, and 320 emery cloth in that order, followed by a finishing polish with crocus cloth. Each polishing cloth was attached in turn to a slotted bar inserted in an electrical hand drill operating at 3500 rpm. The drill was installed in an adjustable frame which could be manipulated so that a 1/2 in. section of polishing cloth, protruding from the slotted bar, would brush the specimen surface. At the same time, the specimen was rotated in the lathe operating at 250 rpm. All polishing was accomplished in the longitudinal direction of the specimen.

2. Equipment

The apparatus for this investigation included the equipment necessary to apply load to the specimens during the static and fatigue tests; and devices designed specifically for measurement of specimen dimensions before and during testing. Much of this apparatus had originally been constructed for an earlier low cycle fatigue study at the University of Illinois.[36]

The initial diameter at the minimum cross-section of the test specimen was measured with the traveling microscope arrangement shown in Fig. 11. The specimen was first positioned in a movable grip which aligned the test section directly beneath the microscope lenses. The microscope, mounted on a geared traveling table, was focused at one edge of the specimen diameter and then traversed to the opposite edge. At each extreme, a reading was taken on a 0.0001 in. dial gage positioned to follow the traveling microscope. The procedure was then repeated with the microscope being traversed in the opposite direction. The diameter was recorded as the average of the two measurements thus obtained. To obtain an indication of roundness, the specimen was rotated

in the grip and other series of diameter measurements recorded. For most of the specimens, the out-of-roundness was less than 0.0005 in.

The device pictured in Fig. 12 was used to continuously measure variations in specimen diameter during both the static and cyclic tests. This diameter gage consists of a rectangular aluminum frame with mounts housing polished plexiglass probes attached at the center of the long axis. Eight Metalfilm C12-121 type strain gages were cemented to the rectangular frame adjacent to the probes. This arrangement provided a linear relationship between the output of the gages and variations in the opening between probe points. The constant of proportionality was found by calibration to be 7.4×10^{-5} in. separation between probe points for each μin.-per-in. output of the strain gages. When positioned at the minimum diameter of the test specimen, the gage thus provided continuous monitoring of diameter changes which in turn permitted the desired control over diametral strains.

A 60,000-lb. hydraulically-operated universal testing machine, Fig. 13, was used to subject specimens to precompression, and for the static tensile fracture tests. In addition, this machine was used for those cyclic tests in which the controlled strain ranges were sufficiently large to cause failure within about 10 cycles.

For the precompressive straining operation, the loading-head and "sleeve" assembly shown in Fig. 14 was utilized. After placing studs in the holes of the specimen heads, the specimen was centered in the slotted heads with brass shims to insure a close fit. Next the sleeve, coated with powdered graphite to prevent binding, was placed over the assembly. The purpose of the sleeve was to prevent buckling of the specimen when subjected to large plastic compressive strains. The entire assembly was then centered on the lower platen of the universal testing machine, Fig. 15, and the desired loads applied.

The same loading-heads, fitted with threaded adaptors for bolting into the testing machine, were also utilized as pull-heads for the static tension tests as shown in Fig. 16. The tensile loads were applied through a pin-connection system provided by passing hardened steel rods through the drilled specimen holes and seating them in receptacles in the pull-heads. In analogous manner, this equipment was used to apply the cyclic loadings for those specimens failing in less than 10 cycles. The sleeve was again used for each compression application to protect against specimen buckling.

For those specimens in which the cyclic strain ranges resulted in failures greater than 10 cycles, a 50,000-lb. Illinois fatigue testing machine, Fig. 17, was employed. There is a 10.5 to 1 force multiplication transmitted between the eccentric and the test specimen by the walking beam. The eccentric, which controls the cyclic displacement of the walking beam, is varied by means of the power operated quadrant control. To apply the tensile and compressive loads to the test specimen, specially constructed[36] pull-heads were adapted to the fatigue machine. The tensile loads were transmitted through bolts pin-connecting these pull-heads to the specimen in a manner similar to that described for the static test arrangement. To apply the compressive forces, a set of adjustable wedge blocks located within the pull-heads were tightened down on the ends of the test specimen. To eliminate as much eccentricity as possible, the bolts and wedge blocks were tightened during the first tensile load application. A photograph of the pull-head apparatus is shown in Fig. 18. The same equipment is shown in Fig. 19 with the specimen and rectangular diameter gage in place.

3. Testing Procedures

(a) Static Precompression and Tension Tests

The 60,000-lb. testing machine was used to precompress the specimens and to perform the static tension tests. A specimen to be precompressed was

first machined and polished using the procedure outlined above. It was then assembled in the special loading-head and sleeve apparatus and placed under load in the testing machine. The desired compressive strain was obtained with the aid of an L-shaped fixture to which a 0.0001 in. diameter gage was mounted. This device was passed through an opening in the sleeve and hooked around the specimen at the minimum section. The application of load was stopped when the gage indicated that the test section had expanded to the proper predetermined diameter. It should be noted that this provided only an approximate indication of the precompressive strain as the titanium was slightly anisotropic and deformed into an ellipse upon loading. To obtain a more accurate measurement, the precompressed specimen was removed from the testing apparatus and the final major and minor axes measured with the traveling microscope. These dimensions were then used to compute an "average" precompressive plastic strain, ϵ_{pc}, based on the change in cross-sectional area relative to the undeformed state.*

The precompressed specimens, an example of which is shown in Fig. 20 beside an undeformed specimen, were then remachined to the original 1/2 in. diameter and polished as before. This was done to restore the initial specimen geometry and surface finish before further testing in either static tension or fatigue.

All the static tension tests were conducted in the universal testing machine. The specimens, either undeformed or precompressed and repolished as described above, were installed in the tensile pull-heads which were then bolted

---

* Using ratios of major to minor axis obtained from the precompressed specimens and from subsequent static tensile tests, it was possible to establish a relationship between these ratios and the corresponding diametral strains. Applying this information to the cyclic tests which followed, it was then necessary to monitor only changes in the major axis to control a desired strain range. The procedure for computing diametral strains from the measured quantities and of converting them to corresponding true longitudinal strains is described in Appendix B.

to the testing machine, Fig. 16. The diameter gage was positioned at the minimum specimen diameter with the plane of the rectangular frame perpendicular to the longitudinal axis of the specimen. The gage probes were placed in line with the direction of the major axis (when deformed) of the specimen cross-section. During the test, both the load and diameter gage output were continuously monitored. Readings were taken at uniform load increments in the elastic region and at uniform increments of diameter change beginning with the onset of plastic deformation. The ultimate load and approximate fracture load were also recorded. It was impossible to obtain an exact load measurement at the instant of fracture as the load was dropping rapidly by that time. After failure, the final major and minor axes at the fractured section were measured with the traveling microscope. The true total fracture strain, ϵ_f or ϵ_f^{pc}, was then computed from these measurements adjusted to include the elastic rebound. The remainder of the stress-strain diagram was obtained from the load and diameter gage readings. True stresses were calculated using the areas determined from the instantaneous cross-sectional dimension measurements.

(b) Cyclic Controlled-Strain Tests

Several cyclic tests at total strain ranges resulting in very low lives (< 10 cycles) were conducted in the universal testing machine. The apparatus and test procedure were generally the same as in the static tests, the loading in this case being reversed as the desired diameter limits were attained. Although it was a simple process to control the tensile strain limit from the diameter gage output, application of compressive strain was somewhat more difficult to regulate. The method of compressive strain control described earlier resulted in diameter variations as large as a few thousandths of an inch from cycle to cycle. The diameter measurements were therefore checked on the

traveling microscope after each half cycle; the cyclic total strain range for the complete test was reported as the average of all cycles. The slight variations from cycle to cycle were actually of little consequence, however, as they represented only small fractions of the total strain ranges involved in these tests ($\Delta\epsilon_t > 0.06$).

The majority of the fatigue tests were conducted in the 50,000-lb. Illinois' fatigue testing machine. The specimen to be cycled was fastened in the pull-heads with the diameter gage attached at the minimum specimen diameter, Fig. 19. The leads from the diameter gage and from the fatigue machine weighbar were connected either directly to SR-4 strain indicators or to a suitably scaled X-Y recorder. Using either system it was possible to control the diametral deformations corresponding to the required total strain range and to record the tensile and compressive loads for each cycle. The specimens (except for three tested at $\Delta\epsilon_t < 0.015$) were then cycled manually, with the loading direction being reversed each time the limiting diameters were reached. The loading direction was reversed immediately upon attaining the appropriate diameter to reduce the possibility of creep at the high stresses and strain ranges studied. The rate of testing varied from about 1/2 to 2 cycles per minute, depending upon the particular strain range. At these speeds, there was no significant temperature change in the specimen during the course of cycling, a factor which can materially affect the fatigue behavior. Cycling was continued to complete specimen failure (separation), the final cycle in each case being accompanied by a loud report as the specimen fractured.

The three specimens tested at $\Delta\epsilon_t < 0.015$ (with corresponding lives beyond 500 cycles) were manually cycled as above for the first 50 cycles. By this time a stable hysteresis loop had been well established. The specimen was

then power cycled using a geared speed reduction system which reduced the normal operating rate of the fatigue machine to 20 cycles per minute. The cycling was continued until there was a noticeable change in the strain and load readings indicating possible fatigue crack growth in the test specimen. At this point the strain range was readjusted and the specimen again hand cycled to complete failure.

V. PRESENTATION AND ANALYSIS OF TEST RESULTS

A. Test Results

1. Static Precompression and Tension Tests

A series of 8 specimens were tested to fracture in static tension. Two of the specimens were tested in the virgin state while the others were first subjected to plastic precompressive strains varying from -0.094 to -0.467. The data from these tests are presented in Table 1. The true stress-true strain diagram for each condition of precompression is shown in Fig. 21. It can be seen that severe compressive prestraining decreased the fracture strain while raising the yield condition. For the virgin material, the static fracture strain, ϵ_f, was 0.473 (average of two specimens); for the maximum precompressive strain of -0.467, the fracture strain was reduced to 0.143. Note, on the other hand, that the true stress at fracture was not appreciably altered by the initial compression.

The fracture appearance of specimens subjected to plastic precompressive strains of 0, -0.162, and -0.321 are pictured in the top row of Fig. 22. All of the specimens exhibited coarse, irregularly contoured fracture surfaces with a distinct shear lip along the circumference. The elliptical shape of the cross-section was also discernible.

2. Cyclic Controlled-Strain Tests

A total of 30 specimens were tested in fatigue. The tests were divided into three groups corresponding to specimens either initially undeformed or subjected to an average precompressive strain of -0.167 or -0.323. Specimens from each of these three groups were then cycled at various constant total

strain ranges, $\Delta\epsilon_t$, and strain ratios, R, of 0, 1/2, and 3/4. (Only specimens not subjected to precompression were tested at R = 3/4.) A schematic diagram illustrating each of the various cyclic test sequences is shown in Fig. 23.

The data for the cyclic tests are presented in Tables 2, 3, and 4. The true longitudinal (normal to plane of initial circular specimen cross-section) strains reported in these tables were calculated from the actual diametral measurements using the procedure detailed in Appendix B. Comparison of the controlled strain ranges and mean strains will show that the listed strain ratios, R, are nominal values with slight deviations from specimen to specimen. These deviations are partly a result of establishing the ratios on the basis of the originally prescribed diametral strains instead of the longitudinal values. Further, the difficulty in controlling the maximum compressive strains for those specimens tested in the universal machine (noted in the tables) also resulted in values of R differing slightly from the desired limits. The listed nominal values are, however, sufficient for purposes of comparison between the test data and theoretical predictions.

The "stable" ranges of true stress reported in the tables are defined in most cases as the conditions existing at half the specimen fatigue life. For certain specimens, tested at very large cyclic strains resulting in lives of less than five cycles, there was no indication of hysteresis stabilization before failure. For those specimens, the "stable" stress recorded is the magnitude at the last full cycle before fracture, this being considered more indicative of the condition necessary for fracture.

The complete stress histories of the fatigue specimens (with the exception of four specimens tested at small cyclic strains that showed only slight variations throughout their lives) are presented in Figs. 24, 25, and 26.

Certain general observations may be drawn from these curves, all plotted on a semi-log basis. The titanium studied, as with other materials, cyclically hardens or softens under controlled-strain testing, the amount being dependent upon conditions of initial prestrain (i.e., precompression and/or large mean strain values) and the magnitude of the cyclic strain range. For moderate strain ranges at $\epsilon_{pc} = 0$, the most pronounced changes in the stress range occurred early in the cyclic life, generally within the first 5 to 10 cycles. Thereafter, the rate of additional adjustment in the hysteresis contour decreased, the material eventually attaining a relatively stable condition with continued cycling.

The magnitude of the eventual stress range approached similar values for tests conducted at the same cyclic total strain range. Compare, for example, the specimens tested at $\Delta\epsilon_t = 0.04$ for precompressive strains of 0 and -0.167. The stable stresses differed by less than 15 ksi whereas the first cycle stress ranges for these specimens differed by as much as 40 ksi. However, for the two specimens tested at $\Delta\epsilon_t = 0.041$ after a precompression of -0.32, the high initial stresses did not soften to the lower stress levels before fracture occurred. Note the shorter fatigue lives of these two specimens relative to the others mentioned.

An indication of the degree of hardening or softening effected by strain cycling is furnished by the cyclic stress-strain diagrams shown in Figs. 27, 28, and 29 for the three conditions of precompression. Each point represents a measure of the statically applied stress and corresponding strain required to reach that state after $N_f/2$ complete cycles at a given $\Delta\epsilon_t$; i.e., the limiting tensile condition of a stress-strain diagram constructed after cycling to a stable hysteresis loop at $\Delta\epsilon_t$. Also plotted in these figures

are the static stress-strain relationships for specimens subjected to similar precompressive strains and tested in tension without cycling (extracted from Fig. 21). It can be seen that, for the initially uncompressed specimens, Fig. 27, all the cyclic data fall above the stress-strain curve of the virgin material, indicative of cyclic hardening during fatigue testing. In Figs. 28 and 29, however, there is little variation between the cyclic data and the static stress-strain relationship, attributed mainly to the severe initial hardening effect of the precompression. At the larger precompressive strain, Fig. 29, some of the points actually fall below the static curve, indicating some softening relative to the initial compressed state. All of the cyclic data, however, lie well above the stress-strain curve of the virgin material.

Examination of the fatigue lives reported in Tables 2, 3, and 4 reveals the decreasing influence of mean strain (for the strain ratios examined) at progressively smaller constant strain ranges. For each of the separate states of precompression, cyclic lives resulting from tests conducted at the different strain ratios converge below total strain ranges of approximately 0.04. The effect of precompression on fatigue resistance at constant $\Delta\epsilon_t$ is also quite evident, being manifested to a minimum of approximately 0.01 strain. These observations of fatigue behavior are more fully discussed in the following section concerned with analysis of the test results.

The modes of fracture observed for the fatigue specimens are also of interest. For those specimens tested at large strain ranges resulting in failures at less than about 20 cycles, the fracture surfaces are similar in appearance to static tensile test specimens. Examples of such failures are shown in the center row of Fig. 22. There is no visual evidence of typical fatigue crack initiation and propagation at or near the fracture surface. These specimens

failed suddenly after having exhausted their ability to resist the repeated gross plastic deformations and very high accompanying stresses.

At the opposite extreme are the specimens with fatigue lives well above 100 cycles. Two examples, specimens TL-13 and TL-23, are pictured in the bottom row of Fig. 22. Examination of the fractured specimens clearly reveals multiple hairline cracks in the vicinity of the test section, these cracks being randomly distributed on several planes around the polished specimen surface. At the circumference of the fracture surfaces a number of the small cracks eventually interconnected and continued to propagate through the remainder of the cross-section. The fracture surfaces are finely textured with striations faintly visible.

At intermediate lives, fatigue apparently occurs as the consequence of a combination of the two mechanisms outlined above. A typical example is specimen TL-24, Fig. 22. Although a number of fine cracks are present on the polished surface, the fracture itself is relatively coarse textured with a shear lip evident at the circumference, indicating either rapid propagation or sudden fracture.

B. Analysis of Results

1. Direct Application of Cyclic Stress-Strain Data

With the data from the experimental program, it is now possible to examine the applicability of the proposed relationship:

$$N_f = \left[\frac{\epsilon_f - \frac{\Delta\epsilon_p}{\Delta\epsilon_t} (\epsilon_r{}^{pc} + \epsilon_m)}{\Delta\epsilon_t} \right]^{1/m} \qquad (3.16)$$

For the pure titanium examined in this investigation, the true fracture strain, ϵ_f, was computed to be 0.473 from the average of two tests. The

relationship between plastic precompressive strain, ϵ_{pc}, and the corresponding reduction in ductility, ϵ_r^{pc}, may be reasonably approximated by a straight line, Fig. 30. The data for this curve is taken directly from Table 1. The linearity of the ϵ_{pc} - ϵ_r^{pc} curve, applicable to the titanium studied, should by no means be construed as necessarily valid for other materials (cf., data by Drucker et al.[35] and Yao[36]).

It should be noted, in Eq. (3.16), that the plastic component of the total strain range, $\Delta\epsilon_p$, is not an arbitrary variable; i.e., it is uniquely determined in a fatigue test by the prescribed magnitude of $\Delta\epsilon_t$, ϵ_m, and ϵ_r^{pc} (or ϵ_{pc}). For the test conditions of the current investigation, the value of $\Delta\epsilon_p$ may be obtained from the stable cyclic stress-strain data presented in Figs. 27, 28, and 29. A more appropriate method of expressing this information is demonstrated by the log $\Delta\epsilon_t$-log $\Delta\epsilon_e/\Delta\epsilon_p$ curves in Figs. 31, 32, and 33. Using these coordinates, the relative order of magnitude of the strain range components are placed in proper perspective. The data for each strain ratio (at a particular precompression) lie sufficiently close to be represented by a single curve. Note also that for large total ranges of strain, the ratio $\Delta\epsilon_e/\Delta\epsilon_p$ is essentially the same regardless of the amount of precompressive strain. The solid lines in these figures are used to determine the value of $\Delta\epsilon_p$ in the theoretical relationship. This is accomplished as follows:

For a selected value of precompression and $\Delta\epsilon_t$, the corresponding cyclic elastic-plastic strain ratio, $\Delta\epsilon_e/\Delta\epsilon_p$, is obtained from the curve in the appropriate figure. This value is then combined with Eq. (3.1) to obtain the plastic strain component, $\Delta\epsilon_p$:

$$\Delta\epsilon_p = \frac{\Delta\epsilon_t}{1 + \left(\frac{\Delta\epsilon_e}{\Delta\epsilon_p}\right)\Big|_{\substack{\text{experimental} \\ \text{curve}}}}$$

For those tests in which the specimens were not subjected to pre-compressive strains, Eq. (3.16) reduces to:

$$N_f \Big|_{(\epsilon_{pc} = 0)} = \left[\frac{0.473 - \frac{\Delta\epsilon_p}{\Delta\epsilon_t}(\epsilon_m)}{\Delta\epsilon_t}\right]^{1/m} \tag{5.1}$$

Since the strain ratio, R, rather than the mean strain per se, was controlled in the fatigue tests, ϵ_m may be replaced by its equivalent in Eq. (5.1):

$$N_f \Big|_{(\epsilon_{pc} = 0)} = \left[\frac{0.473 - \frac{\Delta\epsilon_p}{2}\left(\frac{1 + R}{1 - R}\right)}{\Delta\epsilon_t}\right]^{1/m} \tag{5.2}$$

The basic relationship thus appears directly in terms of the arbitrarily altered test parameters, $\Delta\epsilon_t$ and R. Using the information from Fig. 31 to estimate $\Delta\epsilon_p$, and by suitable curve fitting (between approximately 1 and 10^2 cycles) of the data from the tests performed at R = 0, a value of 1.8 was determined for the exponent 1/m. With this exponent, Fig. 34a shows that reasonably close agreement is obtained between the cyclic data for initially uncompressed specimens at nominal strain ratios of 0, 1/2, and 3/4, and the results predicted by Eq. (5.2). The theoretical curves clearly demonstrate the decreasing detrimental influence of mean strain on fatigue behavior at small total strain ranges, although the data indicate this effect disappeared at a somewhat shorter life than predicted. It can also be seen that, at the longer

fatigue lives, the data lie above the theoretical line, an indication of the aforementioned "transition zone" between low cycle and long life behavior.*

In accordance with the usual method of plotting fatigue data, and to more clearly distinguish the results, the predicted curves are presented with the cyclic maximum strain, ϵ_{max}, rather than $\Delta\epsilon_t$ as the ordinate, Fig. 34b. These curves were obtained by expressing $\Delta\epsilon_t$ in terms of ϵ_{max} and R, and by direct substitution into Eq. (5.2):

$$N_f \Big|_{(\epsilon_{pc} = 0)} = \left[\frac{0.473 - \frac{\Delta\epsilon_p}{2}\left(\frac{1 + R}{1 - R}\right)}{\epsilon_{max}\,(1 - R)}\right]^{1.8} \tag{5.3}$$

The reduction in static tensile ductility, ϵ_r^{pc}, due to a precompressive strain of -0.167, Fig. 30, is 0.120. Introducing this value into the basic fatigue life expression, Eq. (3.16) becomes:

$$N_f \Big|_{(\epsilon_{pc} = -0.167)} = \left[\frac{0.473 - \frac{\Delta\epsilon_p}{\Delta\epsilon_t}\,(0.120 + \epsilon_m)}{\Delta\epsilon_t}\right]^{1.8} \tag{5.4}$$

where the exponent 1.8 is assumed to be the same as that for the initially uncompressed specimens. The ratio $\Delta\epsilon_p/\Delta\epsilon_t$ is determined from the solid line in Fig. 32 for the range of $\Delta\epsilon_t$ examined.

As discussed above, Eq. (5.4) may be expressed in terms of the cyclic maximum strain and the strain ratio:

$$N_f \Big|_{(\epsilon_{pc} = -0.167)} = \left\{\frac{0.473 - \frac{\Delta\epsilon_p}{\Delta\epsilon_t}\left[0.120 + \epsilon_{max}\left(\frac{1 + R}{2}\right)\right]}{\epsilon_{max}\,(1 - R)}\right\}^{1.8} \tag{5.5}$$

---

* To illustrate this transition behavior, a comparison between the current low cycle data and long life fatigue information for commercially pure titanium, reported by Weinberg and Hanna,[50] is presented in Appendix C.

Equation (5.5) is compared in Fig. 35 with the data for the specimens precompressed to an average strain of -0.167 (Table 3). The curves represent the predicted lives for strain ratios of 0 and 1/2. The point on the strain axis at N_f = 1/4 cycle is for specimen TL-3, which was tested in static tension to a fracture strain of 0.357 after being initially compressed to a strain of -0.162, Table 1. The curves are seen to satisfactorily demonstrate the general fatigue behavior, although the deviation between theory and data is somewhat greater than for the uncompressed specimens.

For the group of specimens subjected to an average initial compressive strain of -0.323, the corresponding reduction in static ductility is 0.233, Fig. 30. Using this value of ϵ_r^{pc} in the fatigue life relationship, Eq. (3.16), and by rearranging the variables as before:

$$N_f = \left\{ \frac{0.473 - \frac{\Delta\epsilon_p}{\Delta\epsilon_t}\left[0.233 + \epsilon_{max}\left(\frac{1+R}{2}\right)\right]}{\epsilon_{max}(1-R)} \right\}^{1.8} \qquad (5.6)$$

$(\epsilon_{pc} = -0.323)$

The $\Delta\epsilon_p/\Delta\epsilon_t$ ratios are obtained from the solid line of Fig. 33. A comparison of Eq. (5.6) with the data from Table 4 is represented by the solid curves of Fig. 36. These curves again show a good correlation with the experimental results for both strain ratios examined, R = 0, 1/2. The static tensile ductility is represented in the figure by the fracture strain of specimen TL-8, Table 1.

Finally, Fig. 37 illustrates the convergence of the fatigue life curves for the three values of precompressive strain as predicted by Eq. (3.16). The curves, using $\Delta\epsilon_t$ as the ordinate, are compared with the experimental data for R = 0. Similar convergent curves may be obtained for the other strain

ratios as well. Note that the predicted values are all conservative at the lowest strain ranges corresponding to the transition region between low cycle and long life fatigue behavior.

2. Use of Approximate Relationships

The major disadvantage of the proposed fatigue life relationship is that, for each value of the variable total strain range, the corresponding magnitude of its plastic component (or the ratio $\Delta\epsilon_p/\Delta\epsilon_t$) must be known. These data can only be obtained from actual cyclic measurements by tracing the stress history from tests performed under each individual condition of mean strain and precompression to be evaluated. Obviously, it is far more desirable to be able to predict the entire spectrum of low cycle fatigue behavior based on a minimum of static and cyclic tests. The static tests are required to establish the effect of precompressive strain on the monotonic fracture ductility of the material studied. A sufficient number of tensile tests must, therefore, be performed on initially compressed specimens to obtain a continuous $\epsilon_{pc} - \epsilon_r^{pc}$ curve such as that shown in Fig. 30.

It is possible, on the other hand, to considerably reduce the number of necessary fatigue tests. It may be recalled that the exponent 1/m was determined in this investigation from the fatigue data for $\epsilon_{pc} = 0$, R = 0 alone, the calculated value providing reasonably close agreement between theory and experiment for the other test conditions. It can be shown that the cyclic stress data from these same tests, representing just 6 of the 30 fatigue specimens, can also be satisfactorily used to approximate the ratio $\Delta\epsilon_p/\Delta\epsilon_t$ in Eq. (3.16) for the various states of precompression and mean strain.

Referring again to Figs. 31, 32, and 33, it was noted earlier that the ratio $\Delta\epsilon_e/\Delta\epsilon_p$ is essentially the same in all cases for values of $\Delta\epsilon_t$ above

approximately 0.06. (The dashed lines in Figs. 32 and 33 represent, for purposes of comparison, the curve for $\epsilon_{pc} = 0$, Fig. 31.) This is a result of the severe hardening accompanying the larger cyclic strains, with peak stresses approaching the static fracture stress, even in initially undeformed specimens. At lower total strain ranges the three curves diverge slightly, with the line for $\epsilon_{pc} = 0$ representing the softest cyclic conditions, i.e., lowest $\Delta\epsilon_e$ or $\Delta\sigma_s$ for a particular $\Delta\epsilon_t$.* If continued, these curves would again converge for completely elastic reversals.

The values of $\Delta\epsilon_p$ calculated from the curve for $\epsilon_{pc} = 0$, Fig. 31, were then applied to Eqs. (5.5) and (5.6) to predict the fatigue behavior for the other two levels of precompression. Using these values, the dashed lines in Fig. 36 were obtained. For the specimens precompressed to -0.167 strain, Fig. 35, the divergence of the approximate curves from the original was too slight to be clearly distinguishable.

Since the values of $\Delta\epsilon_p$ computed from the curve for $\epsilon_{pc} = 0$ were larger than those obtained from the actual cyclic data for the precompressed specimens, use of these approximate values resulted in conservative deviations from the original fatigue life predictions.** The actual differences were found to be minor, however, as the $\Delta\epsilon_p/\Delta\epsilon_t$ ratios (and, consequently, the relative weight of ϵ_r^{pc} and ϵ_m) become small in the range for $\Delta\epsilon_t < 0.06$.

The above method of estimating the $\Delta\epsilon_p/\Delta\epsilon_t$ ratio in Eq. (3.16) is equally applicable to other materials and test conditions. The values of $\Delta\epsilon_p$

---

* The softest hysteresis conditions would probably be found in cyclic tests performed on the virgin material at R = -1 as this represents the state of zero prestrain.

** It should be realized that such approximations are not necessarily conservative, however, if fatigue life is to be compared to $\Delta\epsilon_p$ rather than $\Delta\epsilon_t$ using the same equations.

can be obtained from the cyclic stress-strain curves representative of the softest stable cyclic conditions, usually for complete reversal tests with no prestrain.

To conclude this analysis of the commercially pure titanium investigated herein, the important observations discussed above may be condensed as follows:

(1) For lives to approximately 1000 cycles, the proposed fatigue life relationship, Eq. (3.16), satisfactorily predicts fatigue behavior at the various conditions of strain ratio and precompression examined.

(2) The exponent of this expression, $1/m = 1.8$, determined from the test data for $\epsilon_{pc} = 0$, $R = 0$, is similarly applicable to other conditions of prestrain, both tensile and compressive.

(3) When fatigue life is compared to the total strain range, the ratio $\Delta\epsilon_p/\Delta\epsilon_t$ in Eq. (3.16) may be conservatively approximated by data obtained from the cyclic stress-strain curve representing the softest stable cyclic conditions; in this case, for $\epsilon_{pc} = 0$, $R = 0$.

C. Correlation with Existing Data

Considerable information is presently available regarding the low cycle fatigue behavior of aluminum. In a study reviewed earlier, D'Amato[39] presented a comprehensive examination of the effect of large plastic mean strains on the low cycle resistance of aluminum alloy 2024-T4. The data were obtained from axial tests of hourglass-shaped specimens with taper radius of 1-1/2 in. and minimum test section diameter of 0.357 in.

The results of the fatigue tests are reproduced in Table 5. The listed values of cycles to failure, N_f, differ slightly from those reported by D'Amato because of a difference in the method of interpreting the first tensile

strain application. D'Amato considered this initial tensile strain as one cycle whereas it has been recorded as 1/4 cycle for the purposes of the current analysis. The variation is of little consequence, however, beyond approximately 10 cycles to failure.

Also from Table 5, it is seen that three specimens were tested at a cyclic mean strain of -0.075. In order to remain consistent with the present hypothesis, these tests are analyzed as cycling about a zero mean strain following a precompressive strain of -0.075; i.e., $\epsilon_{pc} = -0.075$ and $\epsilon_m = 0$. Furthermore, as there are no results presented for the static tensile fracture strain following a precompression of -0.075, the assumption is made that there was no loss of ductility due to the relatively small compressive prestrain. Thus, for this particular case, it is assumed that $\epsilon_f^{pc} = \epsilon_f$, or $\epsilon_r^{pc} = 0$.

From the static stress-strain diagram for two specimens with a taper radius of 1-1/2 in., the average fracture strain, ϵ_f, is estimated as 0.375 with a corresponding true fracture stress, σ_f, of 104 ksi. Introducing this value of ϵ_f into the fatigue life expression, Eq. (3.16):

$$N_f = \left[\frac{0.375 - \frac{\Delta\epsilon_p}{\Delta\epsilon_t}(\epsilon_m)}{\Delta\epsilon_t}\right]^{1/m} \tag{5.7}$$

From the data presented in Table 5, the curve representing the cyclic elastic-plastic strain ratio for the range of values of $\Delta\epsilon_t$ at $\epsilon_m = 0$ is shown in Fig. 38. The same ratio for the other values of mean strain is presented in Fig. 39, together with the curve for zero mean strain. It can be seen that the data for $\epsilon_m = 0$ represent the softest stable cyclic hysteresis conditions, all the other points falling on or above the dashed curve in Fig. 39. It was possible, therefore, to use this single curve to obtain conservative estimates

of $\Delta\epsilon_p$ for each corresponding total strain range and all mean strains when applied to Eq. (5.7).

The low cycle fatigue lives predicted by Eq. (5.7) are compared with the data in Fig. 40a. The slope of the linear log $\Delta\epsilon_t$-log N_f curve corresponding to the condition of zero mean strain was found to be best represented by the exponent $1/m = 2.2$. Using this value, an excellent correlation is observed between theory and data to approximately 1000 cycles for mean strains of 0, -0.075, 0.075, and 0.135. (Since ϵ_r^{pc} was assumed to be zero for $\epsilon_m = -0.075$, the predicted lives for this condition would be the same as for zero mean strain.) For the most severe mean strain condition, $\epsilon_m = 0.275$, the predicted curve, although correctly representative of the basic behavior pattern, is somewhat unconservative at very low lives. At lives beyond 1000 cycles, however, the convergence of the data for all values of mean strain clearly demonstrates the decreasing influence of even the largest mean strains (prestrains) on low cycle fatigue resistance. Note also that the data lie above the predicted values in this region, a condition indicative of the transition between low cycle and long life fatigue behavior.

The test results and predicted curves are also presented in Fig. 40b using the cyclic maximum strain, ϵ_{max}, as ordinate. The nature of these curves is such that the deviation between theory and data for $\epsilon_m = 0.275$ is not clearly discernible. The curves do, however, satisfactorily indicate the differences between the various conditions of mean strain.

Based on this examination of the data of D'Amato for aluminum, it is anticipated that the fatigue life relationship proposed herein may be equally applicable to other ductile metals subjected to similar conditions of prestrain and fatigue cycling. Until further information is available, however, it should

not be presumed that these fatigue behavior predictions are valid when other test conditions (corrosive atmosphere, elevated temperatures, etc.) are introduced into the cyclic program in addition to variable mean strain.

VI. SUMMARY AND CONCLUSIONS

A. Summary

The purpose of this study has been to evaluate the effect of large plastic prestrains, both tensile and compressive, on the low cycle fatigue behavior of a ductile material subjected to conditions of controlled-strain cycling. Based on information currently available in the literature, the following general relationship was developed, which quantitatively relates the governing test variables to the observed ability of a material to resist failure by fatigue:

$$N_f = \left[\frac{\epsilon_f - \frac{\Delta\epsilon_p}{\Delta\epsilon_t} \left(\epsilon_r^{pc} + \epsilon_m \right)}{\Delta\epsilon_t} \right]^{1/m}$$

where N_f = number of applied cycles to failure

ϵ_f = static tensile fracture strain

ϵ_r^{pc} = reduction in static ductility as a result of precompression

ϵ_m = cyclic mean strain

$\Delta\epsilon_t$ = cyclic constant total strain range

$\Delta\epsilon_p$ = plastic component of the cyclic total strain range

$1/m$ = a constant, considered a material fatigue property

To support the hypothesis, the fatigue behavior of a commercially pure titanium, RS-70, was investigated. A number of polished, hourglass-shaped specimens were initially subjected to axial plastic compressive strains of various magnitudes. Subsequent static tensile fracture tests performed on these

specimens revealed that the loss of ductility resulting from precompression was directly proportional to the magnitude of the applied compressive strain.

Axial controlled-strain fatigue tests were then conducted on specimens of the virgin titanium and on specimens subjected to average precompressive strains of -0.167 and -0.323. The tests were performed at nominal strain ratios, R, of 0, 1/2, and 3/4 to introduce the additional parameter of variable positive mean strain into the cyclic program. The cyclic constant total strain ranges varied from 0.01 to a maximum of approximately 0.2.

For a particular condition of precompression and large total range of strain (> 0.04), an increase in mean strain (or strain ratio) was accompanied by a proportionate reduction in fatigue life. As the constant total strain range was decreased, however, the detrimental influence on fatigue behavior of the positive strain ratios examined was gradually reduced, and became insignificant for strains below 0.04.

The initial hardening effects of the large precompressive strains were also accompanied by decreased fatigue resistance relative to that of the virgin material in the low cycle fatigue region. With continued cycling at the lower constant strain ranges, however, the precompressed material was observed to progressively soften, with the height of the eventual stable hysteresis loop being lower than that for the first strain reversals. As these adjustments were able to develop at the smaller ranges of strain, it was found that the resultant fatigue life curves approached convergence independent of the magnitude of the precompressive strain.

Comparison of the titanium test data with fatigue lives predicted by the proposed expression resulted in reasonably close agreement, at lives to approximately 10^3 cycles, for all values of precompression and strain ratio

examined. An exponent $1/m = 1.8$, determined from the data for virgin specimens cycled at $R = 0$, was applicable as well to the other conditions of prestrain.

The hypothesis was further compared with data obtained from a previous investigation of another ductile material, aluminum alloy 2024-T4. The data were for controlled-strain axial fatigue tests conducted at 6 separate conditions of cyclic mean strain. There was again close agreement between the test results and predicted lives for all but the most severe mean strain condition. The theory did, however, adequately demonstrate the decreasing effect of mean strain on fatigue behavior at the lower total ranges of strain. For the particular aluminum alloy examined, the exponent $1/m = 2.2$ was determined by the constant slope of the log $\Delta\epsilon_t$-log N_f curve for zero mean strain.

B. Conclusions

On the basis of the studies reported herein, the following conclusions have been drawn:

The low cycle fatigue behavior of a ductile material subjected to uniaxial controlled-strain cycling about a zero mean strain may be described by a linear relationship between the cyclic total strain range and the number of applied cycles to failure. This relationship is valid to a maximum life of approximately 10^3 cycles, the failure curve assuming a more gradual slope in the long life fatigue region. The intercept of the log $\Delta\epsilon_t$-log N_f curve on the strain axis, representing a single tensile strain application (static tension test), is closely related to the true fracture ductility of the material. This is valid when the test environment and specimen configuration are the same for both the static tension and the cyclic tests.

As a result of subjecting the material to severe plastic prestrains, either tensile or compressive, the static tensile fracture strain is reduced in

proportion to the amount of initial straining. This decrease in reserve ductility is also manifested by a reduction in low cycle fatigue resistance (relative to the fatigue behavior of the virgin material) for specimens tested at large constant strain ranges associated with gross cyclic plastic deformations. The adverse influence on fatigue life of a prestrain application gradually diminishes at smaller constant ranges of strain, however, as continued cycling produces adjustments in the hysteresis loop to stable stress levels resembling those of initially undeformed specimens. Finally, as the applied cyclic strains approach completely elastic reversals, the resultant fatigue lives (based on the cyclic total strain range) are found to be essentially unaltered by prestraining. This fatigue behavior in the low cycle region may be satisfactorily represented by the relationship:

$$N_f = \left[\frac{\epsilon_f - \frac{\Delta\epsilon_p}{\Delta\epsilon_t} (\epsilon_r^{pc} + \epsilon_m)}{\Delta\epsilon_t} \right]^{1/m}$$

The exponent $1/m$ is considered a material fatigue property which should be determined from the results of actual fatigue tests. For use in the above expression, the plastic component of the total strain range, $\Delta\epsilon_p$, may be conservatively estimated from the cyclic stress-strain relationship representative of the softest stable cyclic hysteresis conditions for the particular material.

The validity of the hypothesis has been supported by low cycle fatigue data obtained for controlled-strain tests of commercially pure titanium, RS-70, and an aluminum alloy, 2024-T4. A satisfactory correlation was found to exist in both materials for most conditions of prestrain to lives approaching a maximum of 10^3 cycles to failure. Based on these observations, it is anticipated

that similar agreement is possible for other ductile materials tested under like cyclic conditions. Of course, it is advisable to examine the behavior of a number of materials as further confirmation of the fatigue evaluations presented in this study.

LIST OF REFERENCES

1. Wood, W. A., "Some Basic Studies in Fatigue in Metals," Conference on Fracture, M. I. T. Technology Press, April 1959.

2. Grover, H. J., Gordon, S. A., and Jackson, L. R , Fatigue of Metals and Structures, Bureau of Aeronautics, Department of the Navy, 1960.

3. Smith, J. O., "The Effect of Range of Stress on the Fatigue Strength of Metals," Engineering Experiment Station, Bulletin Series No. 334, University of Illinois, Urbana, Illinois, Feb. 1942.

4. Benham, P. P., "Fatigue of Metals Caused by a Relatively Few Cycles of High Load or Strain Amplitude," Metallurgical Reviews, vol. 3, no. 11, 1958.

5. Yao, J. T. P., and Munse, W. H., "Low-Cycle Fatigue of Metals - Literature Review," The Welding Journal, Research Supplement, April 1962.

6. Hartmann, E. C., and Stickley, G. W., "The Direct-Stress Fatigue Strength of 17S-T Aluminum Alloy Throughout the Range From 1/2 to 500,000,000 Cycles of Stress," N.A.C.A. Technical Note 865, Sept. 1942.

7. Weisman, M. H., and Kaplan, M. H., "The Fatigue Strength of Steel Through the Range From 1/2 to 30,000 Cycles of Stress," Proceedings, A.S.T.M., vol. 50, 1950.

8. Smith, F. C., Brueggeman, W. C., and Harwell, R. H., "Comparison of Fatigue Strengths of Bare and Alclad 24S-T3 Aluminum-Alloy Sheet Specimens Tested at 12 and 1000 Cycles per Minute," N.A.C.A. Technical Note 2231, Dec. 1950.

9. Grover, H. J., Hyler, W. S., Kuhn, P., Landers, C. B , and Howell, F. M., "Axial-Load Fatigue Properties of 24S-T and 75S-T Aluminum Alloy as Determined in Several Laboratories," N.A.C.A. Technical Note 2928, May 1953.

10. Hardrath, H. F., Landers, C. B., and Utley, E. C., Jr., "Axial-Load Fatigue Tests on Notched and Unnotched Sheet Specimens of 61S-T6 Aluminum Alloy, Annealed 347 Stainless Steel, and Heat-Treated 403 Stainless Steel," N.A.C.A. Technical Note 3017, Oct. 1953.

11. Hardrath, H. F., and Illg, W., "Fatigue Tests at Stresses Producing Failure in 2 to 10,000 Cycles," N.A.C.A. Technical Note 3132, Jan. 1954.

12. Illg, W., "Fatigue Tests on Notched and Unnotched Sheet Specimens of 2024-T3 and 7075-T6 Aluminum Alloys and of SAE 4130 Steel with Special Consideration of the Life Range from 2 to 10,000 Cycles," N.A.C.A. Technical Note 3866, Dec. 1956.

13. Dubuc, J., "Plastic Fatigue under Cyclic Stress and Cyclic Strain, with a Study of the Bauschinger Effect," Ph.D. Thesis submitted to Ecole Polytechnique, Université de Montreal, Montreal, Canada, Jan. 1961.

14. Benham, P. P., and Ford, H., "Low Endurance Fatigue of a Mild Steel and an Aluminum Alloy," Journal of Mechanical Engineering Science, vol. 3, no. 2, June 1961.

15. Bell, W. J., and Benham, P. P., "The Effect of Mean Stress on the Fatigue of Plain and Notched Stainless Steel Sheet in the Range from 10 to 10^7 Cycles," Paper presented at Fourth Pacific Area National Meeting of A.S.T.M., Oct. 1962.

16. Liu, S. I., Lynch, J.J., Ripling, E. J., and Sachs, G., "Low Cycle Fatigue of the Aluminum Alloy 24S-T in Direct Stress," Transactions, A.I.M.E., vol. 175, 1948.

17. Pian, T. H. H., and D'Amato, R., "Low-Cycle Fatigue of Notched and Unnotched Specimens of 2024 Aluminum Alloy Under Axial Loading," W.A.D.C. Technical Note 58-27, Feb. 1958.

18. Coffin, L. F., Jr., and Tavernelli, J. F., "The Cyclic Straining and Fatigue of Metals," Transactions, Metallurgical Society of A.I.M.E., vol. 215, Oct. 1959.

19. Kommers, J. B., "Repeated Stress Testing," Proceedings VIth Congress of the International Association for Testing Materials, New York, 1912. See also, Moore, H. F., and Kommers, J. B., "An Investigation of the Fatigue of Metals," Engineering Experiment Station, Bulletin No. 124, University of Illinois, Urbana, Illinois, Oct. 1921.

20. Coffin, L. F., Jr., "A Study of the Effects of Cyclic Thermal Stresses on a Ductile Metal," Transactions, A.S.M.E., vol. 76, no. 6, Aug. 1954.

21. Baldwin, E. E., Sokol, G. J., and Coffin, L. F., Jr., "Cyclic Strain Fatigue on AISI Type 347 Stainless Steel," Proceedings, A.S.T.M., vol. 57, 1957.

22. Tavernelli, J. F., and Coffin, L. F., Jr., "A Compilation and Interpretation of Cyclic Strain Fatigue Tests on Metals," Transactions, A.S.M., vol. 51, 1959.

23. Tavernelli, J. F., and Coffin, L. F., Jr., "Experimental Support for Generalized Equation Predicting Low Cycle Fatigue," Journal of Basic Engineering, Transactions, A.S.M.E., vol. 84, series D, no. 4, Dec. 1962.

24. Raymond, M. H., and Coffin, L. F., Jr., "Geometric and Hysteresis Effects in Strain-Cycled Aluminum," Acta Metallurgica, vol. 11, no. 7, July 1963.

25. Low, A. C., "The Bending Fatigue Strength of Aluminum Alloy MG5 Between 10 and 10 Million Cycles," Journal of the Royal Aeronautical Society, vol. 59, July 1955.

26. Low, A. C., "Short Endurance Fatigue," International Conference on Fatigue of Metals, London, Sept. 1956.

27. Gross, M. R., "Low-Cycle Fatigue of Materials for Submarine Construction," U. S. Naval Engineering Experiment Station, Annapolis, Maryland, Research and Development Report 91 197D, Feb. 1963.

28. Wells, C. H., and Sullivan, C. P., "The Low-Cycle Fatigue Characteristics of a Nickel-Base Superalloy at Room Temperature," Transactions Quarterly, Transactions, A.S.M., vol. 57, no. 4, Dec. 1964.

29. Smith, R. W., Hirschberg, M. H., and Manson, S. S., "Fatigue Behavior of Materials Under Strain Cycling in Low and Intermediate Life Range," N.A.S.A. Technical Note D-1574, April 1963.

30. Morrow, J., and Tuler, F. R., "Low Cycle Fatigue Evaluation of Inconel 713C and Waspaloy," A.S.M.E. Paper No. 64-Met-15, presented at A.W.S.-A.S.M.E. Metals Engineering Conference, May 1964.

31. Nadai, A., Theory of Flow and Fracture of Solids, vol. 1, 2nd ed., McGraw-Hill Book Co. Inc., New York, 1950.

32. Bridgman, P. W., Studies in Large Plastic Flow and Fracture, McGraw-Hill Book Co. Inc., New York, 1952.

33. Liu, S. I., and Sachs, G., "The Flow and Fracture Characteristics of the Aluminum Alloy 24ST After Alternating Tension and Compression," Transactions, A.I.M.E., vol. 180, 1949.

34. Polakowski, N. H., "Restoration of Ductility of Cold-Worked Aluminum, Copper, and Low-Carbon Steel by Mechanical Treatment," Proceedings, A.S.T.M., vol. 52, 1952.

35. Drucker, D. C., Mylonas, C., and Lianis, G., "Exhaustion of Ductility of E-Steel in Tension Following Compressive Prestrain," The Welding Journal, Research Supplement, March 1960.

36. Yao, J. T. P., "The Effect of Plastic Strains on the Low-Cycle Fatigue Behavior of Steel," Ph.D. Thesis submitted to the Graduate College, University of Illinois, Urbana, Illinois, 1961.

37. Tuler, F. R., and Morrow, J., "Cycle-Dependent Stress-Strain Behavior of Metals," Theoretical and Applied Mechanics Report No. 239, University of Illinois, Urbana, Illinois, March 1963.

38. Liu, S. I., "Effects of Precompression on the Behavior of the Aluminum Alloy 24ST4 During Cyclic Direct Stressing," Journal of Metals, vol. 3, no. 6, 1951.

39. D'Amato, R., "A Study of the Strain-Hardening and Cumulative Damage Behavior of 2024-T4 Aluminum Alloy in the Low-Cycle Fatigue Range," W.A.D.D. Technical Report 60-175, April 1960.

40. Gerberich, W. W., "An Analysis of Several of the Variables Encountered in Low Cycle Fatigue," Metallurgical Engineering Dep't. Report No. MET575-596IT4, Syracuse University Research Institute, Syracuse, New York, June 1959.

41. Sachs, G., Gerberich, W. W., and Weiss, V., "Low Cycle Fatigue of Pressure Vessel Materials," Metallurgical Research Laboratories Report No. MET575-601IT5, Syracuse University Research Institute, Syracuse, New York, Jan. 1960.

42. Weiss, V., Sessler, J., and Packman, P., "Low Cycle Fatigue of Pressure Vessel Materials," Dep't. of Chemical Engineering and Metallurgy Report No. MET.E.575-662-F, Syracuse University Research Institute, Syracuse, New York, June 1962.

43. Weiss, V., Sessler, J., and Packman, P., "Effect of Several Parameters on Low Cycle Fatigue Behavior," Acta Metallurgica, vol. 11, no. 7, July 1963.

44. Orowan, E., "Stress Concentrations in Steel Under Cyclic Load," The Welding Journal, Research Supplement, vol. 31, no. 6, June 1952.

45. Manson, S. S., "Behavior of Materials Under Conditions of Thermal Stress," N.A.C.A. Technical Note 2933, July 1953.

46. Martin, D. E., "An Energy Criterion for Low-Cycle Fatigue," Journal of Basic Engineering, Transactions, A.S.M.E., vol. 83, series D, no. 4, Dec. 1961.

47. Benham, P. P., "Axial-Load and Strain-Cycling Fatigue of Copper at Low Endurance," Journal of the Institute of Metals, vol. 89, May 1961.

48. Majors, H., Jr., "Thermal and Mechanical Fatigue of Nickel and Titanium," Transactions, A.S.M., vol. 51, 1959.

49. Langer, B. F., "Design of Pressure Vessels for Low-Cycle Fatigue," Journal of Basic Engineering, Transactions, A.S.M.E., vol. 84, series D, no. 3, Sept. 1962.

50. Weinberg, J. G., and Hanna, I. E., "An Evaluation of the Fatigue Properties of Titanium and Titanium Alloys," Titanium Metallurgical Laboratory, Report No. 77, Battelle Memorial Institute, Columbus, Ohio, July 1957.

TABLE 1

RESULTS OF STATIC TENSION TESTS FOR SPECIMENS SUBJECTED TO VARIOUS PLASTIC PRECOMPRESSIVE STRAINS

Specimen Number	Plastic Precompressive strain, $-\epsilon_{pc}$	Static Tensile Fracture Strain ϵ_f^{pc}	True Tensile Fracture Stress σ_f, (ksi)	Reduction of Fracture Ductility* $\epsilon_r^{pc} = \epsilon_f - \epsilon_f^{pc}$
TL-1	0	0.474 (ϵ_f)	148	0
TL-5	0	0.471 (ϵ_f)	---	0
TL-2	0.094	0.409	151	0.064
TL-3	0.162	0.357	149	0.116
TL-4	0.228	0.303	150	0.170
TL-8	0.321	0.240	151	0.233
TL-7	0.391	0.191	152	0.282
TL-9	0.467	0.143	153	0.330

* Based on ϵ_f = 0.473 av.

TABLE 2

RESULTS OF FATIGUE TESTS FOR COMMERCIALLY PURE TITANIUM RS-70
INITIALLY UNCOMPRESSED SPECIMENS

Specimen Number*	Plastic Precompressive Strain, $-\epsilon_{pc}$	Cyclic Total Strain Range $\Delta\epsilon_t$	Cyclic Mean Strain ϵ_m	Cyclic Stable True Stress Range** $\Delta\sigma_s$, (ksi)	Cycles to Failure N_f	Nominal Strain Ratio*** R
TL-12(a)	0	0.188	0.109	297 (b)	3.20	0
TL-11	0	0.106	0.050	281	12.25	0
TL-15	0	0.076	0.035	269	23	0
TL-14	0	0.045	0.020	239	74	0
TL-10	0	0.024	0.010	195	296	0
TL-13	0	0.013	0.005	157	1863	0
TL-39(a)	0	0.189	0.225	298 (b)	1.22	1/2
TL-38	0	0.106	0.150	294	9.25	1/2
TL-16	0	0.066	0.090	260	32	1/2
TL-18	0	0.040	0.053	236	89	1/2
TL-40(a)	0	0.097	0.318	291	4.20	3/4
TL- 6	0	0.066	0.210	277	30	3/4
TL-37	0	0.040	0.123	240	95	3/4

* Tested in 50,000 lb. fatigue machine except as noted.
(a) tested in 60,000 lb. universal testing machine.

** Defined as stress range at $N_f/2$ cycles except as noted.
(b) stress range at last complete cycle prior to failure.

*** Slight variation from test to test.

TABLE 3

RESULTS OF FATIGUE TESTS FOR COMMERCIALLY PURE TITANIUM RS-70
SPECIMENS PRECOMPRESSED TO -0.167 AV. STRAIN

Specimen Number*	Plastic Precompressive Strain, $-\epsilon_{pc}$	Cyclic Total Strain Range $\Delta\epsilon_t$	Cyclic Mean Strain ϵ_m	Cyclic Stable True Stress Range** $\Delta\sigma_s$, (ksi)	Cycles to Failure N_f	Nominal Strain Ratio*** R
TL-22(a)	0.166	0.167	0.066	306 (b)	2.22	0
TL-43(a)	0.175	0.104	0.049	286	7.15	0
TL-21	0.164	0.066	0.030	271	15.25	0
TL-20	0.170	0.041	0.018	251	48	0
TL-19	0.172	0.025	0.010	229	137	0
TL-23	0.166	0.014	0.005	199	706	0
TL-25(a)	0.167	0.099	0.145	279	5.22	1/2
TL-27	0.165	0.066	0.090	270	13.25	1/2
TL-24	0.165	0.040	0.053	246	69	1/2
Av., w/TL-3	0.167					

* Tested in 50,000 lb. fatigue machine except as noted.
(a) tested in 60,000 lb. universal testing machine.

** Defined as stress range at $N_f/2$ cycles except as noted.
(b) stress range at last complete cycle prior to failure.

*** Slight variation from test to test.

TABLE 4

RESULTS OF FATIGUE TESTS FOR COMMERCIALLY PURE TITANIUM RS-70
SPECIMENS PRECOMPRESSED TO -0.323 AV. STRAIN

Specimen Number*	Plastic Precompressive Strain, $-\epsilon_{pc}$	Cyclic Total Strain Range $\Delta\epsilon_t$	Cyclic Mean Strain ϵ_m	Cyclic Stable True Stress Range** $\Delta\sigma_s$, (ksi)	Cycles to Failure N_f	Nominal Strain Ratio*** R
TL-32(a)	0.322	0.121	0.053	304 (b)	3.20	0
TL-33(a)	0.327	0.078	0.031	296	8.15	0
TL-28	0.323	0.041	0.018	277	33	0
TL-29	0.322	0.025	0.010	252	143	0
TL-30	0.315	0.014	0.005	199	762	0
TL-36(a)	0.328	0.086	0.122	288	4.20	1/2
TL-35(a)	0.328	0.066	0.088	280	10.25	1/2
TL-34	0.318	0.041	0.053	272	31	1/2
Av., w/TL-8	0.323					

* Tested in 50,000 lb. fatigue machine except as noted.
(a) tested in 60,000 lb. universal testing machine.

** Defined as stress range at $N_f/2$ cycles except as noted.
(b) stress range at last complete cycle prior to failure.

*** Slight variations from test to test.

TABLE 5

RESULTS OF FATIGUE TESTS FOR 2024-T4 ALUMINUM ALLOY

Data by D'Amato, Ref. 39

Specimen Number	Cyclic Total Strain Range $\Delta\epsilon_t$	Cyclic Mean Strain ϵ_m	Cyclic Stable True Stress Range* $\Delta\sigma_s$, (ksi)	Cycles to Failure** N_f
29d	0.345	0	205	1.20
9d	0.1680	0	195	4.25
44d	0.1137	0	181	8.25
25e	0.0735	0	166.5	31
20d	0.0599	0	161	65
6d	0.0519	0	154	77
49d	0.0498	0	163	63
16d	0.0311	0	151	236
24e	0.0263	0	143	400
3d	0.0180	0	138	803
23e	0 0154	0	130	1835
37d	0.0144	0	127	1960
14e	0 1030	-0.075	175	12.25
17e	0.0424	-0.075	156	117
17d	0 0226	-0.075	142	489
16e	0.1060	0.075	189	8.25
15e	0.0419	0.075	157	88
6e	0.0227	0.075	139	359
21e	0.0705	0.135	177	16.25
19e	0.0341	0.135	156	112
1e	0.0259	0.135	151	233
22e	0.0174	0.135	140	710
13e	0.0129	0.135	125	2076
5e	0.1220	0.185	190	2.23

* Average stress range for test.
$\Delta\epsilon_e = \Delta\sigma_s / E_{Al.}$, where $E_{Al.} = 10^4$ ksi

** Lives <1000 cycles differ from those reported by D'Amato because of a difference in method of defining first tensile strain application.

TABLE 5 (CON'T)

RESULTS OF FATIGUE TESTS FOR 2024-T4 ALUMINUM ALLOY

Data by D'Amato, Ref. 39

Specimen Number	Cyclic Total Strain Range $\Delta\epsilon_t$	Cyclic Mean Strain ϵ_m	Cyclic Stable True Stress Range* $\Delta\sigma_s$, (ksi)	Cycles to Failure** N_f
12d	0.0730	0.275	196	2.20
20e	0.0606	0.275	191	4.13
21d	0.0593	0.275	192	2.25
12e	0.0544	0.275	182	7.13
40e	0.0538	0.275	188	5.23
19d	0.0383	0.275	177	14.25
50d	0.0310	0.275	176	36
22d	0.0223	0.275	164	128
14d	0.0161	0.275	155.5	196
4d	0.0150	0.275	146	715
18e	0.0135	0.275	134.5	1720
47d	0.0121	0.275	121	3750
26d	0.0120	0.275	120	2850
3e	0.0107	0.275	108	10900

* Average stress range for test.
$\Delta\epsilon_e = \Delta\sigma_s / E_{Al.}$, where $E_{Al.} = 10^4$ksi

** Lives <1000 cycles differ from those reported by D'Amato because of a difference in method of defining first tensile strain application.

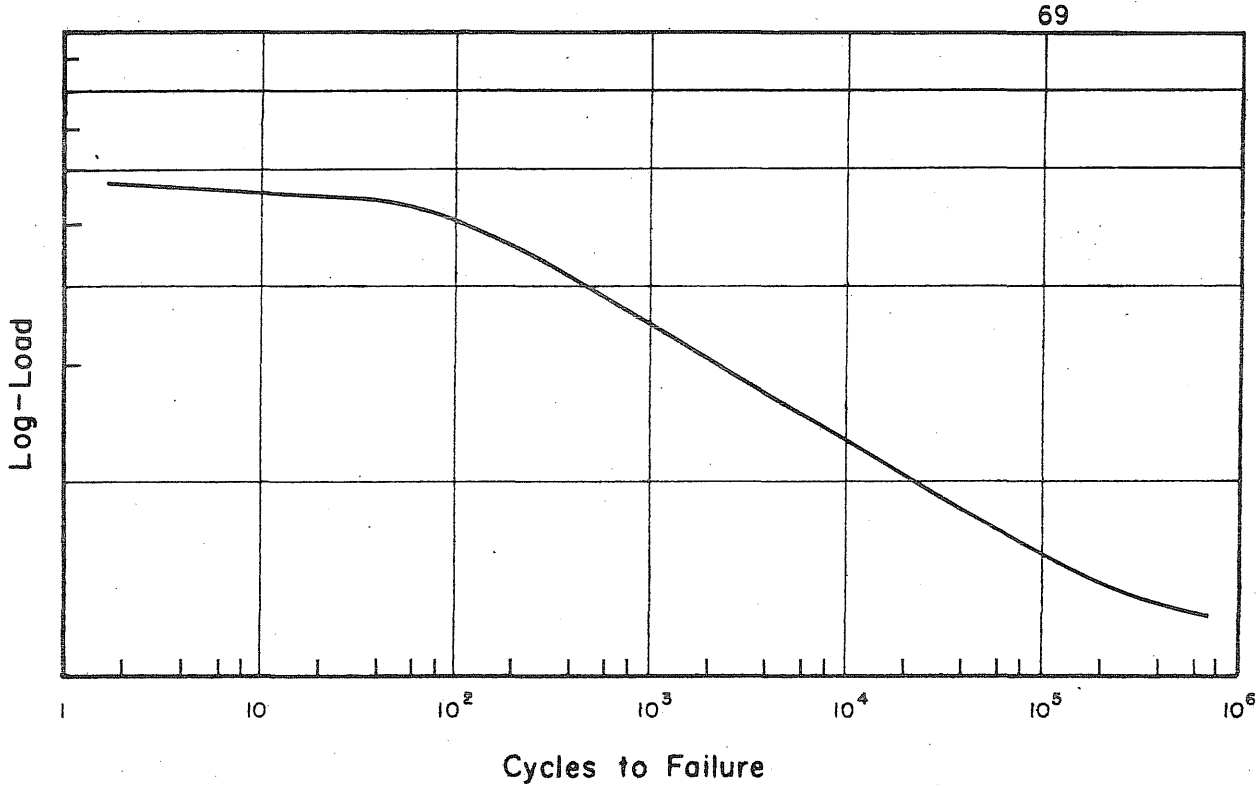

a. Controlled-Load Fatigue Tests

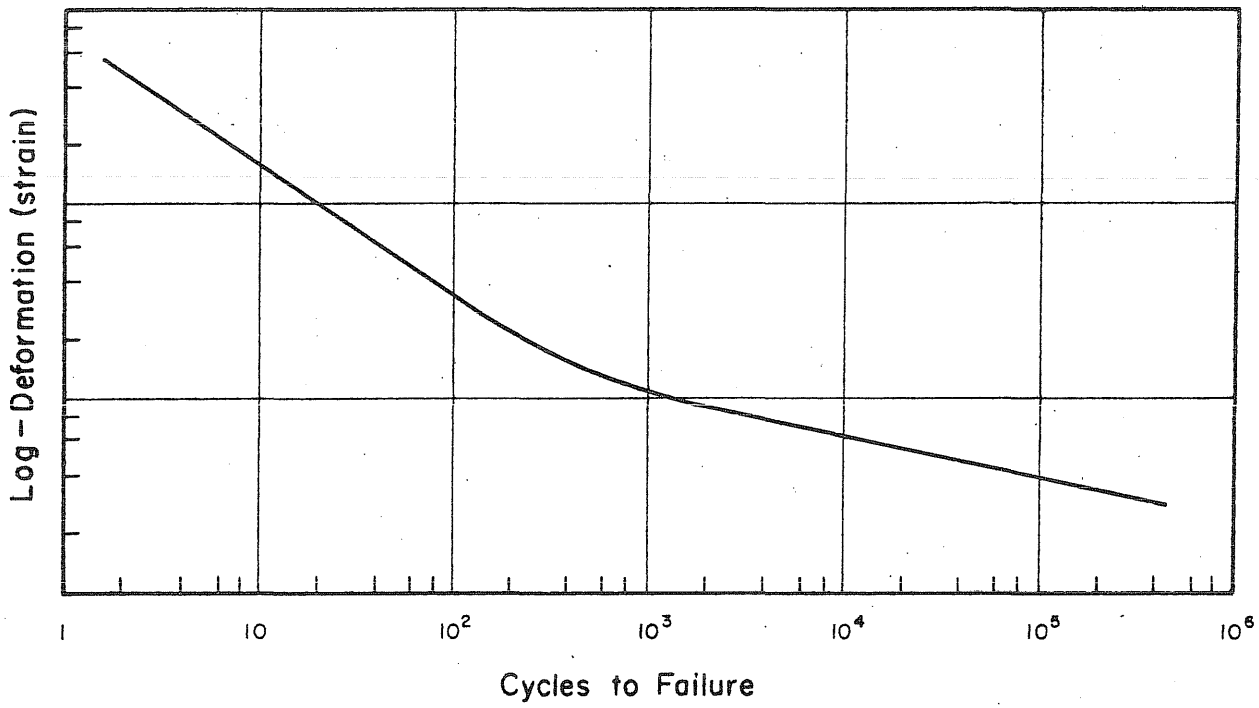

b. Controlled-Deformation Fatigue Tests

FIG. I COMPARISON OF CONTROLLED-LOAD AND CONTROLLED-DEFORMATION FATIGUE BEHAVIOR

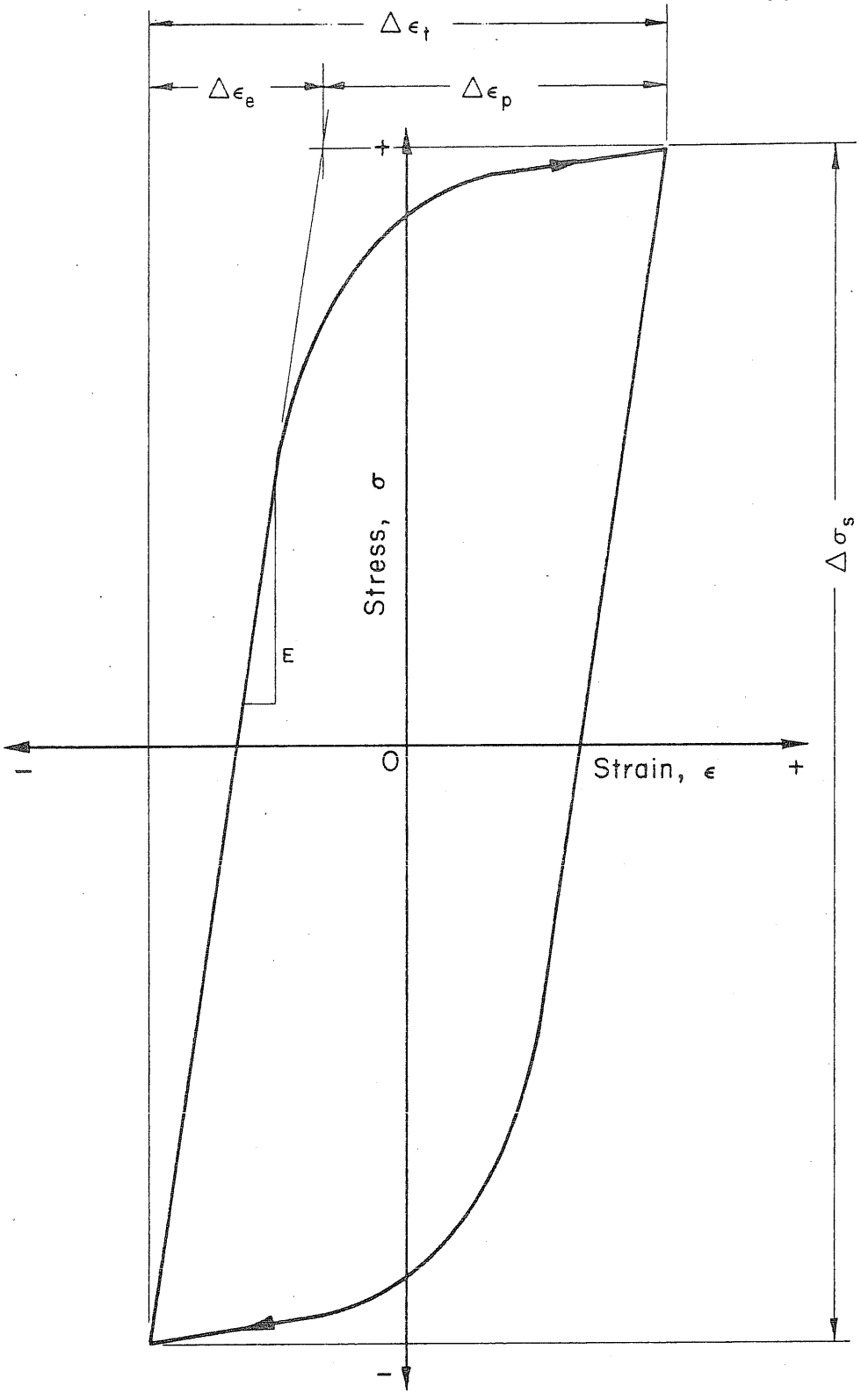

FIG. 2 COMPONENTS OF TOTAL STRAIN RANGE FOR CONTROLLED-STRAIN CYCLING

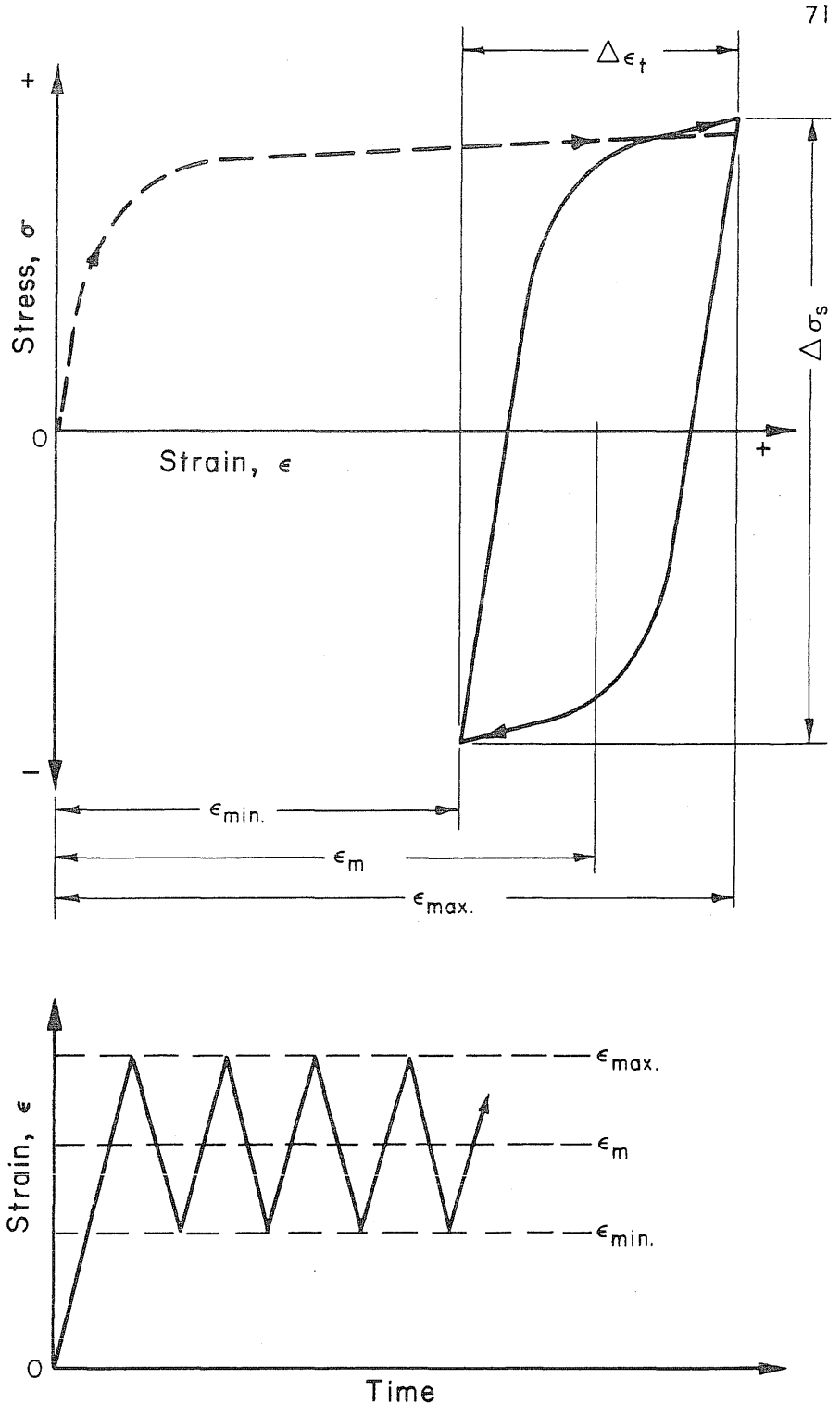

FIG. 3 ILLUSTRATION OF CONTROLLED-STRAIN CYCLING ABOUT A TENSILE MEAN STRAIN

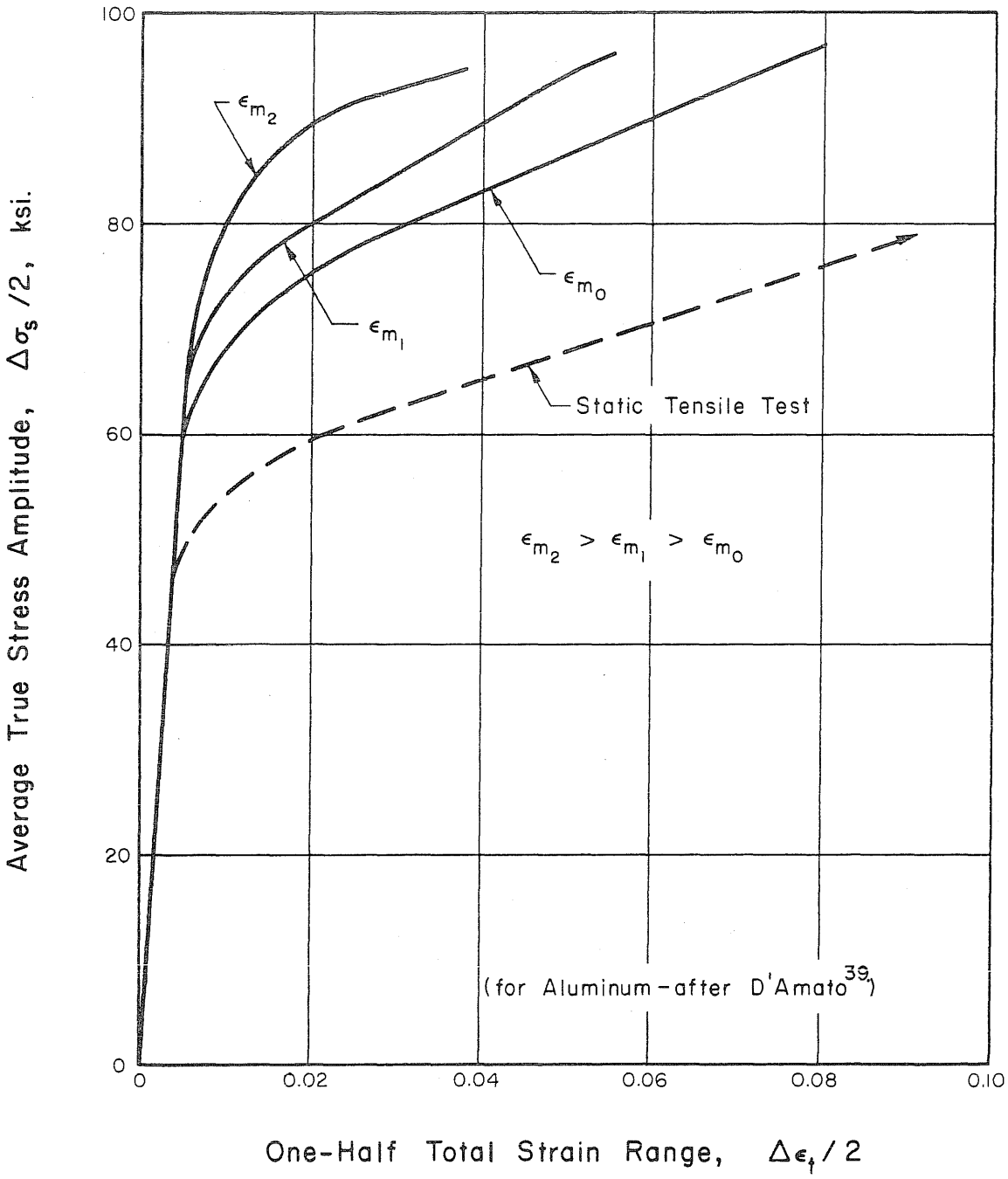

FIG. 4 CYCLIC STRESS–STRAIN DIAGRAMS FOR VARIOUS CONDITIONS OF MEAN STRAIN

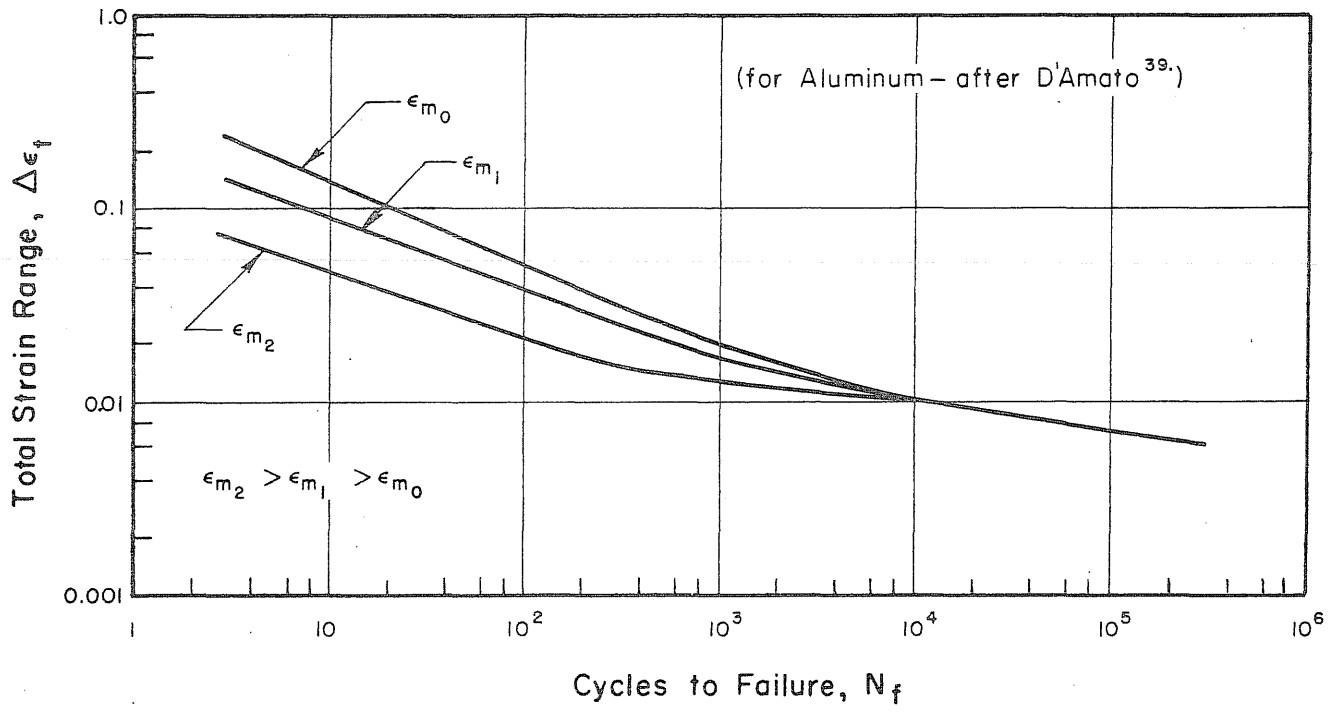

a. Fatigue Behavior Based on Cyclic Total Strain Range

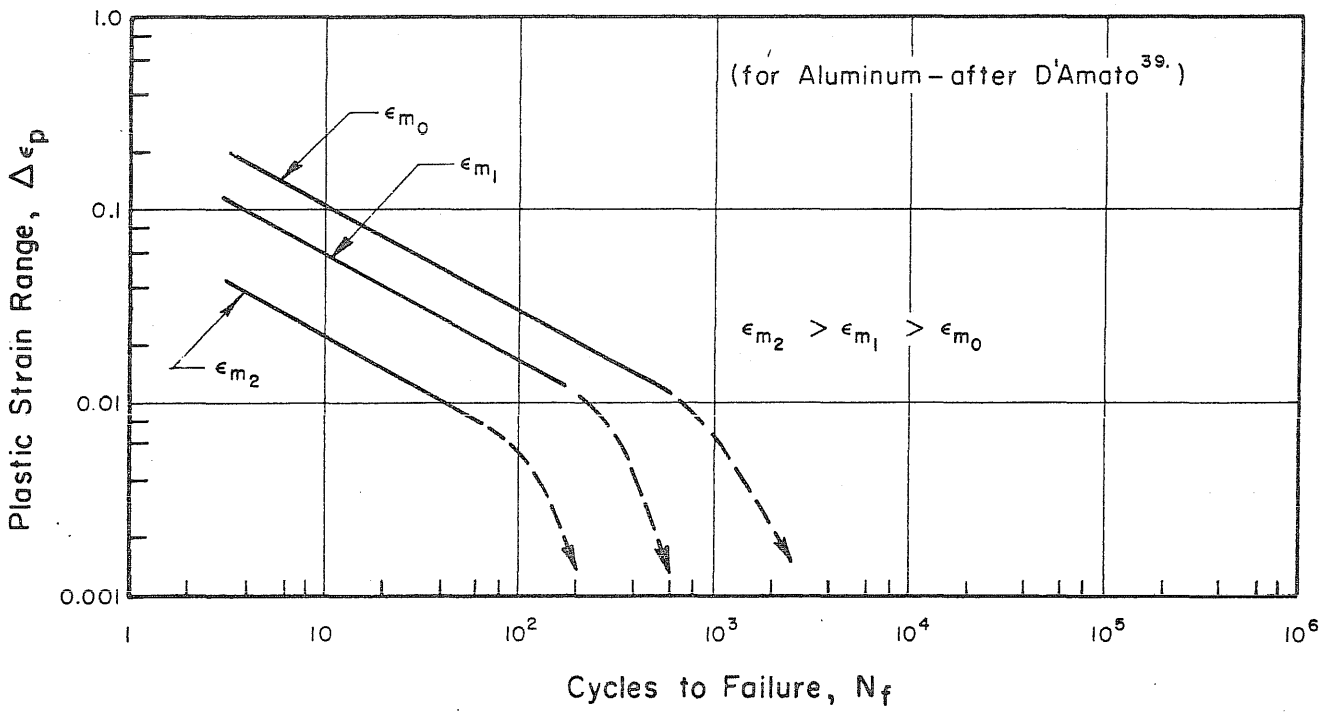

b. Fatigue Behavior Based on Cyclic Plastic Strain Range

FIG. 5 EFFECT OF LARGE TENSILE MEAN STRAINS ON LOW CYCLE FATIGUE BEHAVIOR

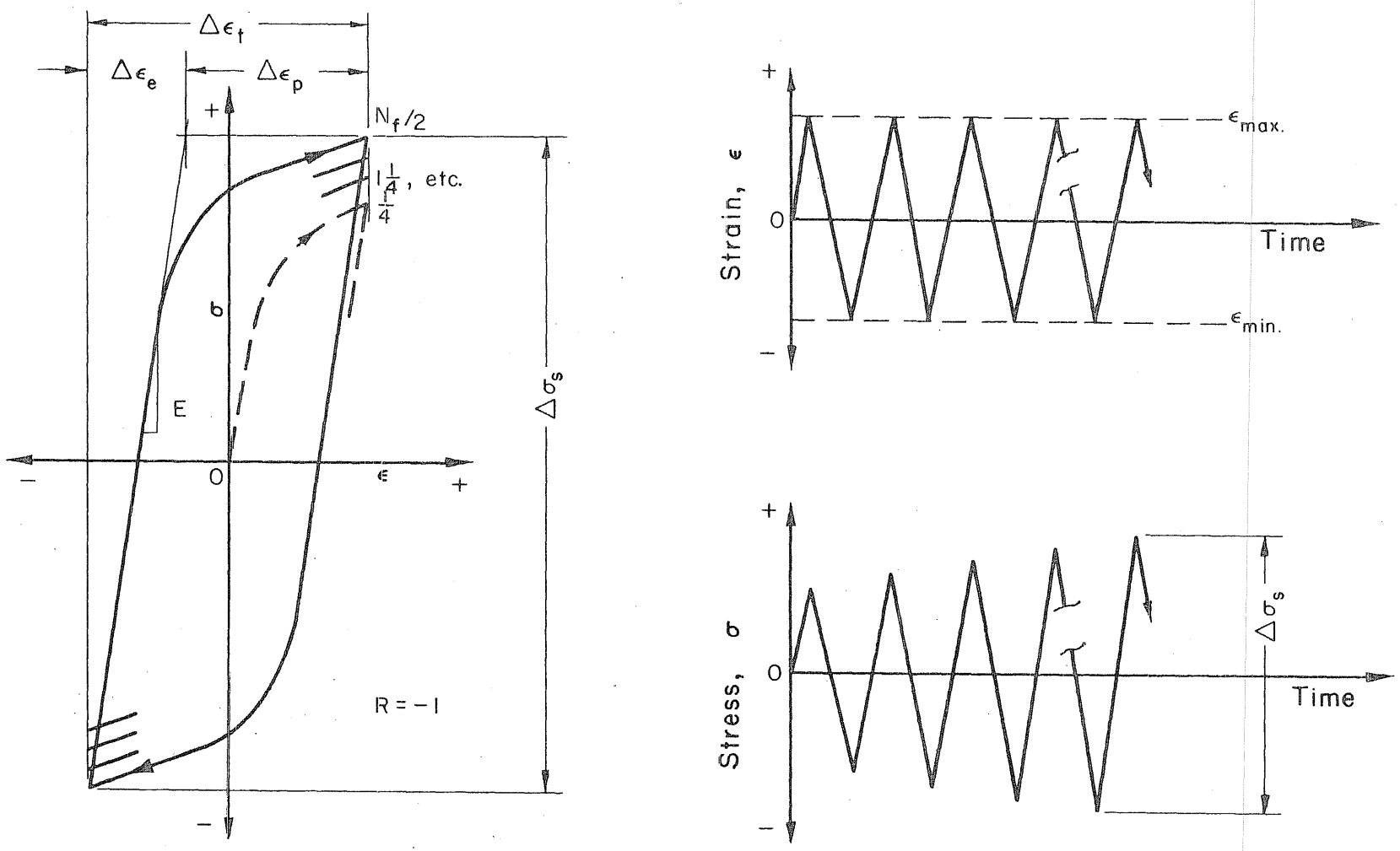

FIG. 6 PARAMETERS ENCOUNTERED IN CONTROLLED-STRAIN CYCLING ABOUT ZERO MEAN STRAIN

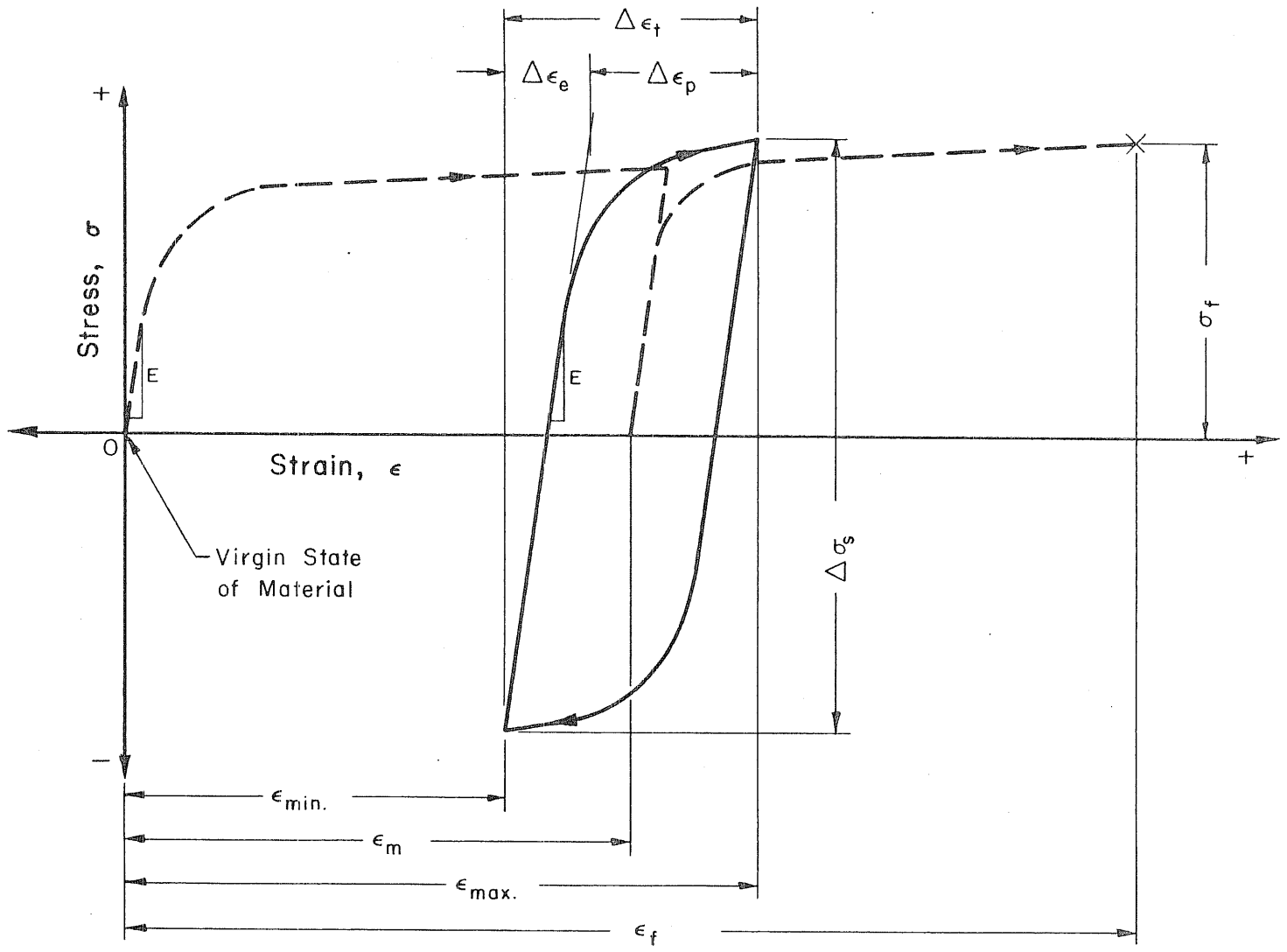

FIG. 7 PARAMETERS ENCOUNTERED IN CONTROLLED-STRAIN CYCLING ABOUT A TENSILE MEAN STRAIN

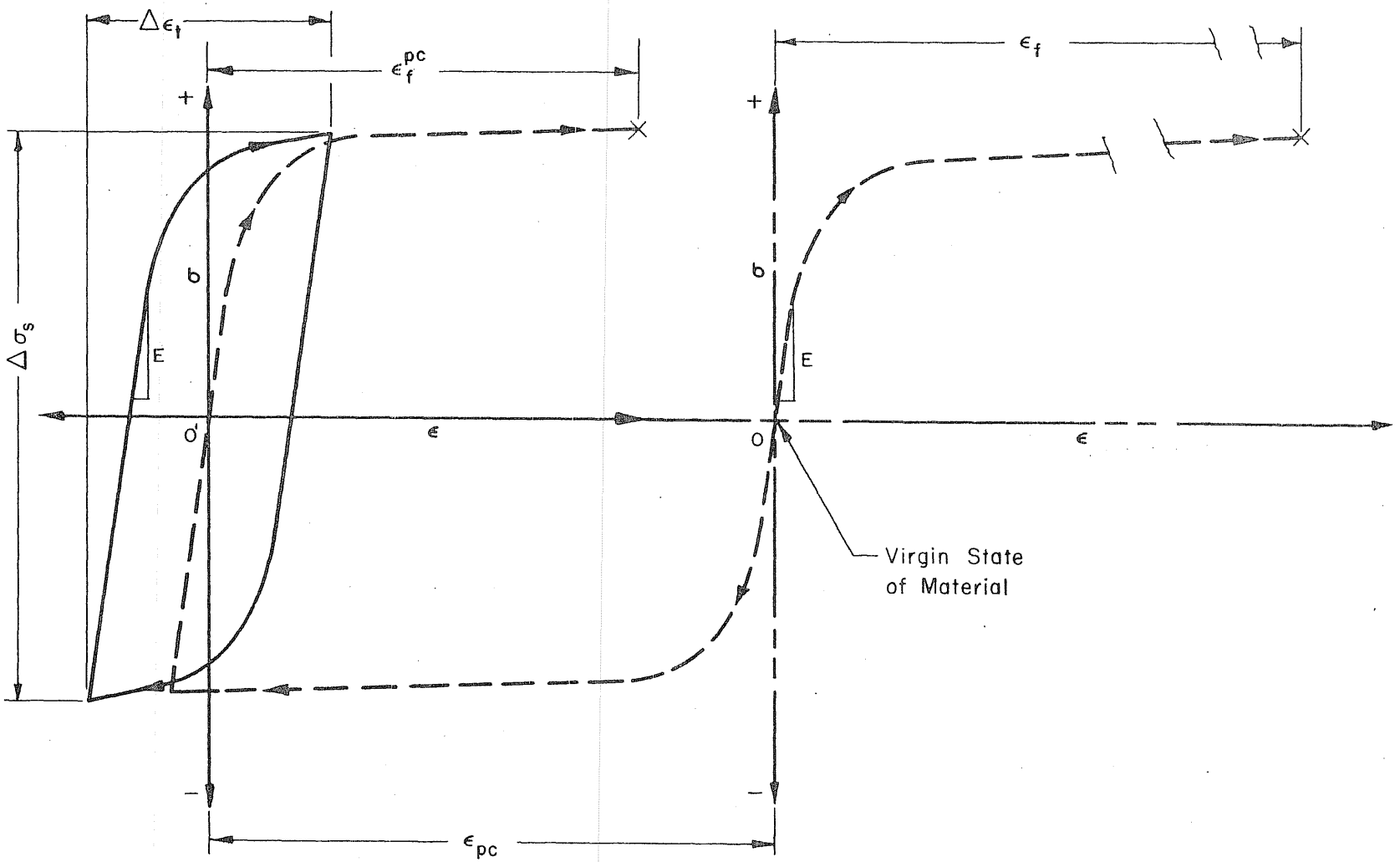

FIG. 8 PARAMETERS ENCOUNTERED IN CONTROLLED-STRAIN CYCLING AFTER PRECOMPRESSION

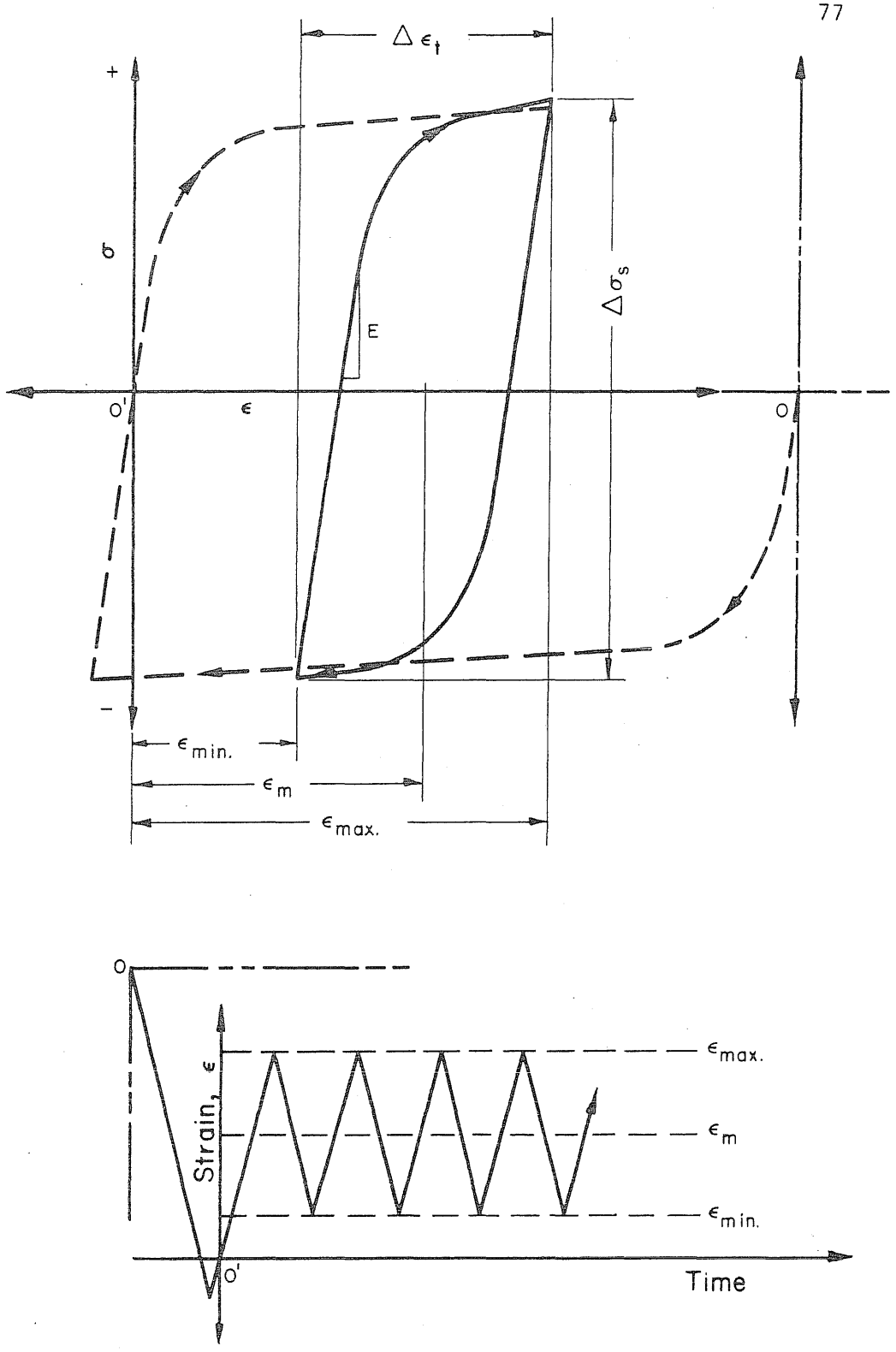

FIG. 9 ILLUSTRATION OF CONTROLLED-STRAIN CYCLING ABOUT A POSITIVE MEAN STRAIN AFTER PRECOMPRESSION

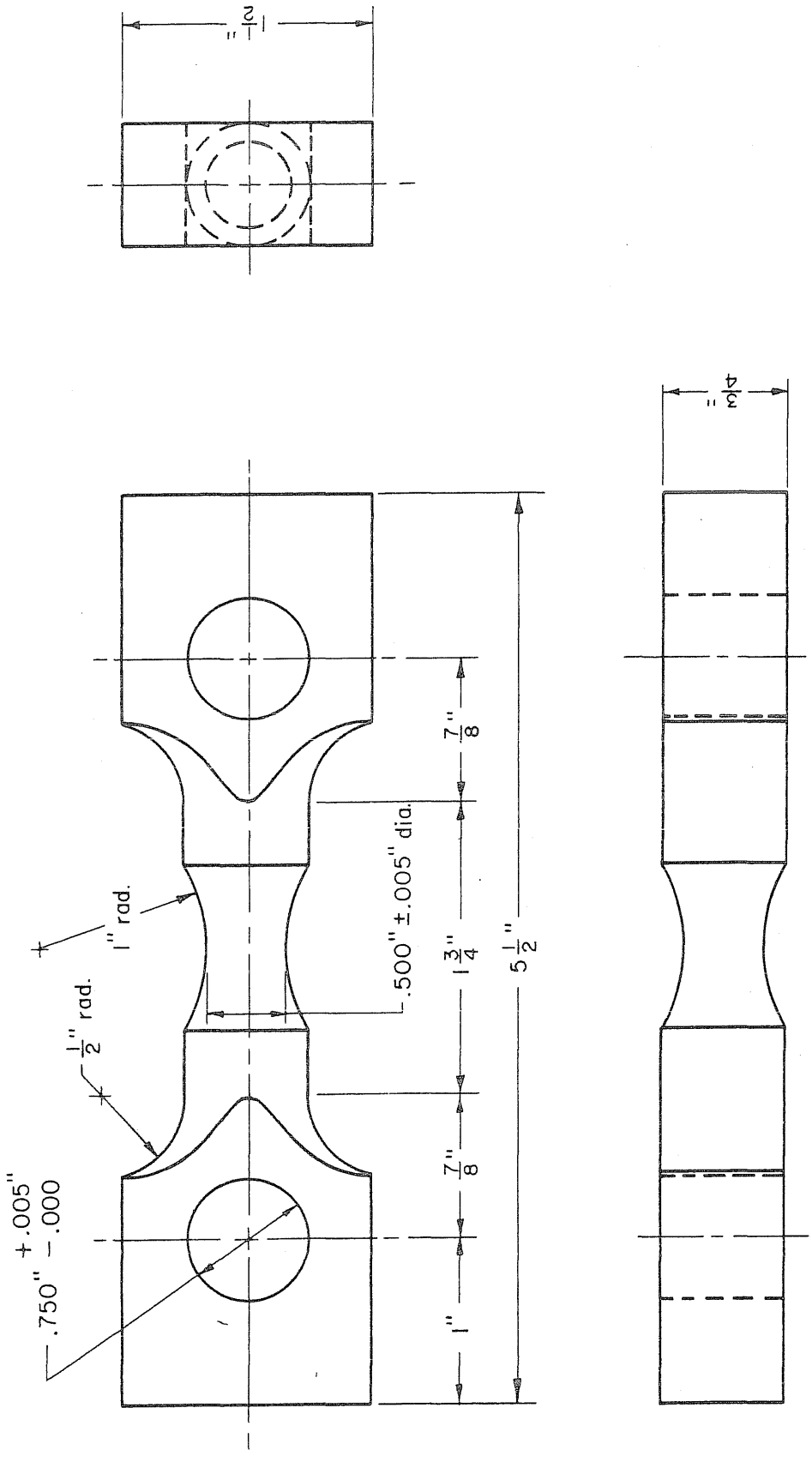

FIG. 10 DETAILS OF TEST SPECIMEN

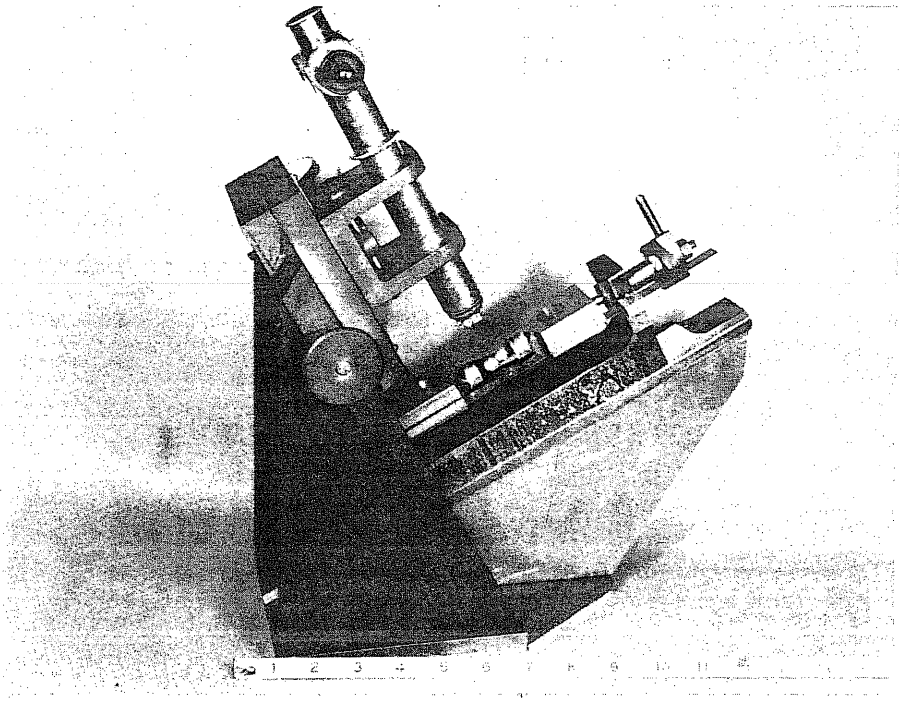

FIG. 11 TRAVELING MICROSCOPE ASSEMBLY

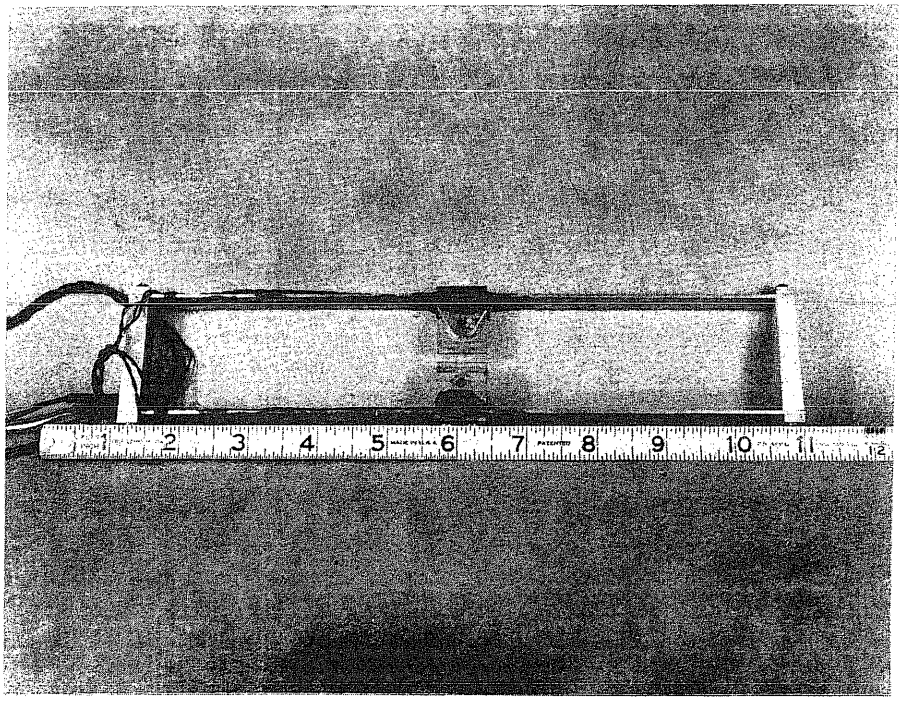

FIG. 12 RECTANGULAR FRAME DIAMETER GAGE

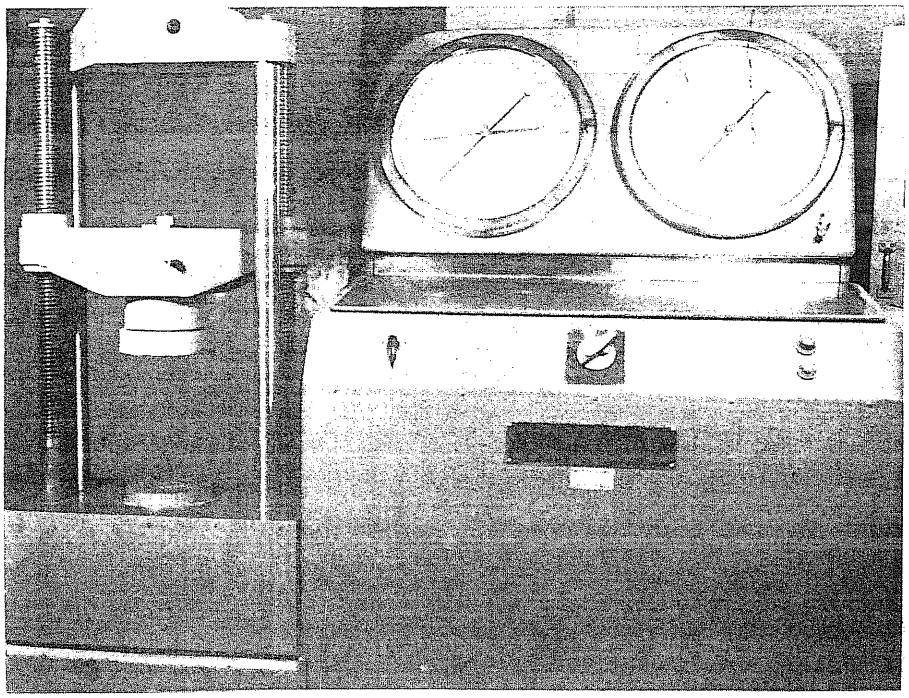

FIG. 13 60,000 LB. UNIVERSAL TESTING MACHINE

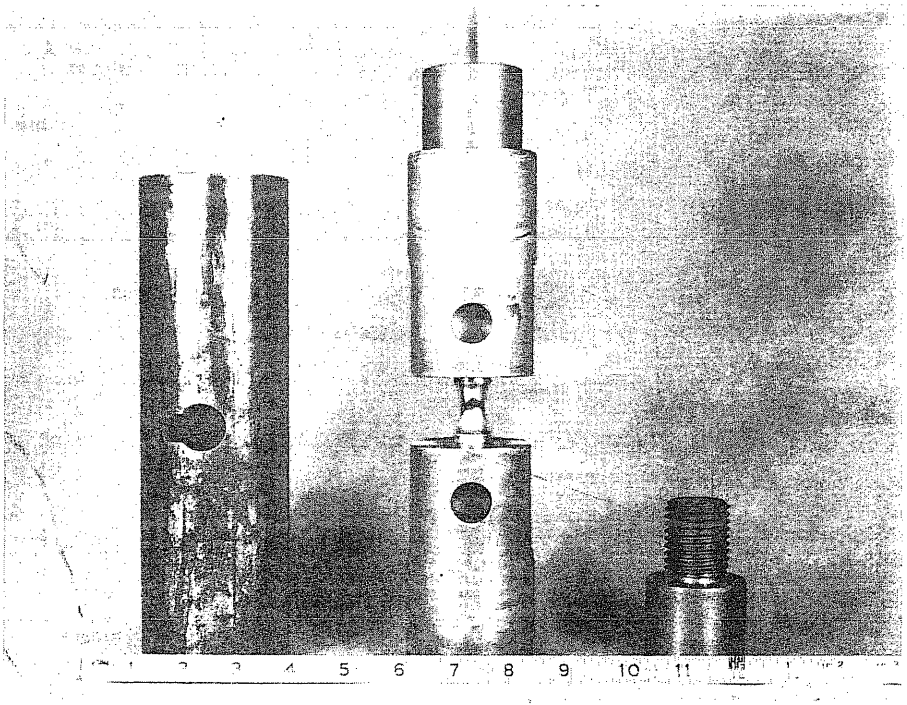

FIG. 14 LOADING-HEAD AND SLEEVE ASSEMBLY

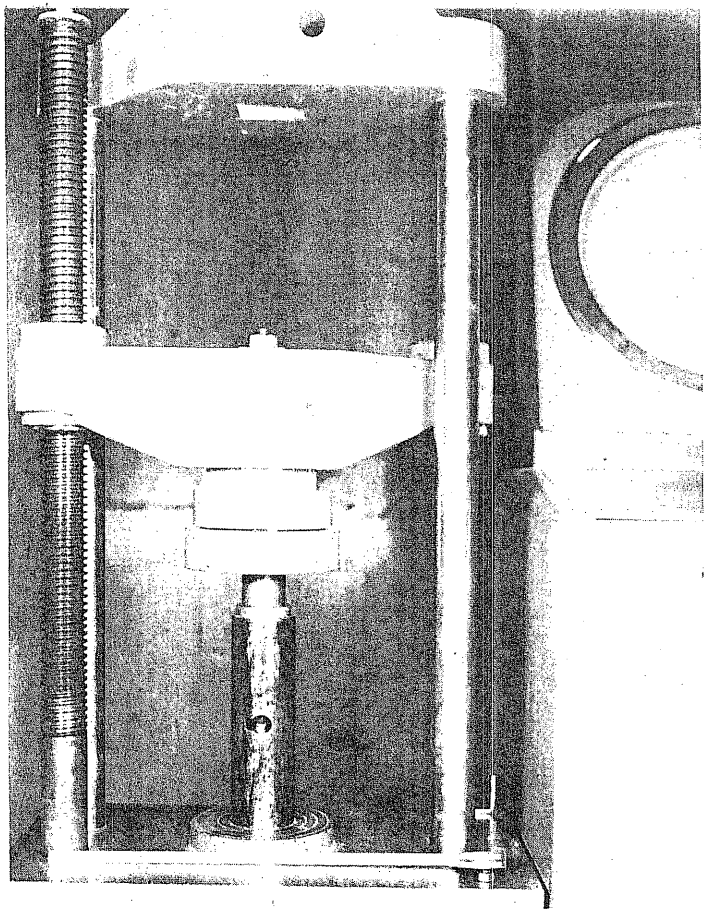

FIG. 15 METHOD OF COMPRESSIVE LOAD APPLICATION

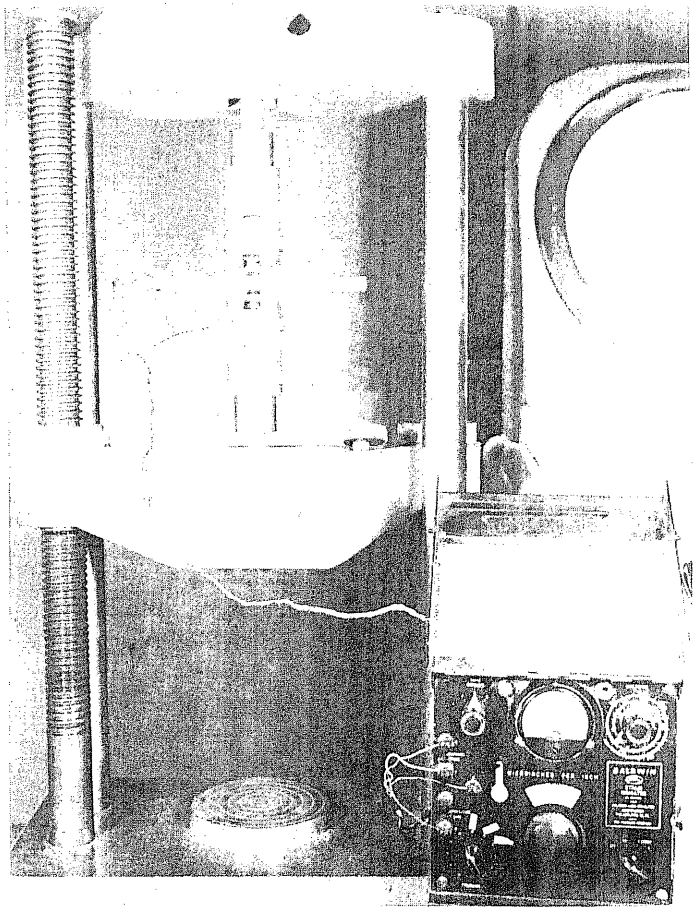

FIG. 16 METHOD OF TENSILE LOAD APPLICATION

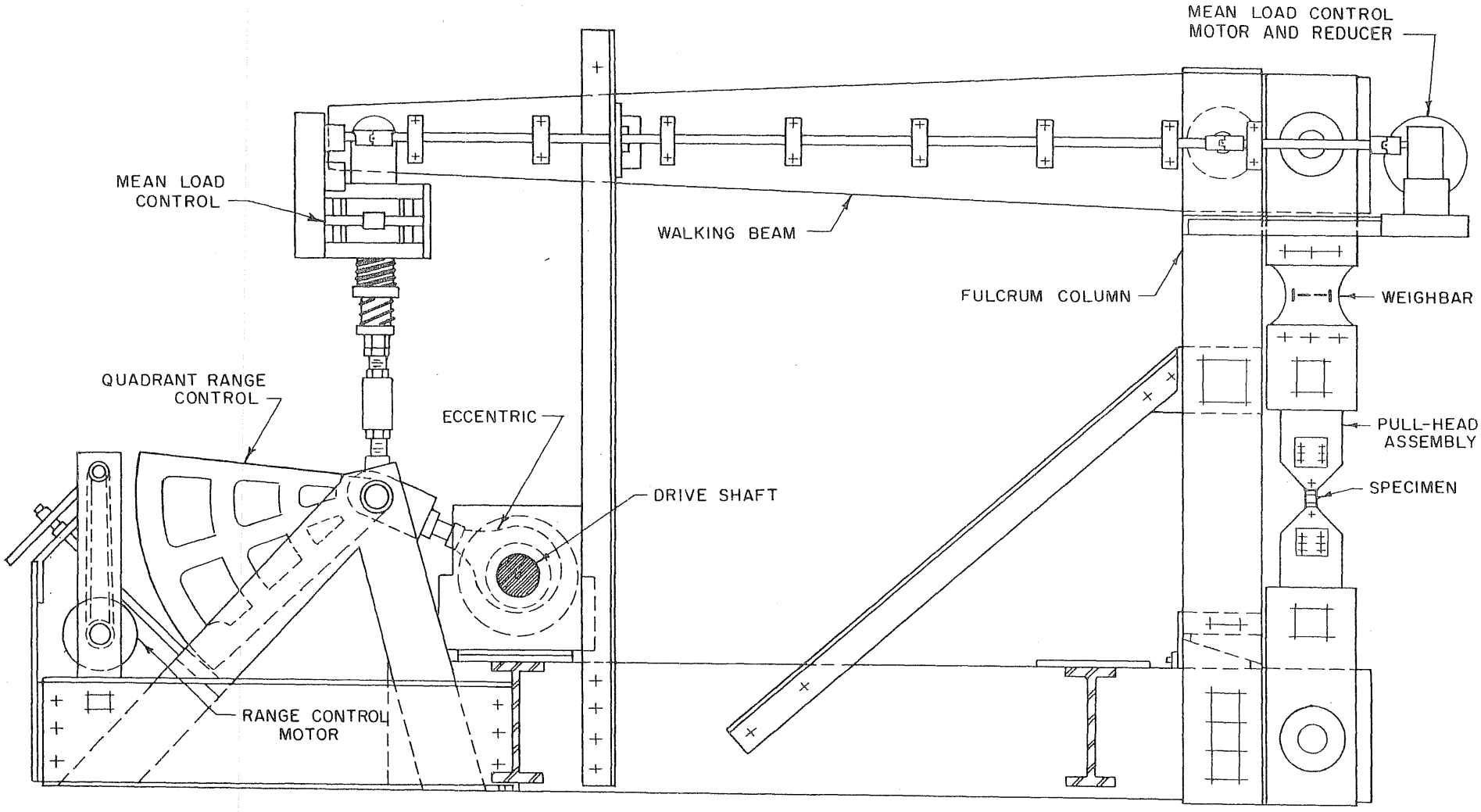

FIG. 17 50,000 LB. FATIGUE TESTING MACHINE

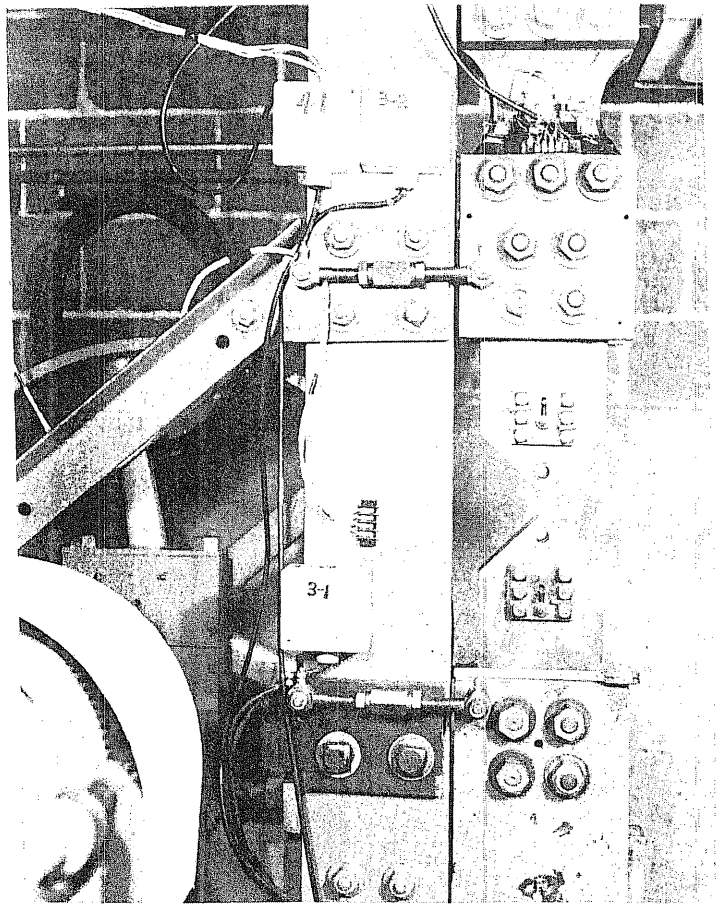

FIG. 18 PULL-HEAD ASSEMBLY FOR FATIGUE MACHINE

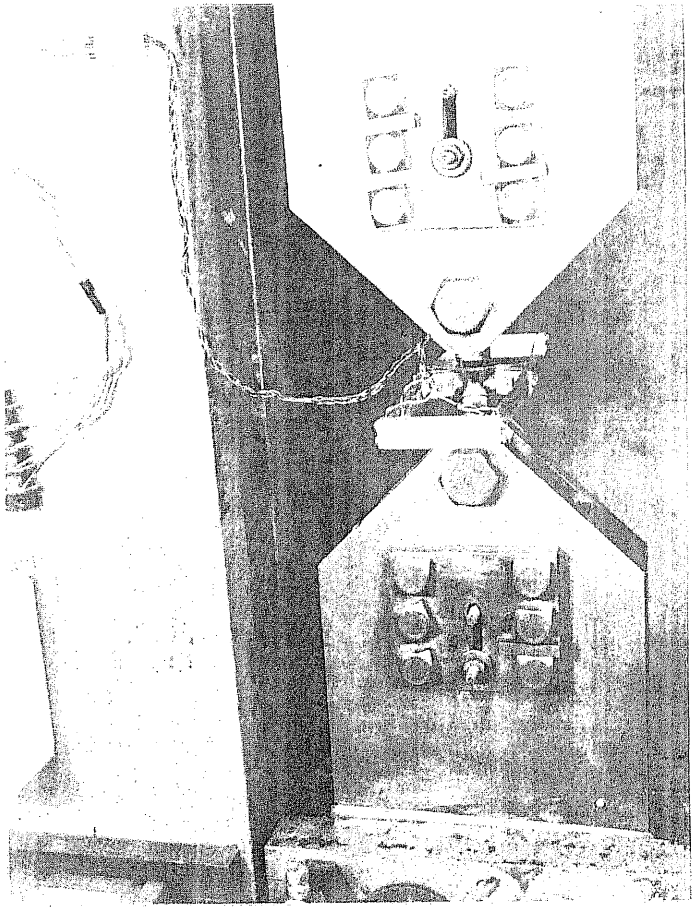

FIG. 19 PULL-HEAD ASSEMBLY WITH SPECIMEN AND GAGE PLACED IN POSITION

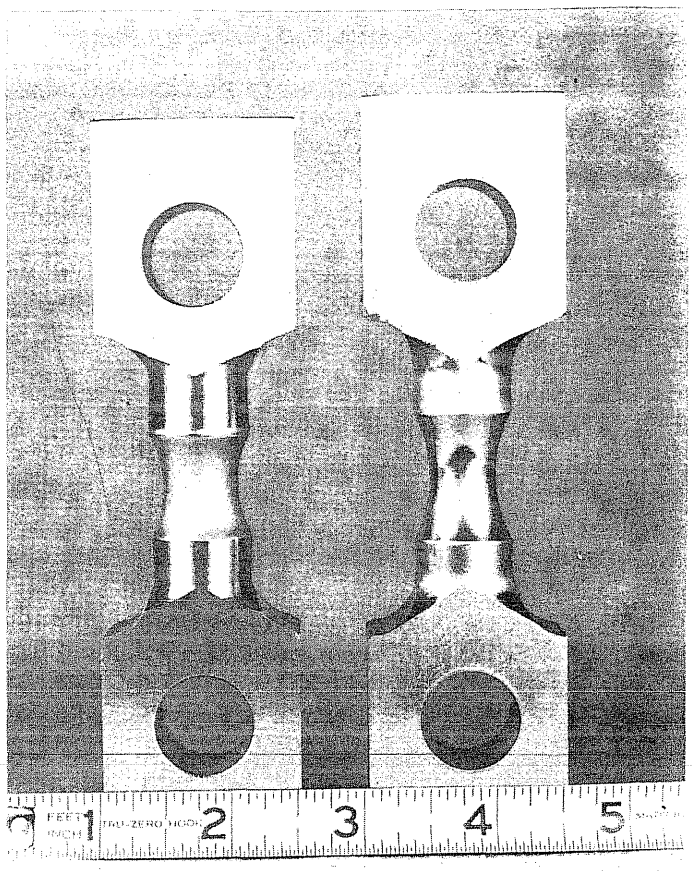

FIG. 20 SPECIMEN PRECOMPRESSED TO – 0.32 STRAIN BESIDE VIRGIN SPECIMEN

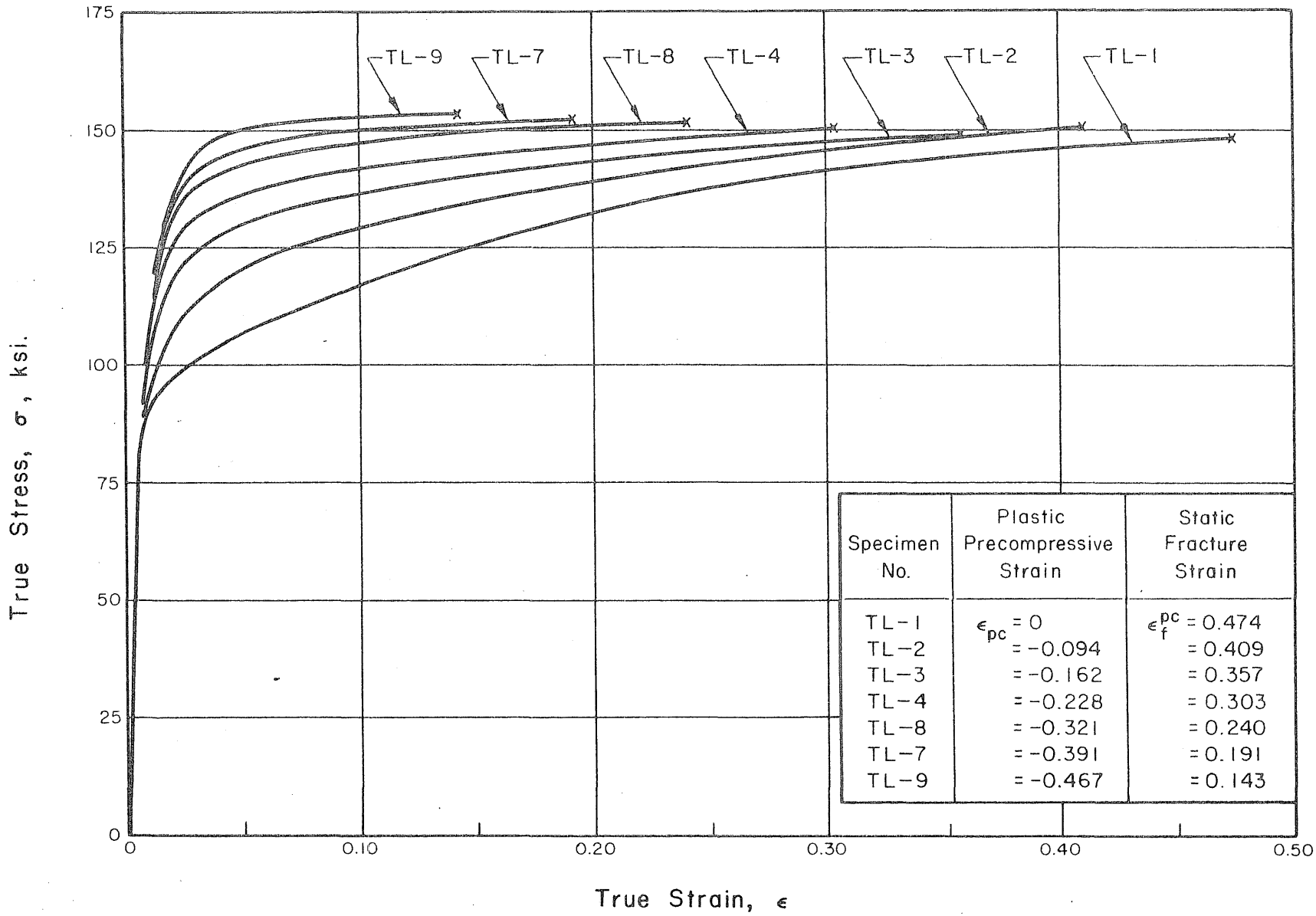

FIG. 21 STATIC STRESS-STRAIN DIAGRAMS FOR SPECIMENS SUBJECTED TO VARIOUS PLASTIC PRECOMPRESSIVE STRAINS

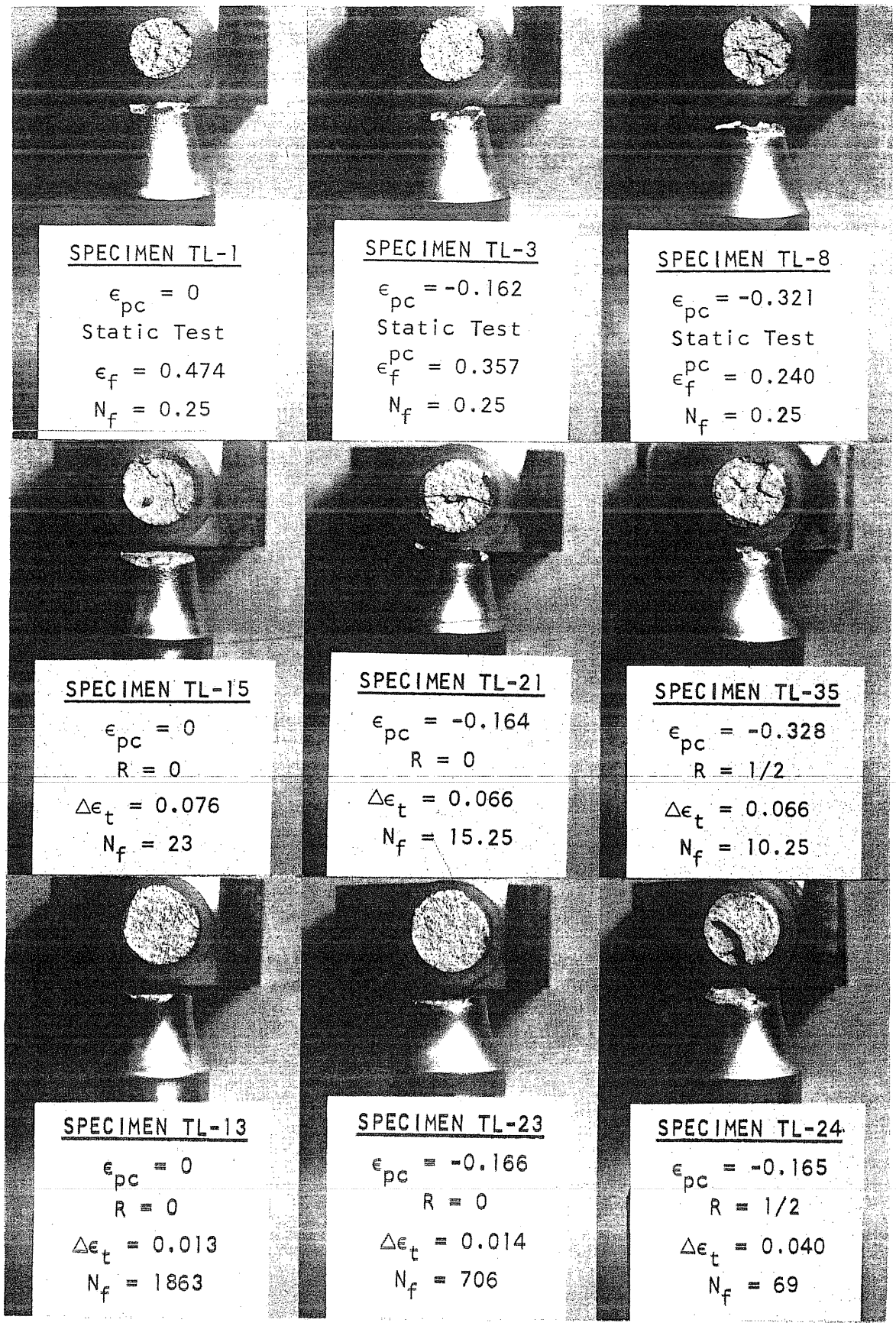

FIG. 22 FRACTURE APPEARANCE OF TYPICAL STATIC AND FATIGUE TEST SPECIMENS

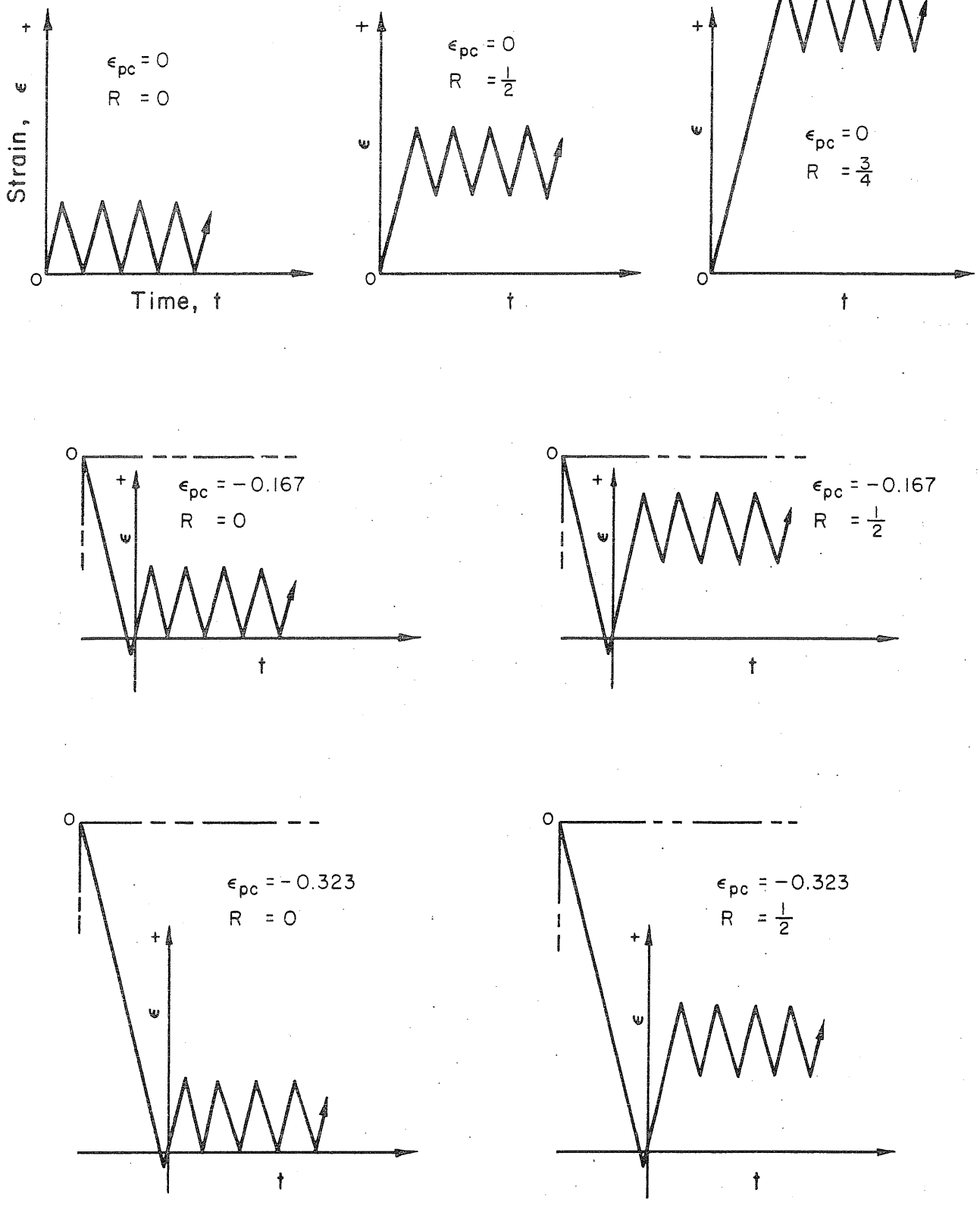

FIG. 23 SCHEMATIC REPRESENTATION OF CYCLIC CONTROLLED-STRAIN TESTS USED IN CURRENT STUDY

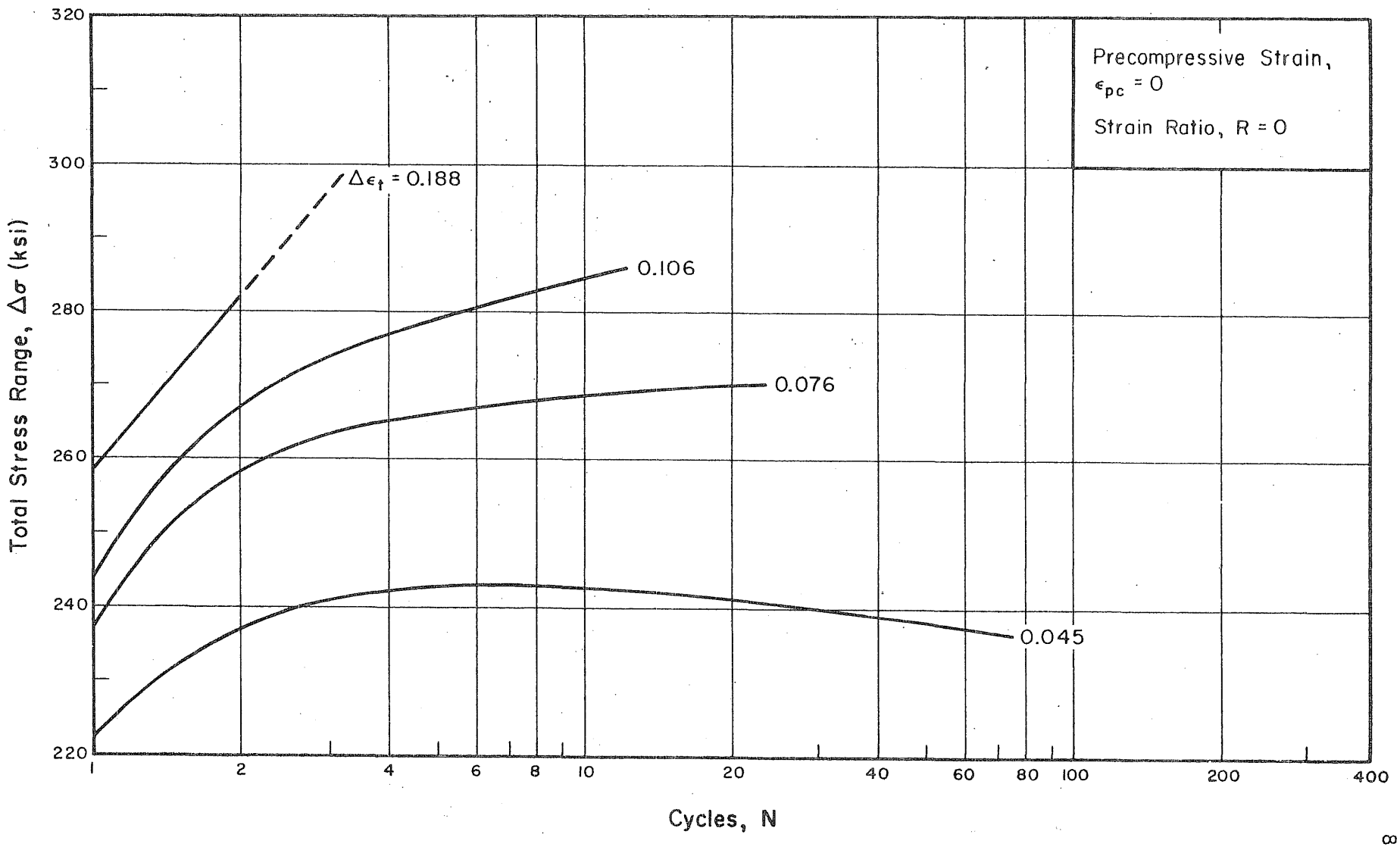

FIG. 24a CYCLIC STRESS HISTORY OF INITIALLY UNCOMPRESSED SPECIMENS, R = 0

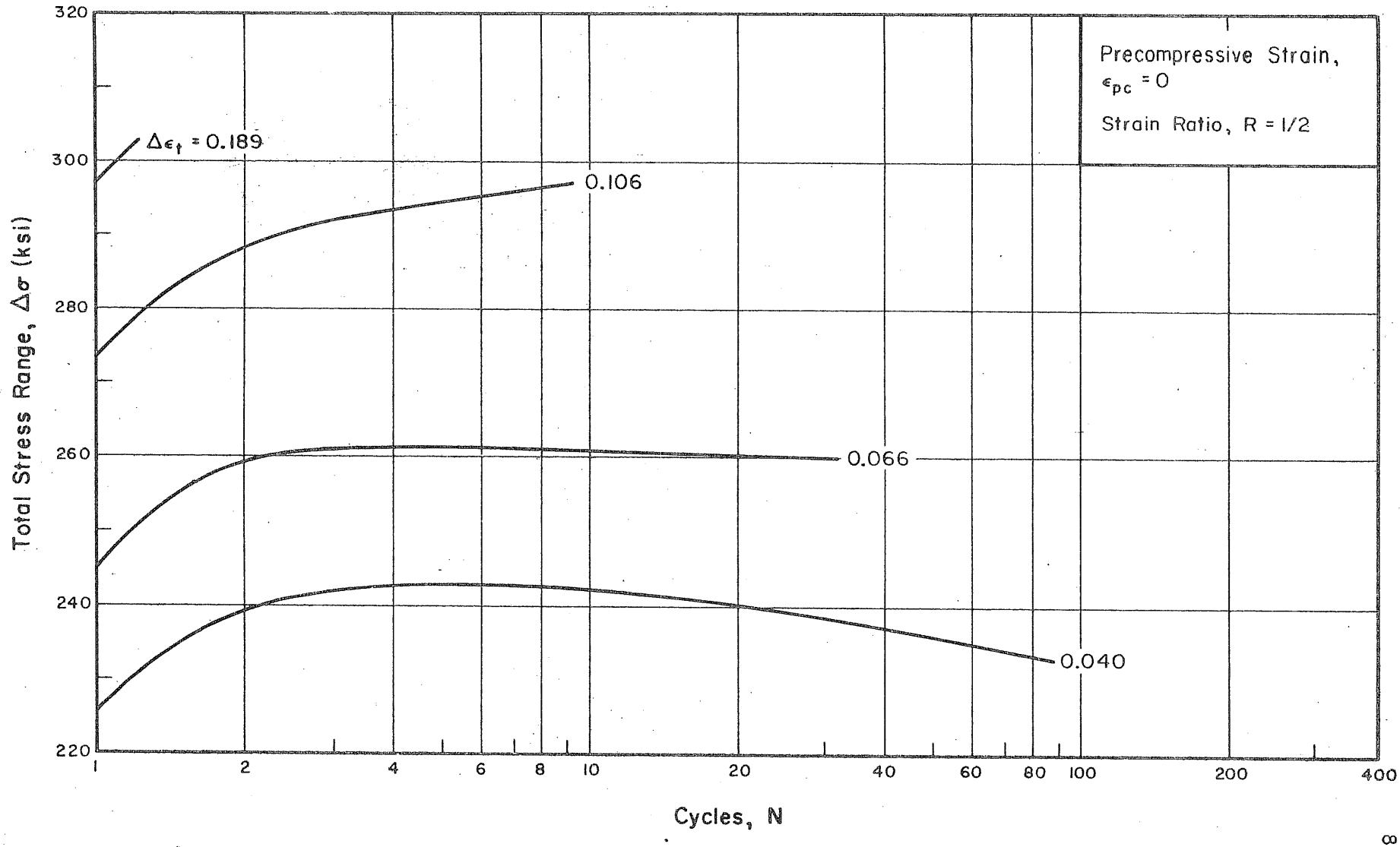

FIG. 24b CYCLIC STRESS HISTORY OF INITIALLY UNCOMPRESSED SPECIMENS, R = 1/2

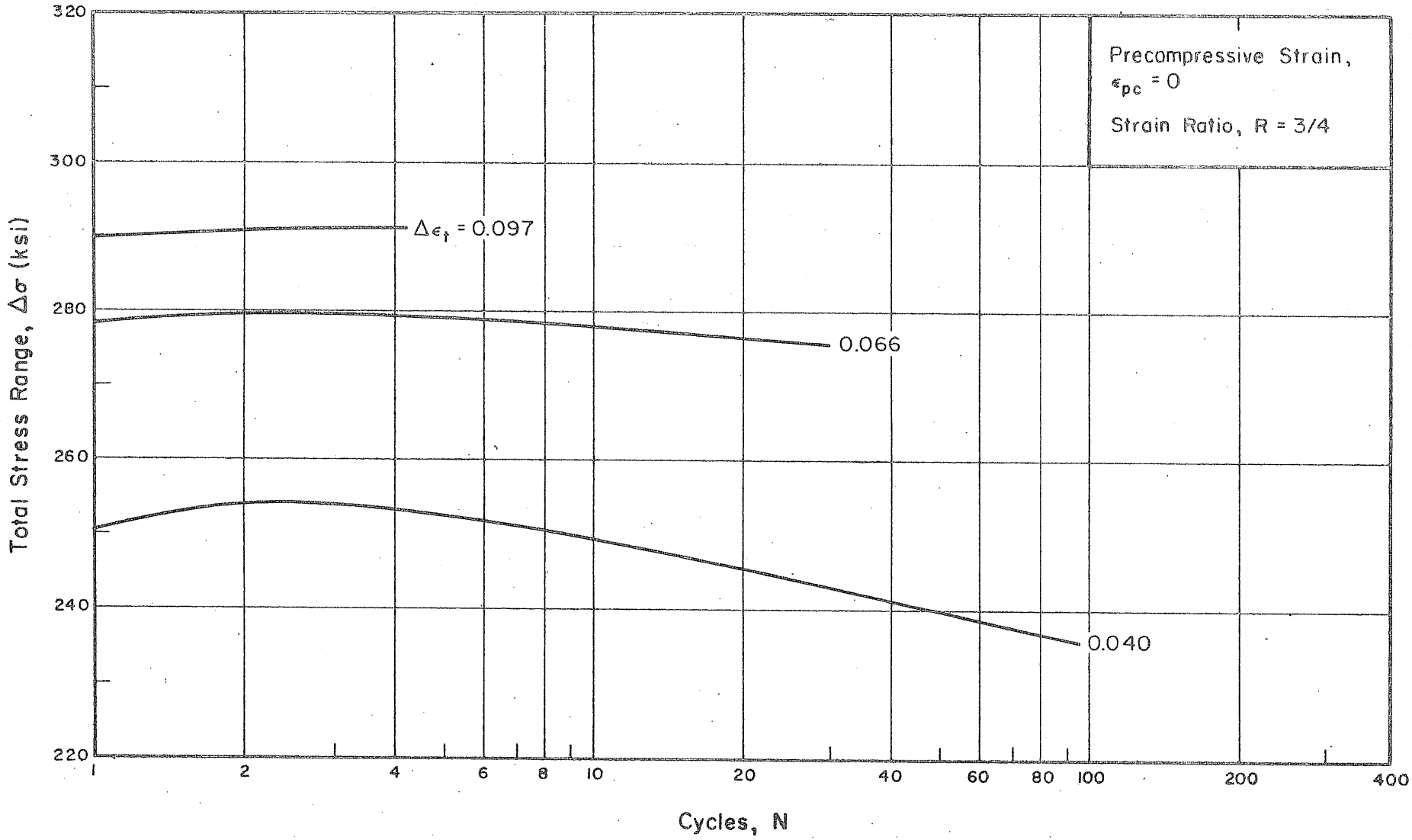

FIG. 24c CYCLIC STRESS HISTORY OF INITIALLY UNCOMPRESSED SPECIMENS, R = 3/4

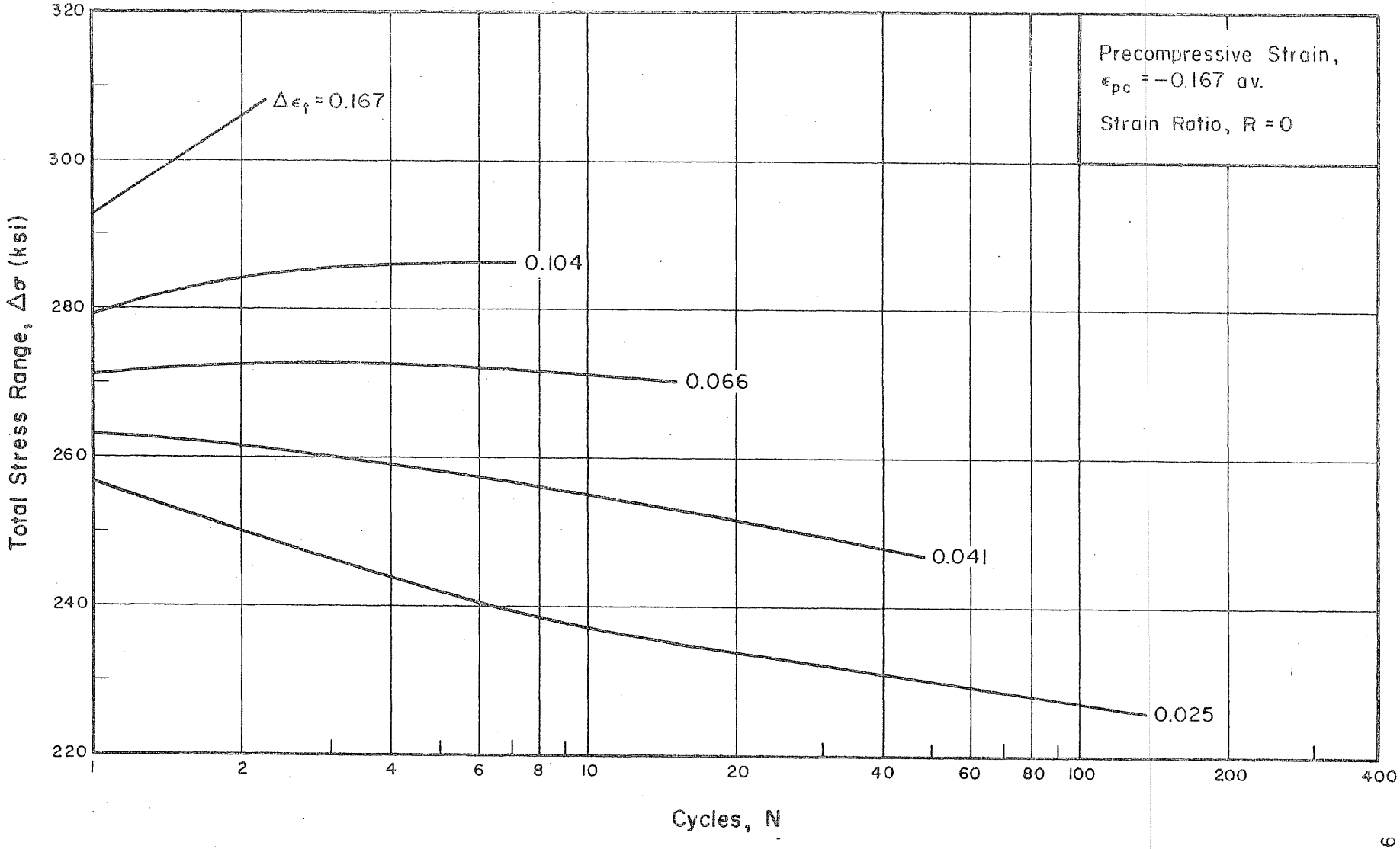

FIG. 25a CYCLIC STRESS HISTORY OF SPECIMENS PRECOMPRESSED TO −0.167 AV. STRAIN, R = 0

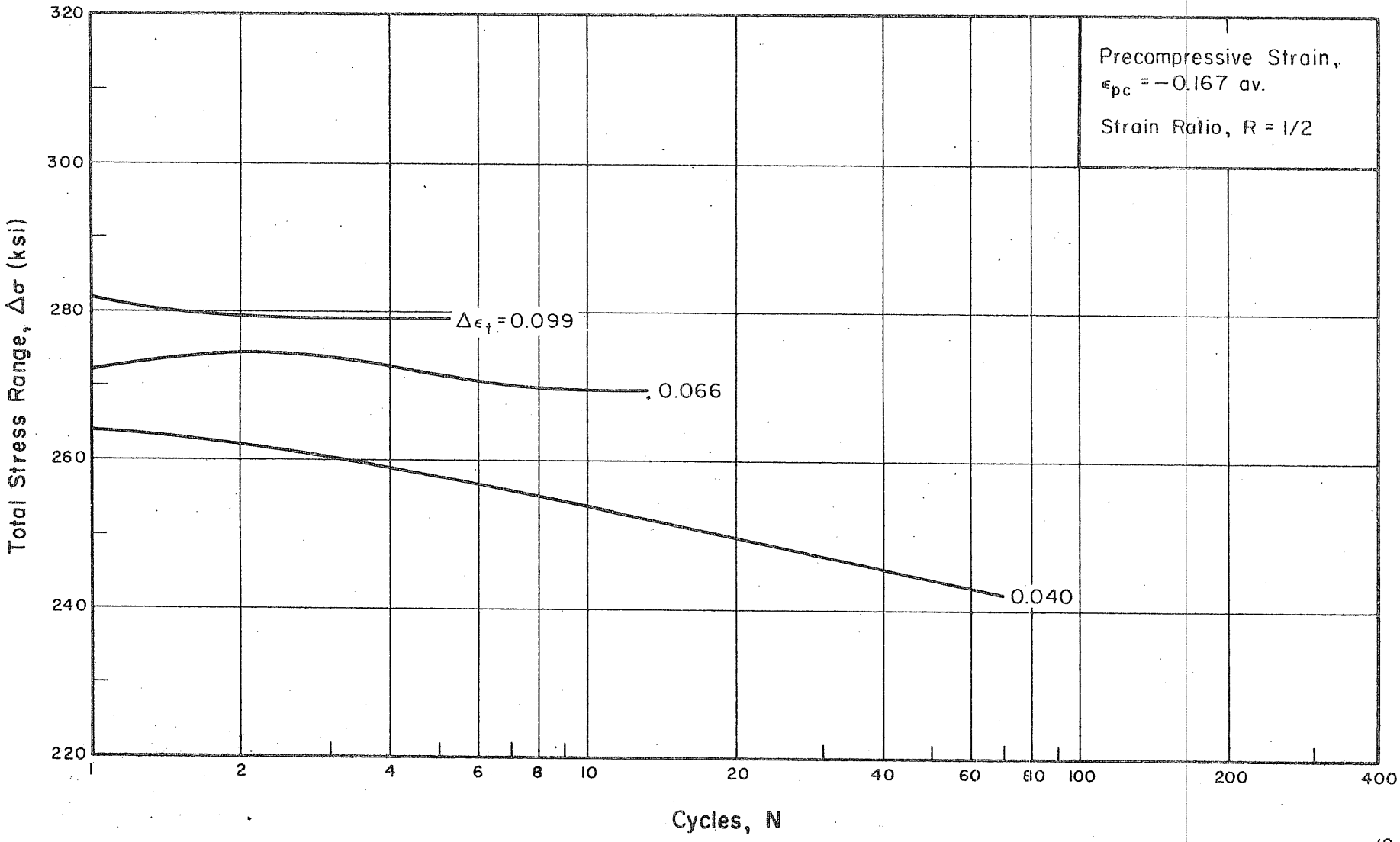

FIG. 25b CYCLIC STRESS HISTORY OF SPECIMENS PRECOMPRESSED TO −0.167 AV. STRAIN, R = 1/2

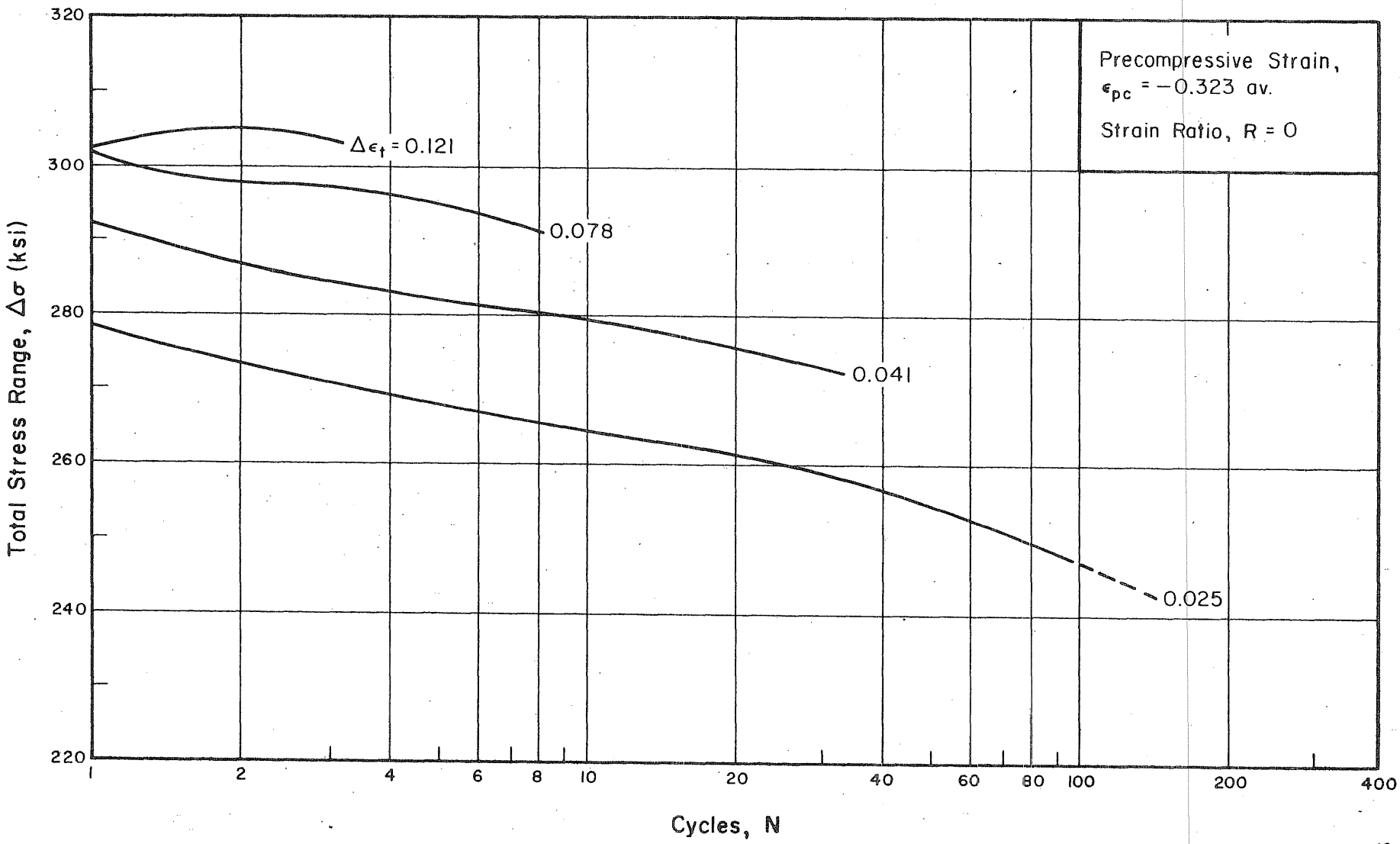

FIG. 26a CYCLIC STRESS HISTORY OF SPECIMENS PRECOMPRESSED TO −0.323 AV. STRAIN, R = 0

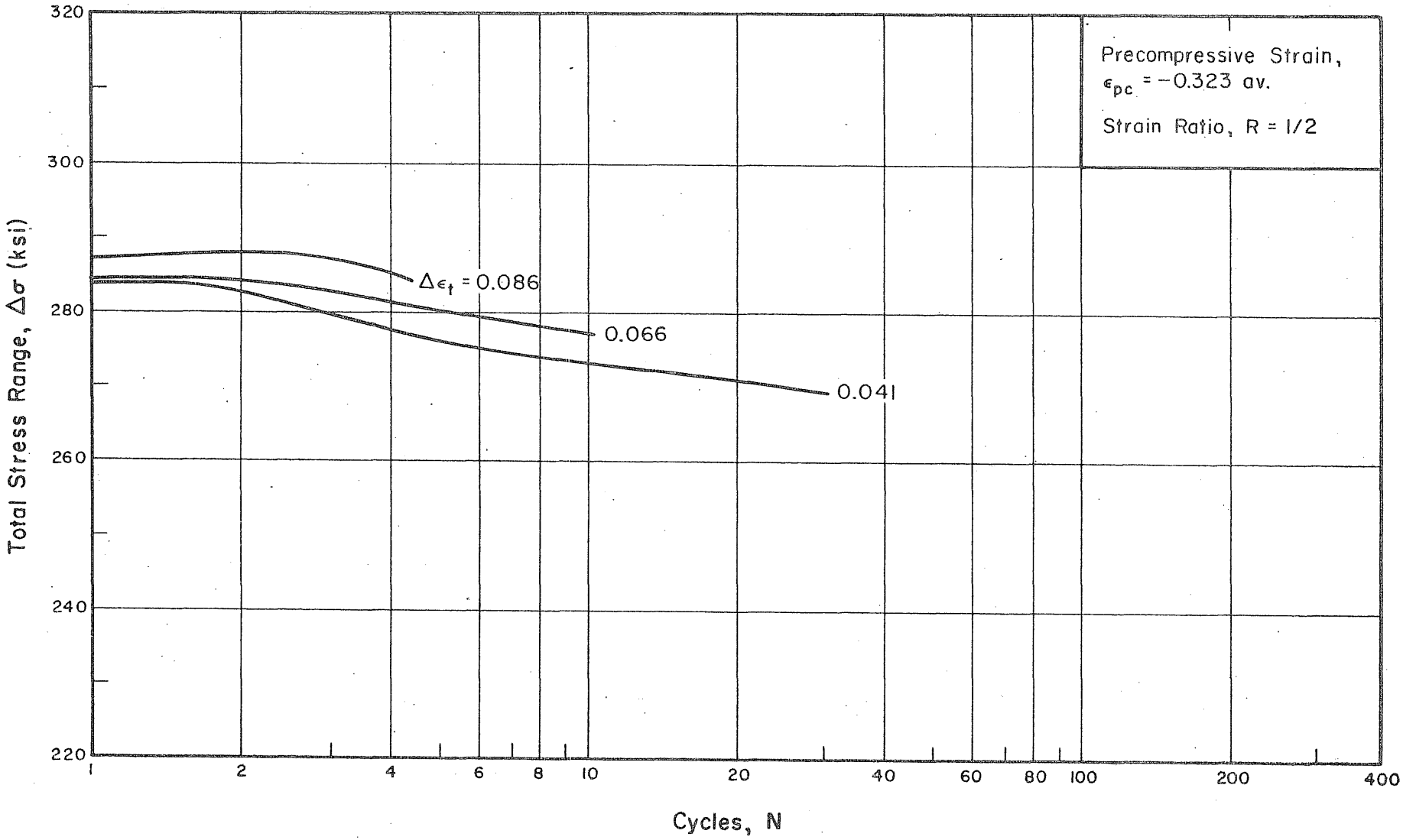

FIG. 26b CYCLIC STRESS HISTORY OF SPECIMENS PRECOMPRESSED TO −0.323 AV. STRAIN, R = 1/2

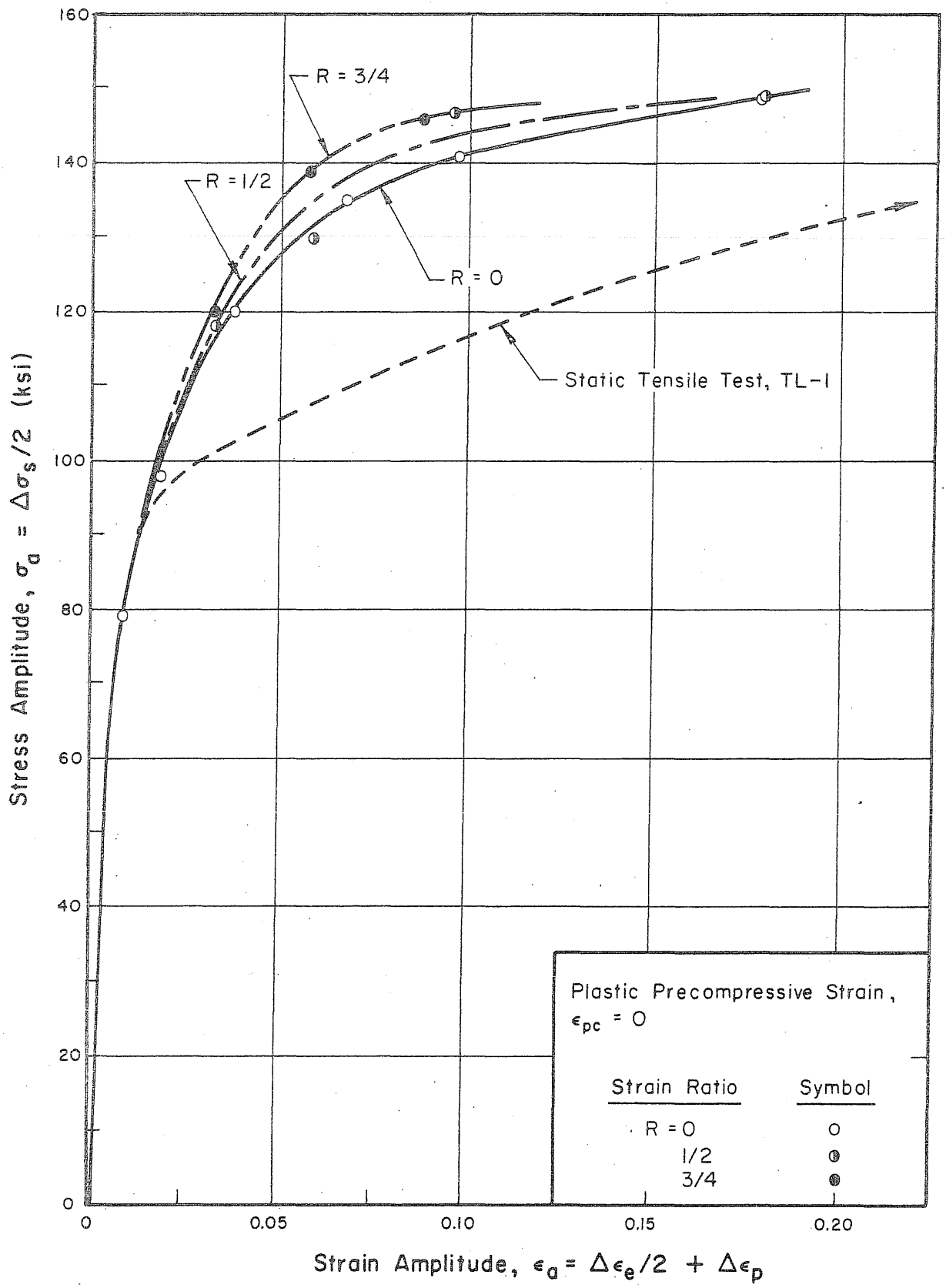

FIG. 27 CYCLIC STRESS-STRAIN DIAGRAMS FOR INITIALLY UNCOMPRESSED SPECIMENS

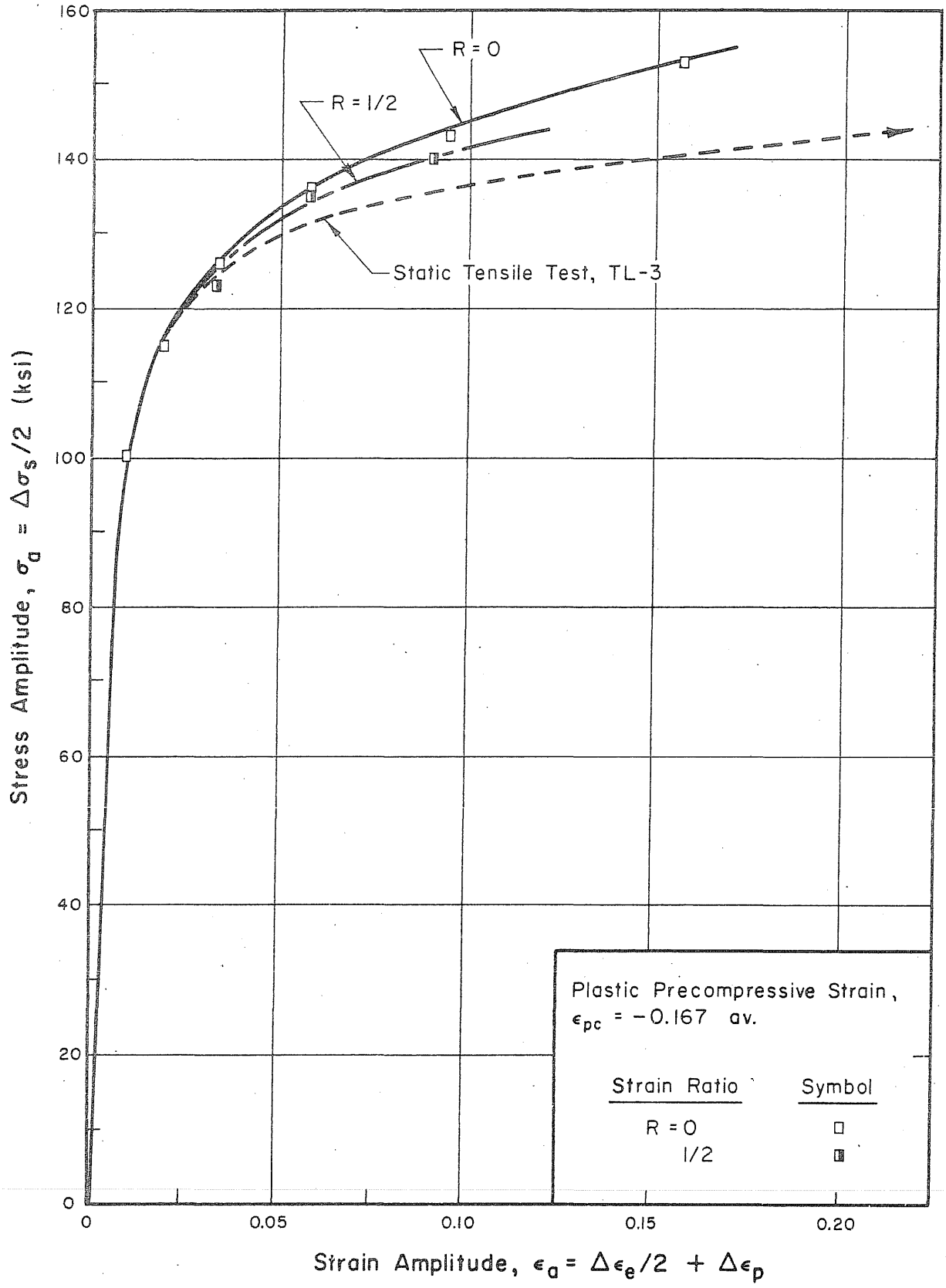

FIG. 28 CYCLIC STRESS-STRAIN DIAGRAMS FOR SPECIMENS PRECOMPRESSED TO -0.167 AV. STRAIN

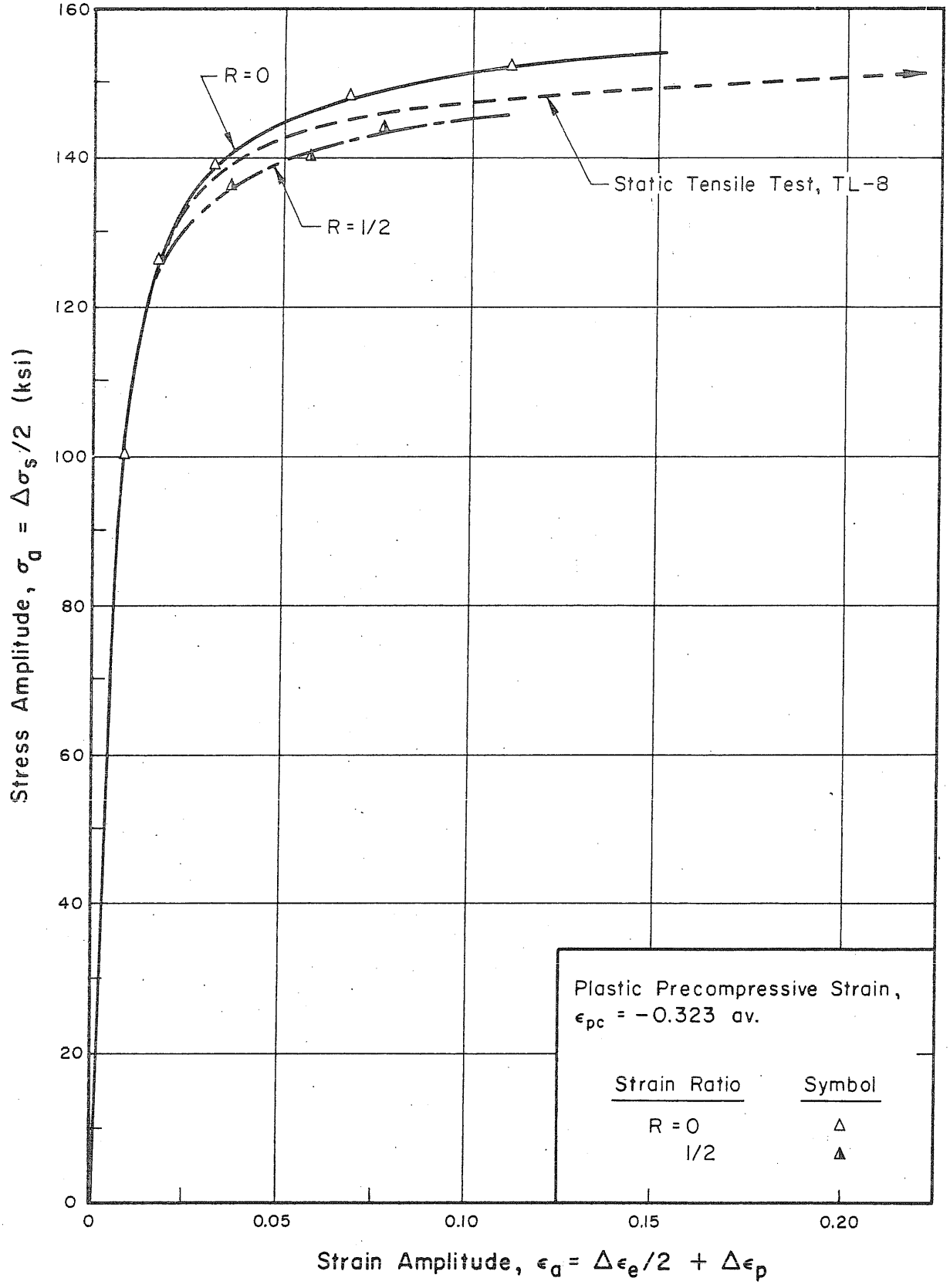

FIG. 29 CYCLIC STRESS-STRAIN DIAGRAMS FOR SPECIMENS PRECOMPRESSED TO −0.323 AV. STRAIN

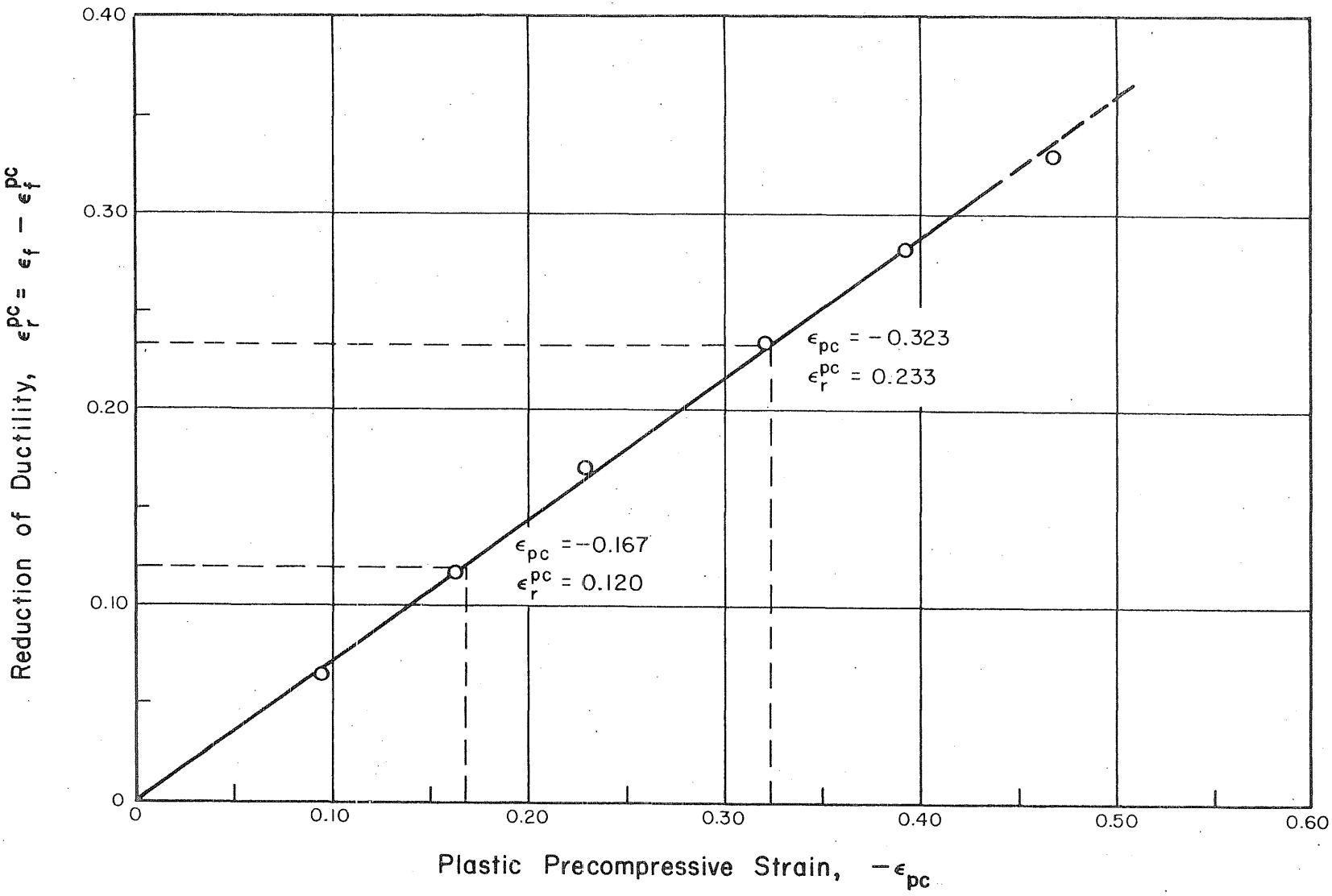

FIG. 30 REDUCTION IN STATIC FRACTURE DUCTILITY AS A RESULT OF PRECOMPRESSION

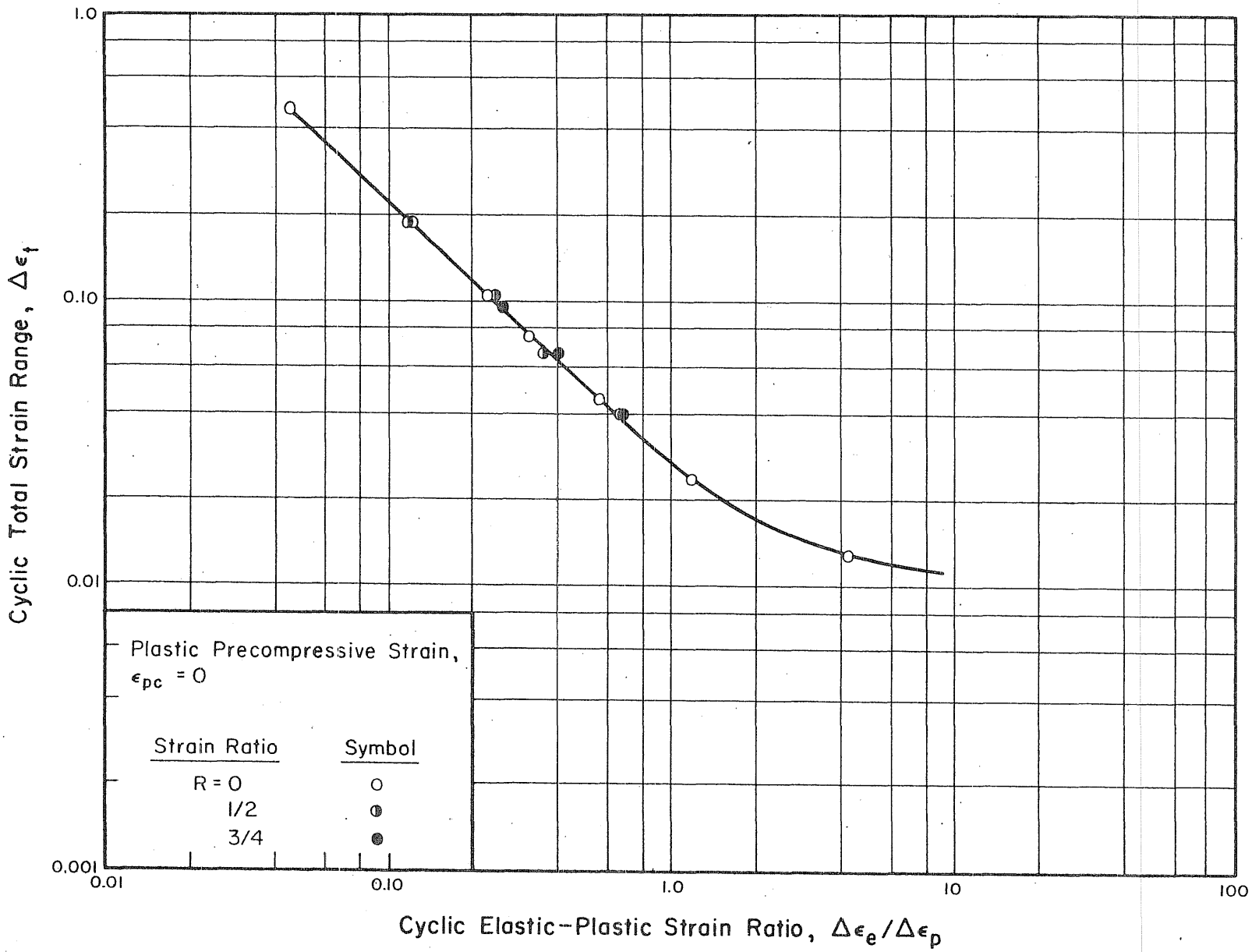

FIG. 31 ELASTIC-PLASTIC STRAIN RATIO FOR INITIALLY UNCOMPRESSED SPECIMENS

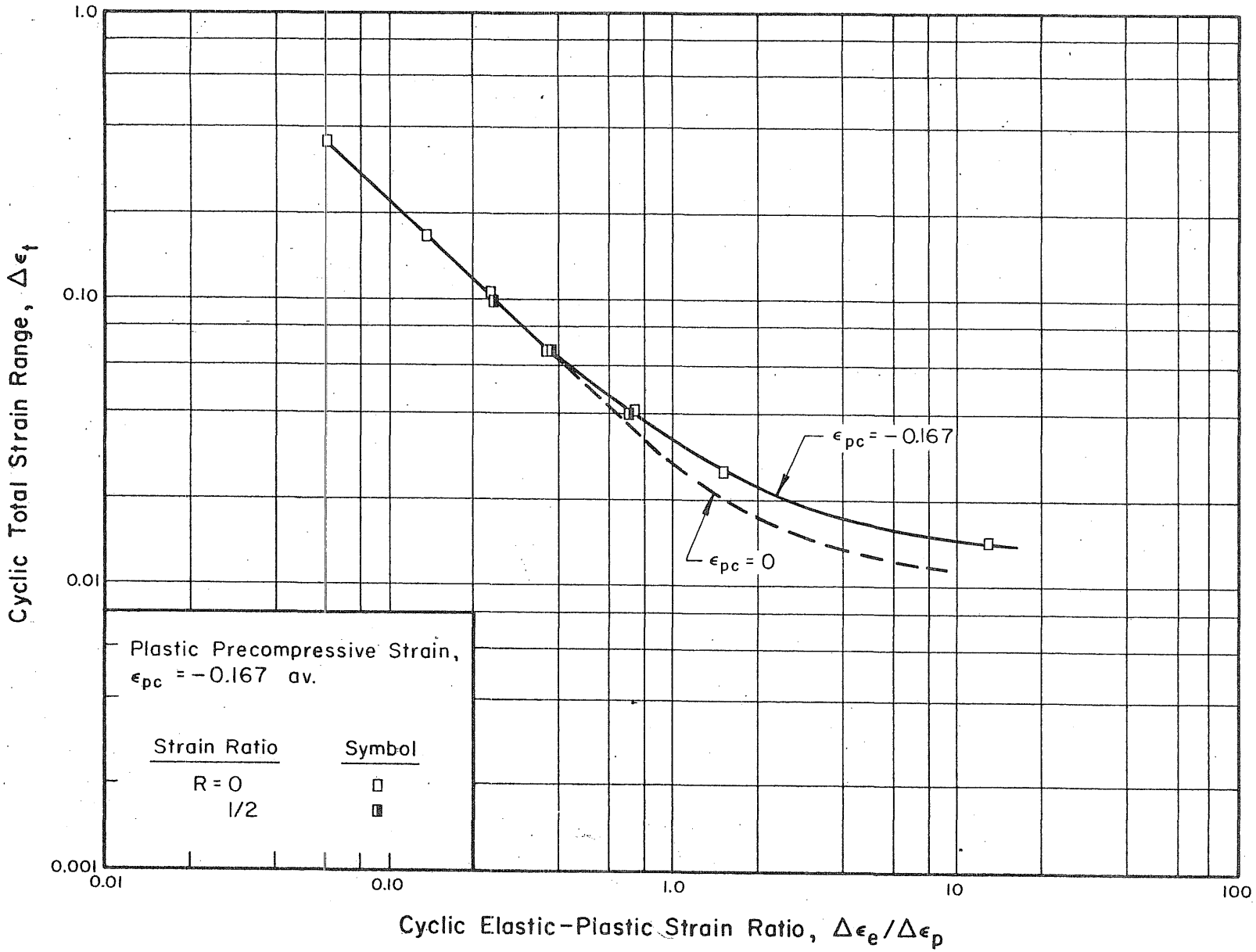

FIG. 32 ELASTIC-PLASTIC STRAIN RATIO FOR SPECIMENS PRECOMPRESSED TO -0.167 AV. STRAIN

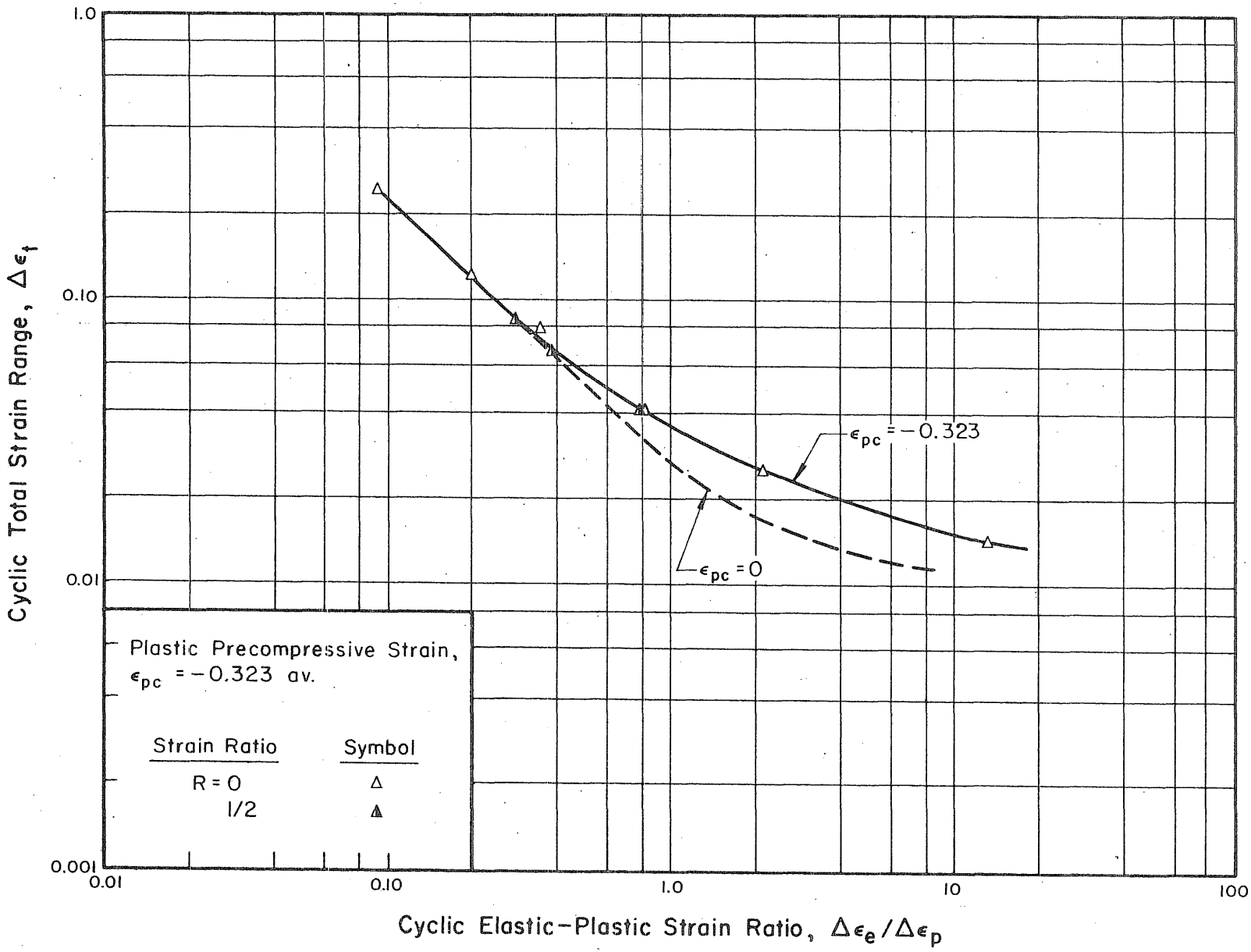

FIG. 33 ELASTIC-PLASTIC STRAIN RATIO FOR SPECIMENS PRECOMPRESSED TO -0.323 AV. STRAIN

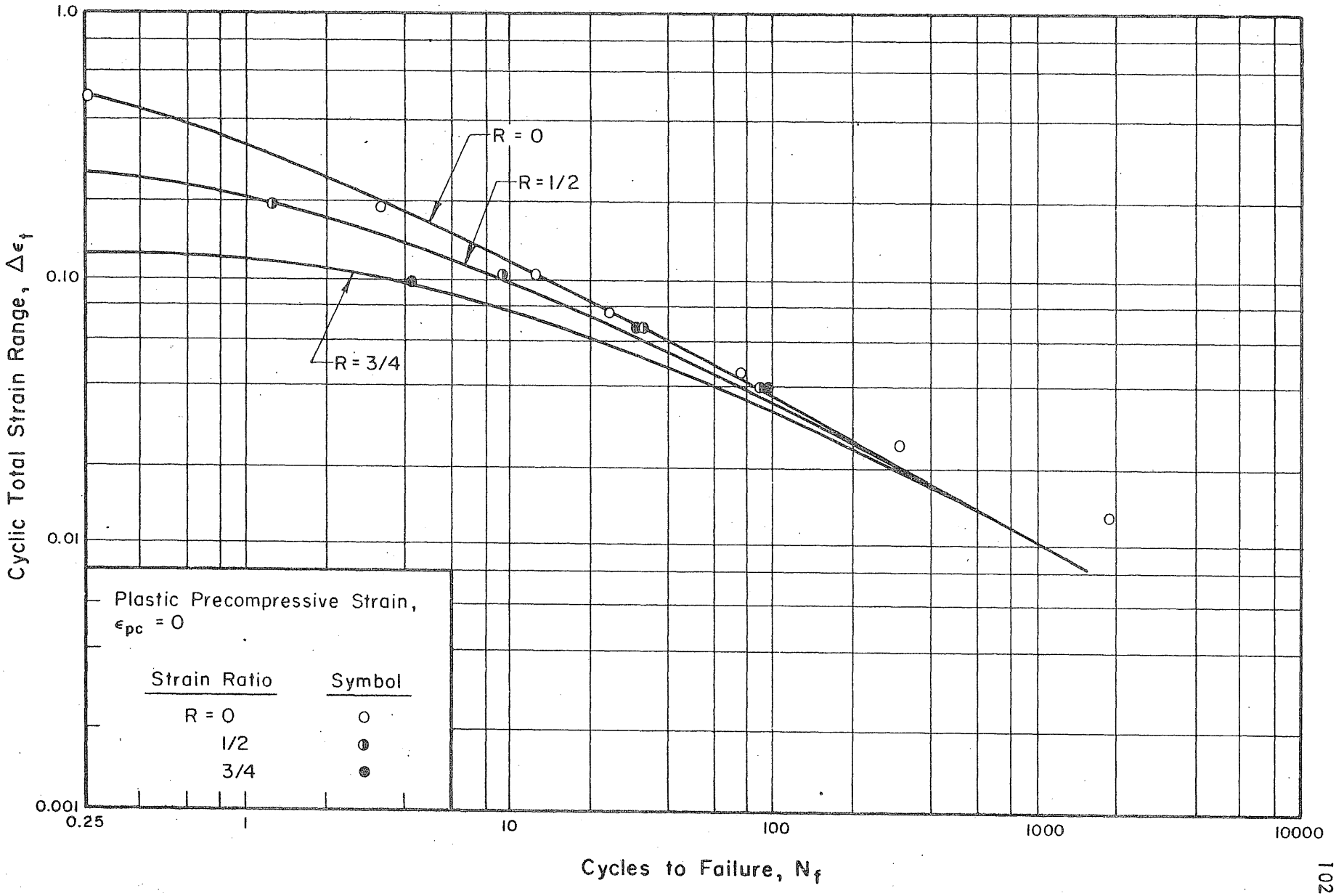

FIG. 34a FATIGUE TEST RESULTS FOR INITIALLY UNCOMPRESSED SPECIMENS

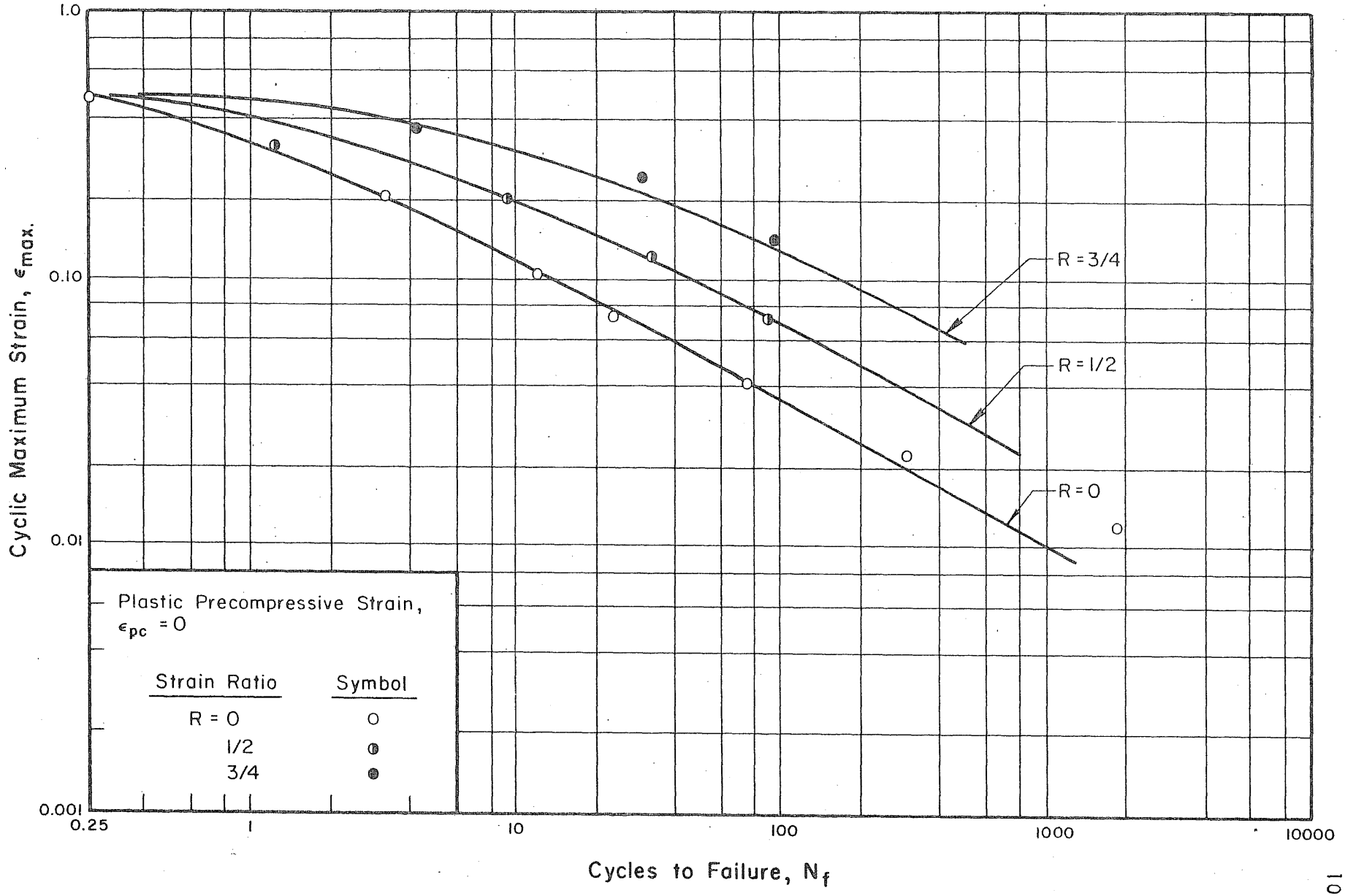

FIG. 34b FATIGUE TEST RESULTS FOR INITIALLY UNCOMPRESSED SPECIMENS

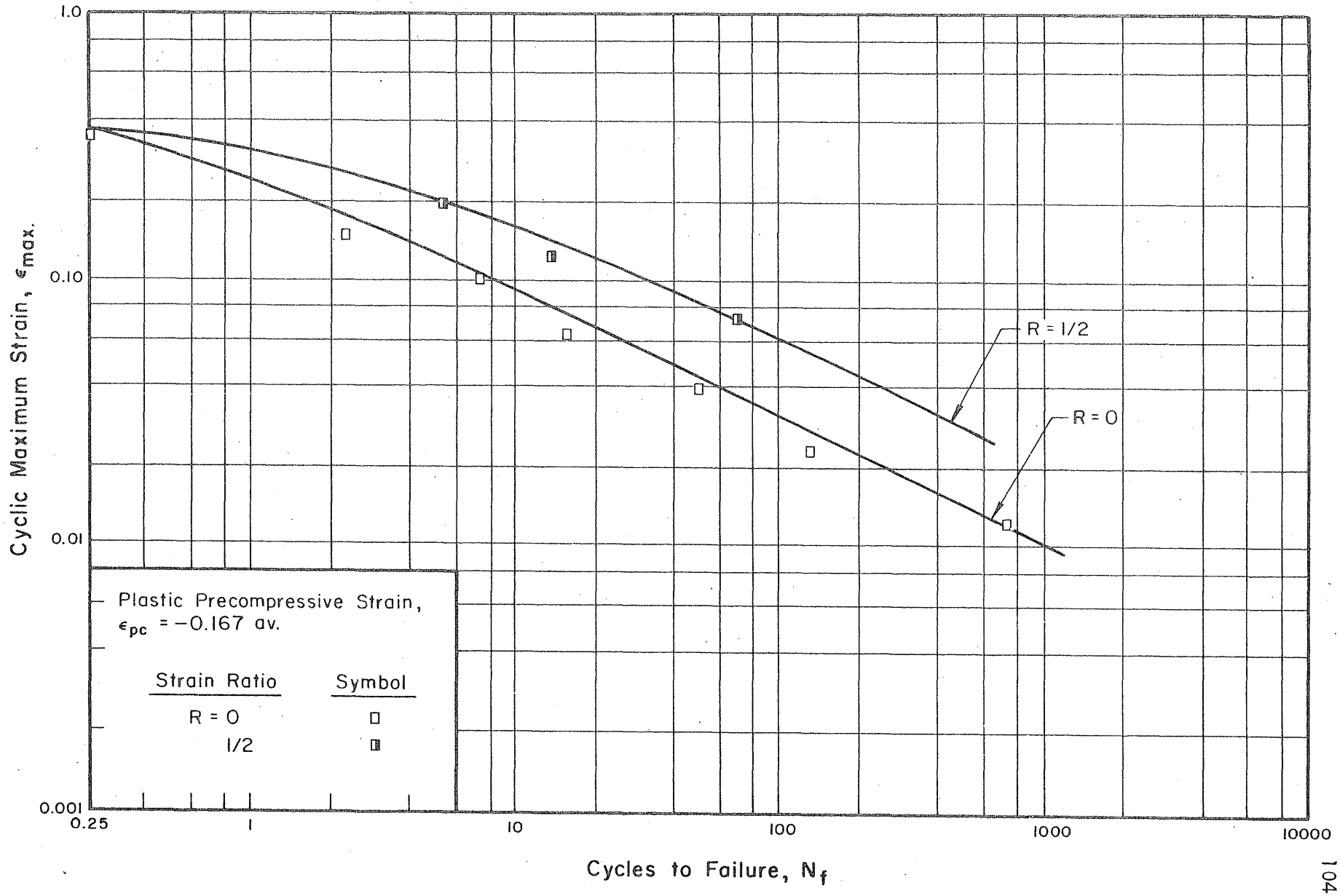

FIG. 35 FATIGUE TEST RESULTS FOR SPECIMENS PRECOMPRESSED TO -0.167 AV. STRAIN

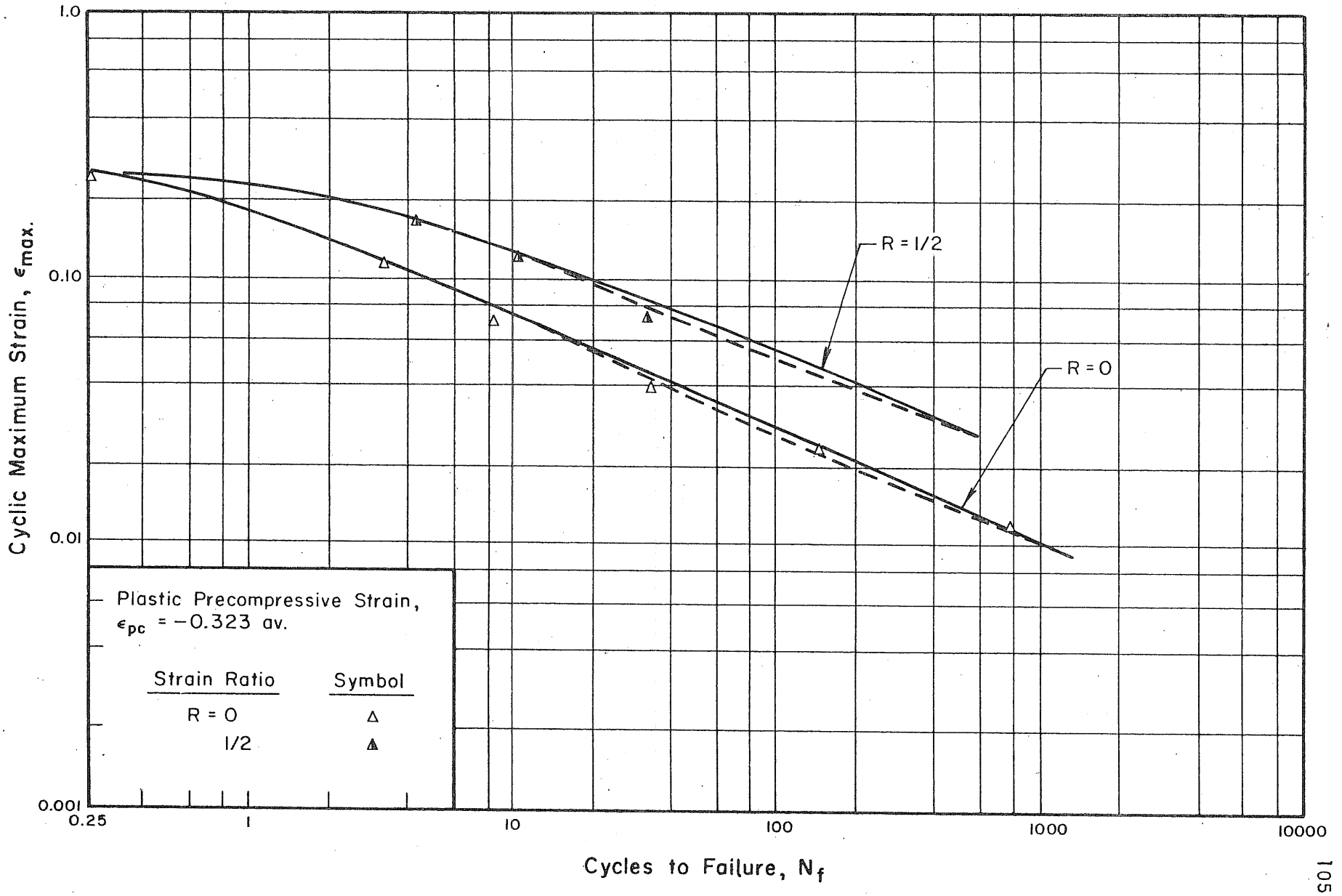

FIG. 36 FATIGUE TEST RESULTS FOR SPECIMENS PRECOMPRESSED TO −0.323 AV. STRAIN

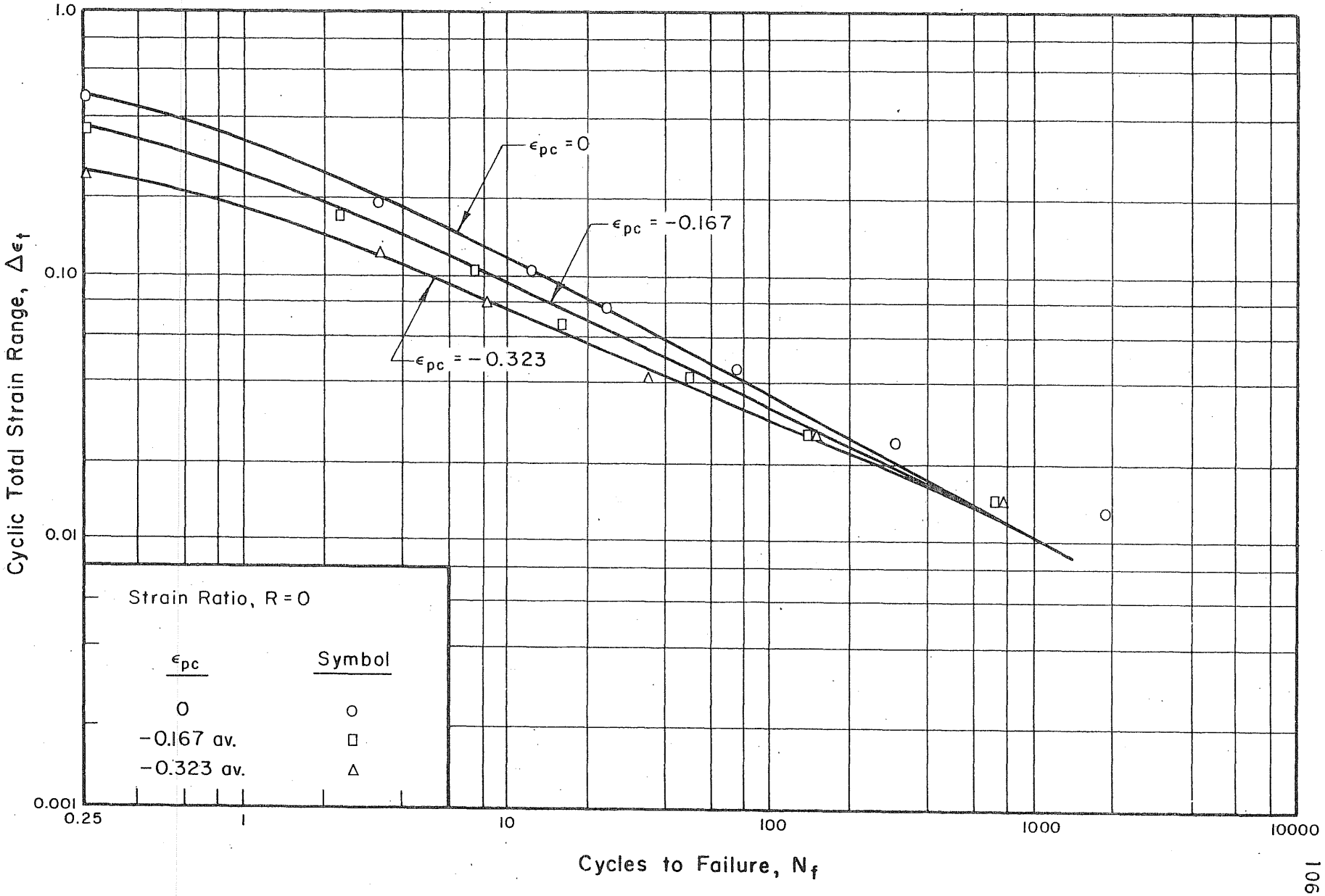

FIG. 37 FATIGUE TEST RESULTS FOR ALL SPECIMENS STRAIN CYCLED AT R = 0

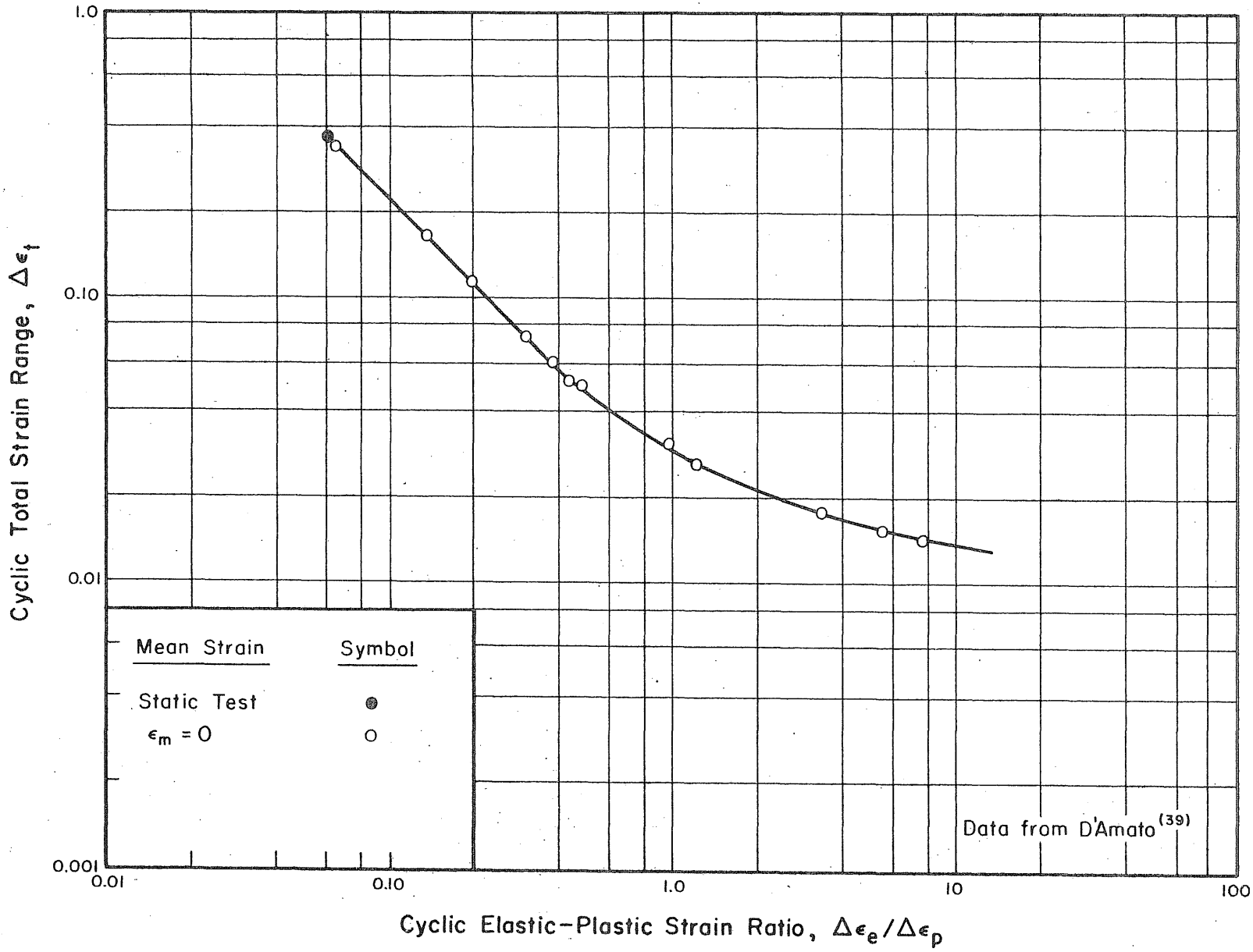

FIG. 38 ELASTIC-PLASTIC STRAIN RATIO FOR 2024-T4 ALUMINUM ALLOY, ZERO MEAN STRAIN

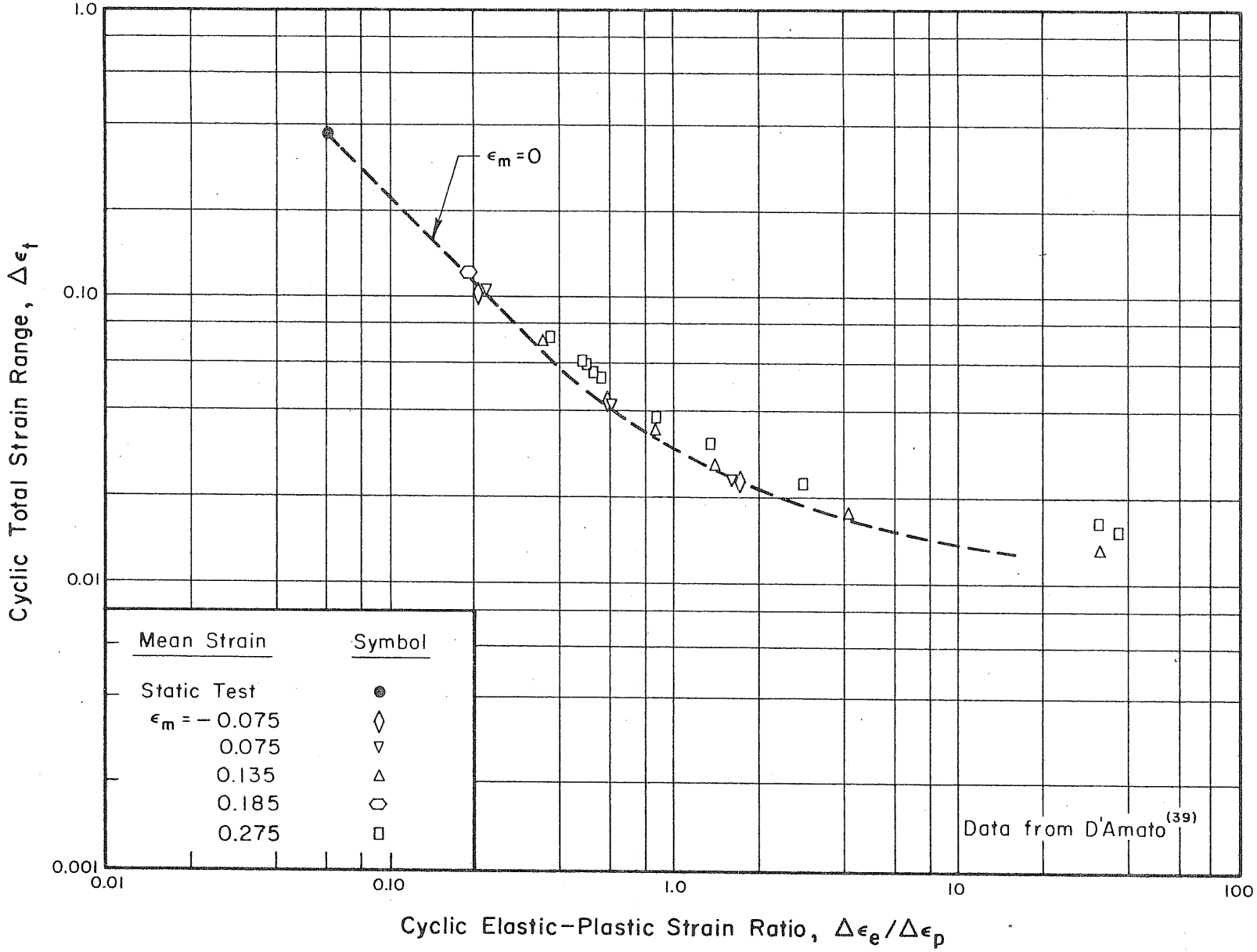

FIG. 39 ELASTIC-PLASTIC STRAIN RATIO FOR 2024-T4 ALUMINUM ALLOY, VARIOUS MEAN STRAINS

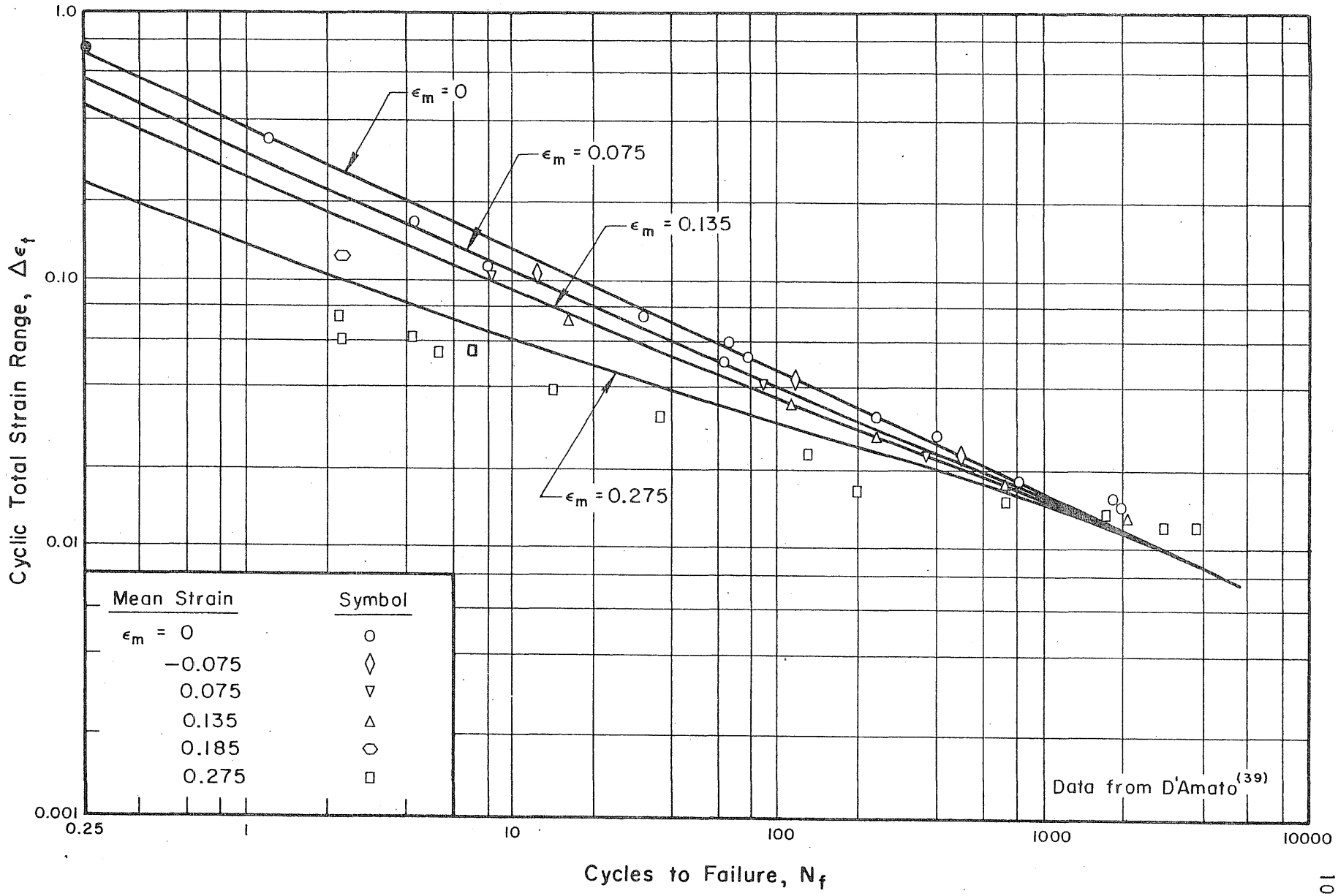

FIG. 40a FATIGUE TEST RESULTS FOR 2024-T4 ALUMINUM ALLOY

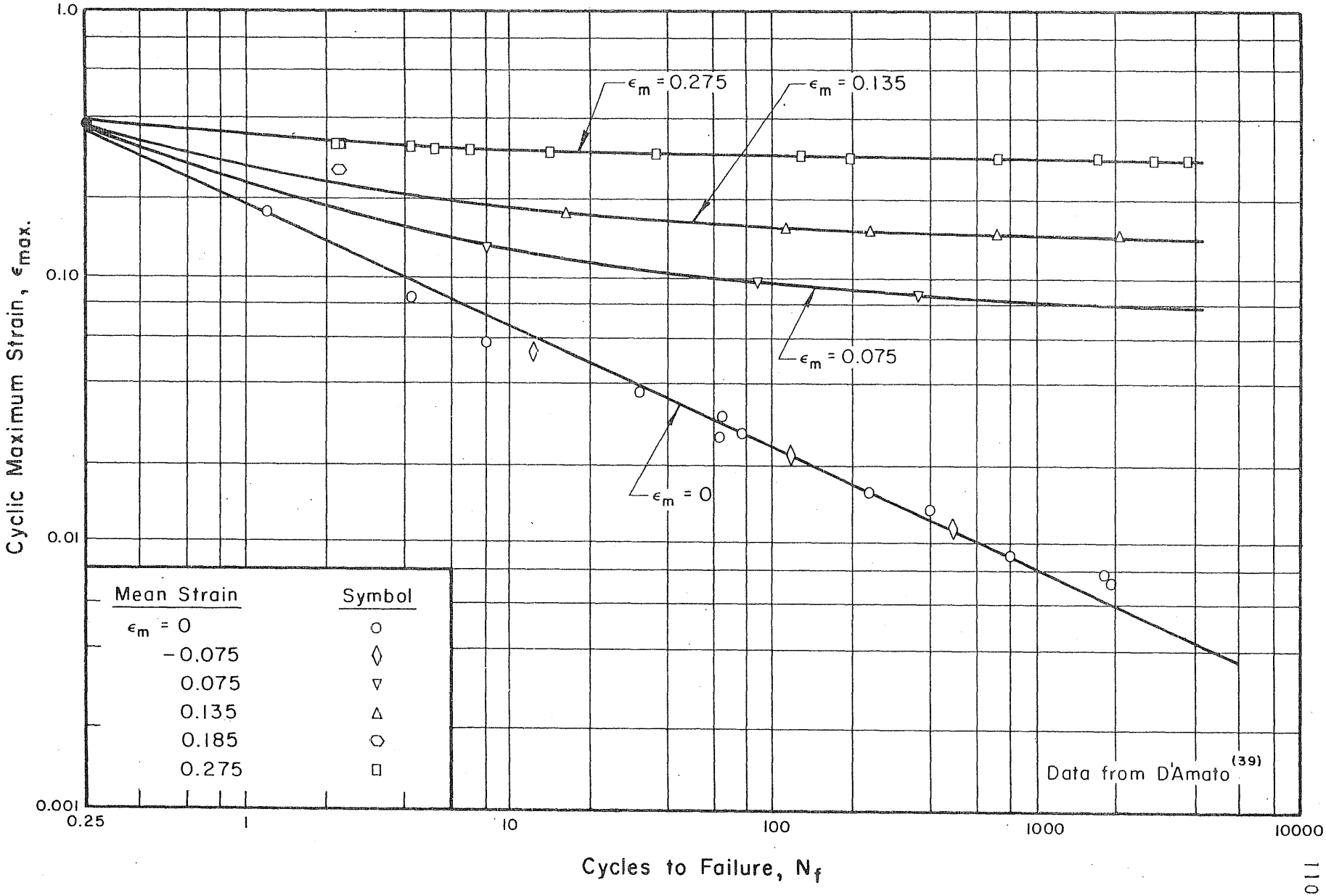

FIG. 40b FATIGUE TEST RESULTS FOR 2024-T4 ALUMINUM ALLOY

APPENDIX A

GLOSSARY OF TERMS

A	Instantaneous specimen cross-sectional area
A_f	Specimen cross-sectional area at fracture in static tension test
A_o	Initial specimen cross-sectional area
C	A constant, related to material tensile fracture strain
E	Elastic modulus
m	An empirical constant, considered a material fatigue property - negative of constant slope of log $\Delta\epsilon_t$-log N_f curve when $\epsilon_{pc} = 0$, $R = -1$
N	Number of applied strain cycles
N_f	Cycles to failure
P	External axial load
R	Cyclic constant strain ratio
S	Nominal stress
$\Delta\epsilon_e$	Cyclic elastic strain range
$\Delta\epsilon_p$	Cyclic plastic strain range
$\Delta\epsilon_t$	Cyclic total strain range
$\Delta\sigma_s$	Cyclic "stable" range of true stress (defined at $N_f/2$)
ϵ	"True" (logarithmic) strain
ϵ_a	Cyclic strain amplitude
ϵ_f	Fracture strain in static tension test
ϵ_f^{pc}	Static tensile fracture strain after precompression
ϵ_m	Cyclic mean strain (plastic tensile prestrain)
ϵ_{max}	Cyclic maximum strain
ϵ_{min}	Cyclic minimum strain

ϵ_{pc}	Plastic precompressive strain
ϵ_r^{pc}	Reduction in static tensile ductility as a result of precompression, $\epsilon_f - \epsilon_f^{pc}$
ν	Poisson's ratio
σ	"True" stress
σ_a	Cyclic stress amplitude
σ_f	Fracture stress in static tension test

APPENDIX B

CALCULATION OF DIAMETRAL AND LONGITUDINAL STRAINS

The titanium tested in this investigation was found to be slightly anisotropic. Under direct axial loading, Fig. B-1, the strains in the x and y directions, ϵ_x and ϵ_y, respectively, are, therefore, not identical. To obtain a consistent "average" measure of strain, the true* total diametral strain range, $\Delta\epsilon_t^d$, has been defined as:

$$\Delta\epsilon_t^d = \frac{1}{2}(\Delta\epsilon_x + \Delta\epsilon_y) = \frac{1}{2}\int_{A_{min}}^{A_{max}} \frac{dA}{A} = \frac{1}{2}\ln\frac{A_{max}}{A_{min}} \qquad (1)$$

where A_{max} and A_{min} are the limiting cross-sectional areas controlled during the test. Approximating the hysteresis loop by a perfectly elastic, perfectly plastic curve (dashed lines in Fig. B-2), the elastic and plastic components of the total diametral strain range are:

$$\Delta\epsilon_t^d = \Delta\epsilon_e^d + \Delta\epsilon_p^d \qquad (2)$$

The cyclic "true" stable stress range, $\Delta\sigma_s$, is found from:

$$\Delta\sigma_s = \frac{P_t}{A_{min}} + \frac{P_c}{A_{max}} \qquad (3)$$

where P_t and P_c are the absolute values of the limiting tensile and compressive loads, respectively, after a stable hysteresis loop has been established.

The longitudinal (in direction normal to xy plane) strain components can now be determined from the measured quantities presented above. The elastic component of the longitudinal strain range, $\Delta\epsilon_e$, is:

---

* "True" refers to logarithmic concept of strain.

$$\Delta\epsilon_e = \frac{\Delta\sigma_s}{E} \tag{4}$$

also,

$$\Delta\epsilon_e = \frac{\Delta\epsilon_e^{\,d}}{\nu} \tag{5}$$

$$\therefore \quad \Delta\epsilon_e^{\,d} = \frac{\nu\Delta\sigma_s}{E} \tag{6}$$

where E is the elastic modulus, 15×10^3 ksi; and $\nu = 1/3$ is Poisson's ratio for pure titanium.

Since plastic deformation occurs at essentially constant volume, the plastic component of the longitudinal strain range, $\Delta\epsilon_p$, is related to the measured quantities by:

$$\Delta\epsilon_p = 2\Delta\epsilon_p^{\,d} = 2(\Delta\epsilon_t^{\,d} - \Delta\epsilon_e^{\,d}) \tag{7}$$

Substituting Eq. (6) into the above:

$$\Delta\epsilon_p = 2\Delta\epsilon_t^{\,d} - \frac{2\nu\Delta\sigma_s}{E} \tag{8}$$

By summing its components, Eqs. (4) and (8), the total longitudinal strain range, $\Delta\epsilon_t$, becomes:

$$\Delta\epsilon_t = \Delta\epsilon_e + \Delta\epsilon_p$$

$$= 2\Delta\epsilon_t^{\,d} + \frac{\Delta\sigma_s}{E}(1 - 2\nu)$$

$$\therefore \quad \Delta\epsilon_t = \ell n \frac{A_{max}}{A_{min}} + \frac{\Delta\sigma_s}{E}(1 - 2\nu) \tag{9}$$

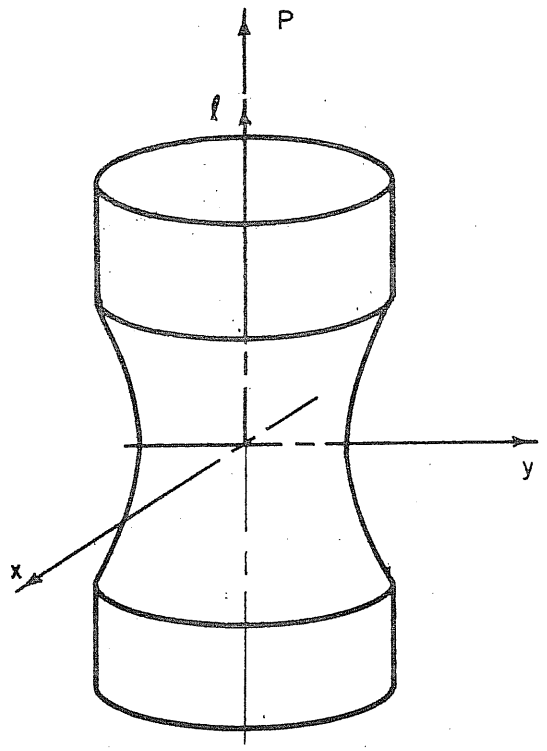

FIG. B-1 SPECIMEN COORDINATE AXES

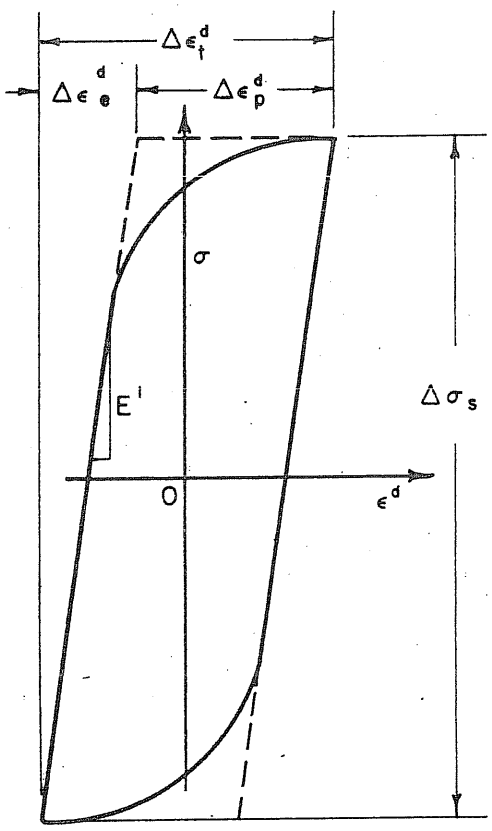

$E' = E/\nu$

FIG. B-2 STABLE CYCLIC HYSTERESIS CONDITION

APPENDIX C

COMPARISON OF LOW CYCLE AND LONG LIFE FATIGUE OF TITANIUM

A study of the long life fatigue behavior of commercially pure titanium, conducted at Carnegie Institute of Technology, has been reported by Weinberg and Hanna[50] of Battelle Memorial Institute. The test material consisted of two separate heats of titanium bar stock, manufacturer's designation Ti-75A. The chemical composition and mechanical properties of this material are similar to the RS-70 titanium used in the current investigation.

Rotating beam fatigue tests were performed on both heats to produce a completely reversed stress cycle. Since the material remains essentially elastic for the ranges of stress examined (i.e., constant-stress and constant-strain cycling are equivalent), a fair comparison is possible between this data and the results of the present study. A composite diagram indicating the entire range of fatigue lives from 1/4 to 10^7 cycles is shown in Fig. C-1. The low cycle fatigue results are from the initially uncompressed specimens tested at R = 0. In the long life region, the data for both heats of the Ti-75A titanium, converted to strain, are presented.

The solid line in Fig. C-1 represents the curve predicted by Eq. (5.1). The dashed line shows the transition behavior evidenced at about 10^3 cycles, the gradually sloping straight line corresponding to the long life region, and the approach toward an apparent endurance limit at about 10^7 cycles.

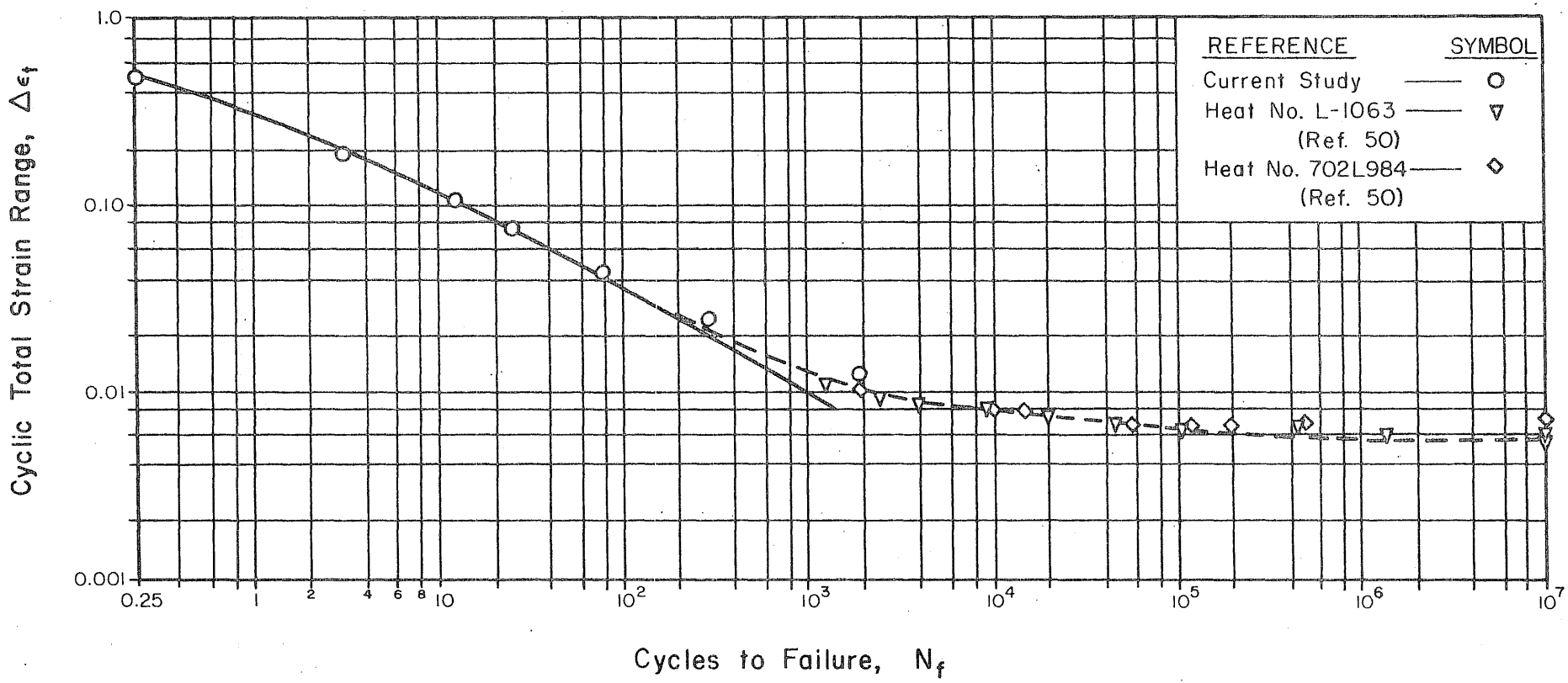

FIG. C-1 COMPLETE RANGE OF FATIGUE BEHAVIOR FOR PURE TITANIUM